GENIORS

Research and Innovation Action (RIA)

This project has received funding from the European Union's Horizon 2020 research and innovation programme under grant agreement No 755171.

Start date : 2017-06-01 Duration : 48 Months
http://geniors.eu/

Impacts of solvent degradation and recycle on the EURO-GANEX process

Authors : Dr. Hitos GALAN (CIEMAT), Iván Sánchez-García, Ana Núñez, Hitos Galán, Sofía Durán and Lorena Serrano (CIEMAT); Colin Boxall (ULANC);Andreas Wilden, Giuseppe Modolo (Juelich); Bart Verlinden and Rainier Hermans (SCK?CEN); Patrik Wessling and Andreas Geist (KIT-INE); Wim Verboom (TWE); X. Heres, S. Costenoble, S. Broussard, J. Sinot, L. Guillerme, J. Vincent, C. Sorel, M.C. Charbonnel (CEA); Dimytro Bavol and Bohumir Gruner (IIC); Peter Distler and Jan John (CTU); Thea Lyseid Authen and Christian Ekberg (CHALMERS)

GENIORS - Contract Number: 755171

Project officer: Roger Garbil

Document title	Impacts of solvent degradation and recycle on the EURO-GANEX process
Author(s)	Dr. Hitos GALAN, Iván Sánchez-García, Ana Núñez, Hitos Galán, Sofía Durán and Lorena Serrano (CIEMAT); Colin Boxall (ULANC);Andreas Wilden, Giuseppe Modolo (Juelich); Bart Verlinden and Rainier Hermans (SCK?CEN); Patrik Wessling and Andreas Geist (KIT-INE); Wim Verboom (TWE); X. Heres, S. Costenoble, S. Broussard, J. Sinot, L. Guillerme, J. Vincent, C. Sorel, M.C. Charbonnel (CEA); Dimytro Bavol and Bohumir Gruner (IIC); Peter Distler and Jan John (CTU); Thea Lyseid Authen and Christian Ekberg (CHALMERS)
Number of pages	103
Document type	Deliverable
Work Package	WP5
Document number	D5.2
Issued by	CIEMAT
Date of completion	2021-06-24 10:19:47
Dissemination level	Public

Summary

The present deliverable collects all the studies carried out within GENIORS project about the impact of solvent degradation and recycle on the EURO-GANEX process as well as all those degradation studies related to the other options of GANEX-2 cycle, such as the recent solvents optimization of EURO-GANEX (New EURO-GANEX) and CHALMEX process. It has been collected the last studies and conclusions extracted for the different systems mentioned, however, deeper degradation studies about some of ligands involved have been previously reported in D2.1 Stability and safety studies of hold extraction systems (1 for each CyMe4BTBP, HydroBTBP, TODGA & PTD) and D2.2 Stability studies of stripping agents of the project; and the studies related to TODGA-based solvents recycling have been included in the corresponding D3.4 Status on solvent clean- up & recycling. Additionally, D5.2 collects the design and set-up of two irradiation loops developed within GENIORS project and the comparative study performed for EURO-GANEX systems. This work has been performed within the GENIORS/INL-USA collaboration for the comparison of the three irradiation loops: Marcel (CEA), Náyade (CIEMAT) and Idaho Falls (INL).

Approval

Date	By
2021-06-24 12:15:24	Pr. Christian EKBERG (Chalmers)
2021-06-24 12:23:34	Dr. Jean-Marc ADNET (CEA)
2021-06-30 22:40:51	Mr. Stéphane BOURG (CEA)

CONTENTS

This project has received funding from the EURATOM research and training programme 2014–2018 under grant agreement No. 755171. The content of this deliverable reflects only the authors' view. The European Commission is not responsible for any use that may be made of the information it contains.

This project has received funding from the EURATOM research and training programme 2014–2018 under grant agreement No. 755171. The content of this deliverable reflects only the authors' view. The European Commission is not responsible for any use that may be made of the information it contains.

EXECUTIVE SUMMARY

The present deliverable collects all the studies carried out within GENIORS project about the impact of solvent degradation and recycle on the EURO-GANEX process as well as all those degradation studies related to the other options of GANEX-2 cycle, such as the recent solvents optimization of EURO-GANEX (New EURO-GANEX) and CHALMEX process. It has been collected the last studies and conclusions extracted for the different systems mentioned, however, deeper degradation studies about some of ligands involved have been previously reported in D2.1 Stability and safety studies of hold extraction systems (1 for each CyMe4BTBP, HydroBTBP, TODGA & PTD) and D2.2 Stability studies of stripping agents of the project; and the studies related to TODGA-based solvents recycling have been included in the corresponding D3.4 Status on solvent clean- up & recycling.

Additionally, D5.2 collects the design and set-up of two irradiation loops developed within GENIORS project and the comparative study performed for EURO-GANEX systems. This work has been performed within the GENIORS/INL-USA collaboration for the comparison of the three irradiation loops: Marcel (CEA), Náyade (CIEMAT) and Idaho Falls (INL).

INTRODUCTION

Two possible concepts of MAs recycling have been considered, the heterogeneous or homogeneous recycling [1]. In the first one, a sequential separation of elements is needed starting from already implemented U and Pu recovering, to finally isolate MAs from the previous raffinate; by contrast, the homogeneous recycling lies on the separation of all the TRU together after the previous recovering of U, the so-called GANEX concept (Grouped Actinide Extraction) [2, 3]. The GANEX process was first developed by the CEA and designed as a 2-stage solvent extraction process, where the bulk uranium is extracted in the primary stage (GANEX-1) [4], while the TRU/fission product separation is achieved in the secondary stage – this has been termed CEA-GANEX [5]. In the ACSEPT project the EURO-GANEX cycle was developed and tested [6-8] as well as the initial formulation of the Chalmers-GANEX (CHALMEX) [9-12]. In the CEA-GANEX and the EURO-GANEX processes, the actinides and lanthanides are co-extracted from the GANEX 1st cycle (GANEX-1) raffinate. The actinide/fission product separation is achieved through subsequent selective stripping. In the CHALMEX process, the An/Ln separation occurs by the selective extraction of An [9-11].

The control of the normal and safe performance during the operation of these processes is one of the most important security keys for the demonstration of its industrial applicability, since these processes are kept in continue operation as much as possible. For that reason, one of the limiting points for the development of these extraction processes is their resistance to the highly radioactive field where they must be used. Therefore, to ensure a safe and stable operation, the stability studies are the cornerstone to understand, simulate and predict what would happen along a real separation process.

The GANEX 1st cycle is common for all the variants of the GANEX processes and it has been assessed to be at TRL 5 [13, 14]). The studies performed up to now regarding the resistance to radiation of the main molecule involved, DEHiBA (*N*,*N*-di(2-ethylhexyl)isobutyramide), as well as its behaviour under an irradiation loop test (MARCEL GANEX-1 test loop, 2010 CEA) [15, 16] have shown promising results. DEHiBA degrades into carboxylic acids and secondary amines, which have little to no effect on the separation of uranium from the raffinate [17-19]. Therefore, the current challenge for GANEX process development relies on GANEX-2 cycle studies, for which the EURO-GANEX is considered as the reference option.

This project has received funding from the EURATOM research and training programme 2014–2018 under grant agreement No. 755171. The content of this deliverable reflects only the authors' view. The European Commission is not responsible for any use that may be made of the information it contains.

EURO-GANEX SOLVENT DEGRADATION STUDIES

Authors: Iván Sánchez-García, Hitos Galán, Sofía Durán and Lorena Serrano (CIEMAT); Colin Boxall (ULANC).

SUMMARY OF PREVIOUS RESULTS

The EURO-GANEX process is one of the most successful options develop for the second cycle of GANEX process [5, 8, 12]. During the first cycle (GANEX-1) U(VI) is selectively extracted leaving TRU, trivalent lanthanides (Ln(III)) and the other fission products (FPs) in the aqueous phase [20]. Then the EURO-GANEX solvent, consisting in a mixture of the DGA TODGA and the malonamide DMDOHEMA (*N*,*N*'-dimethyl-*N*,*N*'-dioctylhexyloxyethyl malonamide), co-extracts An and Ln from GANEX-1 raffinate. To avoid the co-extraction of some FPs such as Zr(IV) and Pd(II), the masking agent CDTA (trans-1,2-cyclohexanediaminetetraacetic acid) is used. After that, all TRU are stripped by using the combination of the water soluble SO_3-Ph-BTP and AHA (acetohydroxamic acid) (Figure 1) [8]. The role of DMDOHEMA in EURO-GANEX solvent is to increase the Pu loading capacity of the organic phase [8] and of AHA is to strip Pu(IV), Np(VI), and Np(VI) into the aqueous phase [21, 22].

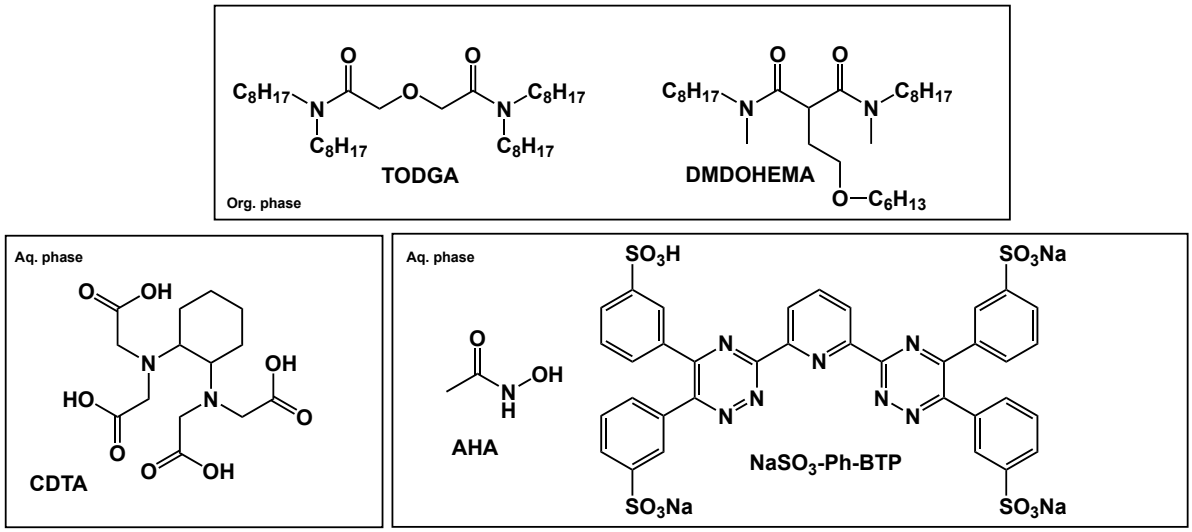

Figure 1. Structures of the molecules involved in the EURO-GANEX process: TODGA, DMDOHEMA, CDTA, $NaSO_3$-Ph-BTP

In general, the individual resistance to radiation of main molecules involved in EURO-GANEX process, TODGA [23-26], DMDOHEMA [27-29] and SO_3-Ph-BTP [30-32], has already been studied. However, it is known that the chemical composition of the solvent modifies the stability studies results. For example, factors such as the presence of nitric acid during the irradiation, oxygen content, the composition of diluents, the contact between phases etc., could lead a scavenger process that may act as radio-protection agent for ligands degradation. In consequence, due to the not simple composition of EURO-GANEX solvent and the different experimental conditions chosen for the individual studies published for each molecule, results are not always adequate to explain the resistance of the full EURO-GANEX system.

At the end of SACSESS project it was evaluated the resistant of the full organic EURO-GANEX solvent [33-36], concluding that even after an accumulated dose such us 1MGy, the system keeps well the co-extraction of Ln and An. Although an important reduction in TODGA and DMDOHEMA concentration was observed, the system was able to keep Ln loading capacity, probably due to extraction properties of new species formed, the degradation compounds (DCs). In that sense, a total of fourteen DCs was identify, 9 from TODGA and 5 from

This project has received funding from the EURATOM research and training programme 2014–2018 under grant agreement No. 755171. The content of this deliverable reflects only the authors' view. The European Commission is not responsible for any use that may be made of the information it contains.

DMDOHEMA, giving place to a complicate mixture where at least three of those compounds could form insoluble aggregates. In relation to FPs, the performance of EURO-GANEX solvent also showed some modification after irradiation. On the one hand, it was observed a reduction of the extraction of Zr and Pd, probably due to TODGA degradation since this experiment was performed without masking agents; and on the other hand, an increase in the extraction of other metals occurred that can be explained also by the extraction properties of some TODGA DCs. The extraction properties and impact of main TODGA DCs and their washing strategies have been intensively studied and reported during ACSEPT [23], SACSESS [37] and GENIORS projects [38].

An stripping studies into 1 mol/L HNO_3 from a loaded (An and Ln) and irradiated (1MGy) organic EURO-GANEX solvent revealed that Ln/An separation could be affected during this step, since An but also Ln were worse kept in the organic phase during this step. By contracts, more Ln stripping steps with diluted nitric acid were needed for a quantitative Ln back-extraction. The measurement of distribution ratio of Ln and An after the irradiation of the organic EURO-GANEX solvent as a function of nitric acid concentration agreed with those results, a higher impact on the original performance of EURO-GANEX solvent was observed at diluted nitric acid concentration, specially for the An extraction. As it was mentioned before, most of reported effects in the performance of the organic EURO-GANEX solvent can be mainly explained due to the presence of DC formed.

From the point of view of aqueous phases, although it is not expected they be recycled their degradation could lead mass transference and accumulation into the recycled organic phases, as well as condition its resistance to radiation. At the end of SACSESS project, some experiments contacting organic and aqueous phases that had been irradiated individually were carried out [36]. For example, a fresh and irradiated organic EURO-GANEX solvent, up to an accumulated dose of 1MGy, were contacted with aq. EURO-GANEX phases submitted to 50, 100, and 300 kGy. These first approaches towards the full system study, although still far from a realistic experiment, evidenced the importance of exploring the interaction and impact of the aqueous phases degradation to study the real EURO-GANEX systems behaviour under radiation conditions.

During GENIORS project it has also been performed the gamma irradiation of CDTA. The irradiation study of CDTA included in D2.1 (Stability and safety studies of hold extraction systems (1 for each CyMe4BTBP, HydroBTBP, TODGA& PTD)) revealed that even at a low accumulated dose of 5-50 kGy, it could exit problems to keep Zr and Pd in the aqueous phase or third phase formation due to the presence of CDTA DCs. These effects do not interfere with An and Ln co-extraction but dose estimation and more realistic experiments should be considered for future irradiation test loops. Other way, experiments to investigate the irradiation of 304L stainless steel flags in 3.7 and 7.4 M HNO_3 solutions, in both the presence and absence of CDTA, were conducted within the gamma irradiator at the Dalton Cumbrian Facility. Results reported in D9.6 (Assessment of the corrosion vulnerability of common plant materials in the presence of key process streams) indicate that the CDTA acted to inhibit intergranular corrosion on the steel surface with greatest protection being shown at the lower acidity. This corrosion inhibiting effect of CDTA in radiation fields is most likely due to one or both of two effects: a) CDTA is adsorbing at the steel surface, said adsorption providing a degree of protection to the Cr_2O_3 passivation layer, preventing oxidative attack by oxidants generated by the radiolysis of water; b) the presence of CDTA may suppress nitrous acid production – either via providing a substrate that the nitrous may participate with in nitrating reactions or by the provision of CDTA radical species during irradiation that interrupt nitrous production

AHA radiolysis studies included in D2.1 [39], concluded that radiolysis effects over the extraction behaviour of systems studied were negligible compared with those coming from its hydrolysis in nitric acid. As consequence and to be comparable, all radiolysis studies involving AHA were fixed in a period of two hours. Other way, it was observed that the irradiation of aqueous phases containing AHA and SO_3-Ph-BTP lets a protection over the degradation of SO_3-Ph-BTP.

This project has received funding from the EURATOM research and training programme 2014–2018 under grant agreement No. 755171. The content of this deliverable reflects only the authors' view. The European Commission is not responsible for any use that may be made of the information it contains.

Unfortunately, conflicting results were found in the past regarding the resistance of SO_3-Ph-BTP against γ-radiation [30, 32, 40, 41]. In general, latest results point out that to simulate the effects of radiations over SO_3-Ph-BTP aqueous phases and the systems related it is essential to design the irradiation experiments carefully according to realist process conditions [42]. A real process involved many different factors that hardly be simulated in a simple and easy way in the lab but also in radiation plants. Therefore, to gain a better understanding of the radiolytic degradation of SO_3-Ph-BTP but also of the full EURO-GANEX system, further studies have been addressed to design reliable experimental strategies to simulate the impact of degradation on EURO-GANEX process performance. On the one hand, it has been explored which are the problems and the most process-relevant conditions to simulate the effects of radiation on EURO-GANEX process in a simple way, it means, with static experiments [41, 42]; and on the other hand, it has been designed and set-up an irradiation loop device at Náyade facility able to check the effects of radiation considering the most relevant process conditions of EURO-GANEX process.

PROCESS-RELEVANT CONDITIONS TO SIMULATE EFFECTS OF RADIATION ON EURO-GANEX PROCESS

First of all, it was studied the interaction between the solvent and aqueous phase containing the main extractants, TODGA or SO_3PhBTP, against γ-irradiation; and them, these studies have been extended to the full systems including the phase modifiers, it means, it has also been considered the interaction of degradation of TODGA-DMDOHEMA solvents and AHA-SO_3PhBTP. Figure 2 shows the schematic representation of the strategy of study followed for the different irradiations performed, where three experimental conditions leading to increase the contact between phases and the content of oxygen have also been considered (air and argon atmosphere and an air sparging flow). For a rightful comparison of the distribution ratios obtained, after irradiation, the organic phases and aqueous consisting in partial compositions i.e. kerosene, nitric acid, etc. were replaced by the corresponding fresh organic or aqueous phase.

All details related to the stability of the stripping agent SO_3-Ph-BTP have been already collected in D2.2 Stability studies of stripping agents of the project [42] and D2.1 Stability and safety studies of hold extraction systems (1 for each CyMe4BTBP, HydroBTBP, TODGA & PTD) [43] and can be summarised as follow:

- All studies performed until now point out towards SO_3-Ph-BTP aqueous phases show a better resistance against γ-irradiation when the irradiation takes place in contact with the organic phases (OK, TODGA in OK or TODGA-DMDOHEMA in OK). Besides, it seems that TODGA or TODGA-DMDOHEMA solvents could have a higher protector effect than kerosene over SO_3-Ph-BTP aqueous phase. In general, the extraction system keeps the performance around 200 kGy, a much higher accumulated doses than expected from our previous results [30].
- Besides, these results are independent of the atmosphere used and bubbled provides by an air sparging flow. Therefore, it would be the contact between phases and not the O_2 of the air-sparging which provides such protection over SO_3-Ph-BTP.
- The effects of the presence of AHA in the aqueous phases must be depth-studied for a better understanding of the full system and the design of strategies of study, since for example, when the aqueous phase contains AHA during the irradiation, An(III) seem to be better kept in the aqueous phase after irradiation and a reduction An/Ln SF is observed due to a decrease of D_{Eu}. These results can be mainly explained due to the AHA hydrolysis reaction in acid media to form NH_2OHNO_3 and the

This project has received funding from the EURATOM research and training programme 2014–2018 under grant agreement No. 755171. The content of this deliverable reflects only the authors' view. The European Commission is not responsible for any use that may be made of the information it contains.

corresponding increase of pH [44, 45]. Besides, studies included in D2.1 corroborated a higher remaining concentration of SO_3-Ph-BTP after irradiation when it takes place in presence of AHA.

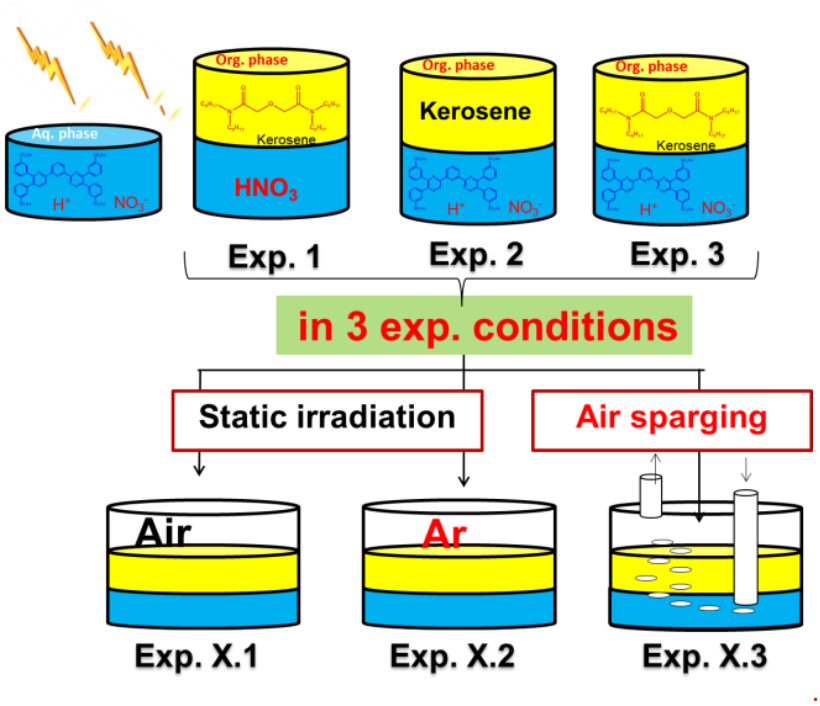

Figure 2. Schematic representation of irradiation performed experiments for TODGA/SO_3-Ph-BTP system.

Following the strategy showed in Figure 2 for TODGA/SO_3-Ph-BTP systems, the results about the effects over organic phase can be summarised as follow: An and Ln extraction properties were kept, but in the case of experiments performed in presence of air flow sparging, TODGA concentration decreased to 70% of the initial concentration after 500 kGy, meanwhile for experiments performed under air and Argon atmosphere where phases were not mixed, just contacted, the concentration decreased to 50%. Besides, only when an air flow is used to mix the organic and aqueous phases during the irradiation, a different proportion of TODGA DCs was found and new possible DCs were identified, pointing out to a change in the degradation pathway [46]. Hence, from the point of view of TODGA-based solvent, Euro-GANEX stability studies should be performed by simulating both phases contact by increasing contact between them with air sparging methods.

The same methodology has been also applied to study TODGA-DMDOHEMA / AHA-SO_3PhBTP system, performing in parallel experiments with and without DMDOHEMA but also with and without AHA. The composition of different samples studied during the corresponding irradiation (200 and 500 kGy) and extraction experiments are summarised in Table 2. System_1 and system_2 correspond to studies performed in absence and presence of AHA during irradiation respectively, where it has been also considered the presence and absence of TODGA+DMDOHEMA and SO_3PhBTP.

This project has received funding from the EURATOM research and training programme 2014–2018 under grant agreement No. 755171. The content of this deliverable reflects only the authors' view. The European Commission is not responsible for any use that may be made of the information it contains.

Table 1. Composition of the organic and aqueous phases (System 1 and 2): a) during irradiation up to 200 and 500 kGy. The concentrations are: 0.2 mol/L TODGA, 0.5 mol/L DMDOHEMA, 0.5 mol/L HNO_3, 0.018 mol/L SO_3-Ph-BTP and 1 mol/L AHA.

System 1	Phases	Irradiation experiment		Extraction experiment	
System 1_1	Org.	OK TODGA DMDOHEMA	IRR	OK TODGA DMDOHEMA	IRR
	Aq.	HNO_3 - -	IRR	HNO_3 SO_3-Ph-BTP -	FRESH
System 1_2	Org.	- - OK	IRR	OK TODGA DMDOHEMA	FRESH
	Aq.	HNO_3 SO_3-Ph-BTP -	IRR	HNO_3 SO_3-Ph-BTP -	IRR
System 1_3	Org.	OK TODGA DMDOHEMA	IRR	OK TODGA DMDOHEMA	IRR
	Aq.	HNO_3 SO_3-Ph-BTP -	IRR	HNO_3 SO_3-Ph-BTP -	IRR

System 2	Phases	Irradiation experiment		Extraction experiment	
System 2_1	Org.	OK TODGA DMDOHEMA	IRR	OK TODGA DMDOHEMA	IRR
	Aq.	HNO_3 - AHA	IRR	HNO_3 SO_3-Ph-BTP AHA	FRESH
System 2_2	Org.	OK - -	IRR	OK TODGA DMDOHEMA	FRESH
	Aq.	HNO_3 SO_3-Ph-BTP AHA	IRR	HNO_3 SO_3-Ph-BTP AHA	IRR
System 2_3	Org.	OK TODGA DMDOHEMA	IRR	OK TODGA DMDOHEMA	IRR
	Aq.	HNO_3 BTP AHA	IRR	HNO_3 BTP AHA	IRR

Figure 3 a) shows the fresh and irradiated samples containing kerosene as org. phase and SO_3PhBTP in HNO_3 with and without AHA as aqueous phase (System 1.2 and 2.2 in Table 1). And, Figure 3 b) shows the fresh and irradiated Euro-GANEX samples containing TODGA-DMDOHEMA in kerosene as org. phase and SO_3PhBTP in HNO_3 with and without AHA as aqueous phase (System 1.3 and System 2.3). On the one hand, as it can be seen in Figure 3, SO_3PhBTP aq. phase gets a darkness colour when irradiation is done in presence of AHA, pointing out towards a higher degradation or oxidation of SO_3PhBTP in HNO_3. However, in absence of AHA (system 1.2) a third phase formation occurred after irradiation but not in system 2.2 where AHA was added. On the other hand, after the irradiation of the full Euro-GANEX systems (system 1.3 and system 2.3) it can be seen that AHA presence does not give place to a darkening of aq. phase and avoid again the third phase formation after irradiation, but also avoids changes of colours in the organic phase.

This project has received funding from the EURATOM research and training programme 2014–2018 under grant agreement No. 755171. The content of this deliverable reflects only the authors' view. The European Commission is not responsible for any use that may be made of the information it contains.

a) *System 1.2 and System 2.2*

Organic: kerosene (OK)
Aqueous: 0.018 mol/L SO_3PhBTP in 0.5 mol/L HNO_3 with and without AHA

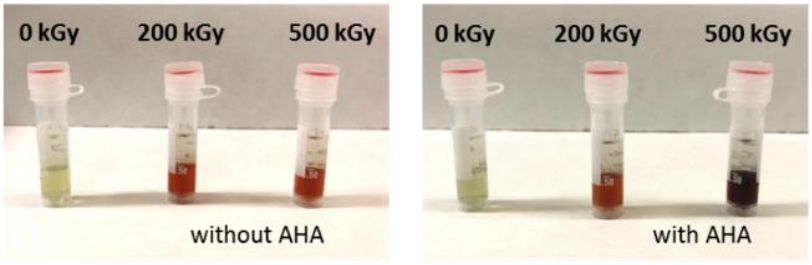

b) *System 1.3 and System 2.3*

Organic: 0.2 mol/L TODGA 0.5 mol/L DMDOHEMA in OK
Aqueous: 0.018 mol/L SO_3PhBTP in 0.5 mol/L HNO_3 with and without AHA

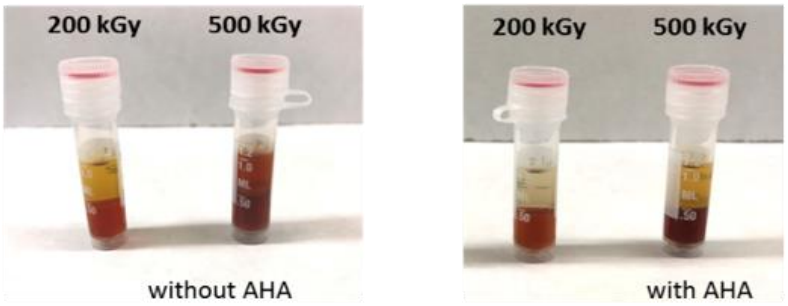

Figure 3. a) Fresh and irradiated aqueous phases of Euro-GANEX system with and without AHA (system 1.2 and 2.2 in Table 1) in contact with kerosene. b) Irradiated Euro-GANEX system, organic + aqueous phases, with and without AHA (system 1.3 and 2.3 in Table 1).

The extraction behaviour of the different samples was analysed by comparing the D_{Am} and D_{Eu} values obtained. Figure 4 shows Am(III) and Eu(III) extraction by TODGA-DMDOHEMA/ SO_3PhBTP-AHA systems studied as it shown Table 1. As it was done in previous studies, for a real comparison of the extraction experiments and D_M values obtained, aqueous phases consisting in 0.5 mol/L HNO_3 or 1 mol/L AHA in 0.5 mol/L HNO_3 were replaced for the corresponding fresh aqueous phase indicated in Table 1; as well as, organic phases consisting in kerosene during irradiation were replaced by 0.2 mol/L TODGA + 0.5 mol/L DMDOHEMA in OK for the extraction experiments (see Table 1).

Figure 4a shows the extraction capacity after irradiation of samples corresponding to *System* 1_1 and *System* 2_1, it means, SO_3-Ph-BTP is not present in the aqueous phase during the irradiation. Therefore, since the irradiated organic phase is the same for both experiments, the differences observed for Eu and Am distribution ratio should be explained only because of the presence or absence of AHA during the irradiation.

Figure 4b shows the extraction capacity after irradiation of samples corresponding to *System* 1_2 and *System* 2_2, it means, SO_3-Ph-BTP or AHA-SO_3-Ph-BTP in nitric acid irradiated in presence of kerosene. After 200 kGy, we can see that after irradiation of OK/SO_3-Ph-BTP, D_{Am} does not show the same stabilization on the performance previously observed and reported for TODGA/ SO_3-Ph-BTP system. These distribution ratios can be explained because TODGA-DMDOHEMA solvent formulation has a higher Am extraction capacity than TODGA solvent and the reduction in SO_3-Ph-BTP concentration are more perceived. For the same experiment containing AHA in the

This project has received funding from the EURATOM research and training programme 2014–2018 under grant agreement No. 755171. The content of this deliverable reflects only the authors' view. The European Commission is not responsible for any use that may be made of the information it contains.

aqueous phase (*System* 2_2) a completely different situation was observed, D_{Am} increases slightly as function of dose and D_{Eu} decrease. The higher D_{Am} could be explained by a higher stabilization of SO_3-Ph-BTP in presence of AHA, but as long as similar behaviour of D_{Eu} was observed for *System* 2_1 (Figure 4a), where the aqueous phase containing SO_3-Ph-BTP-AHA used for the extraction was not irradiated, a mixture of effects is taking place. Therefore, factors like AHA hydrolysis in acidic media have to also be considered to evaluate these results.

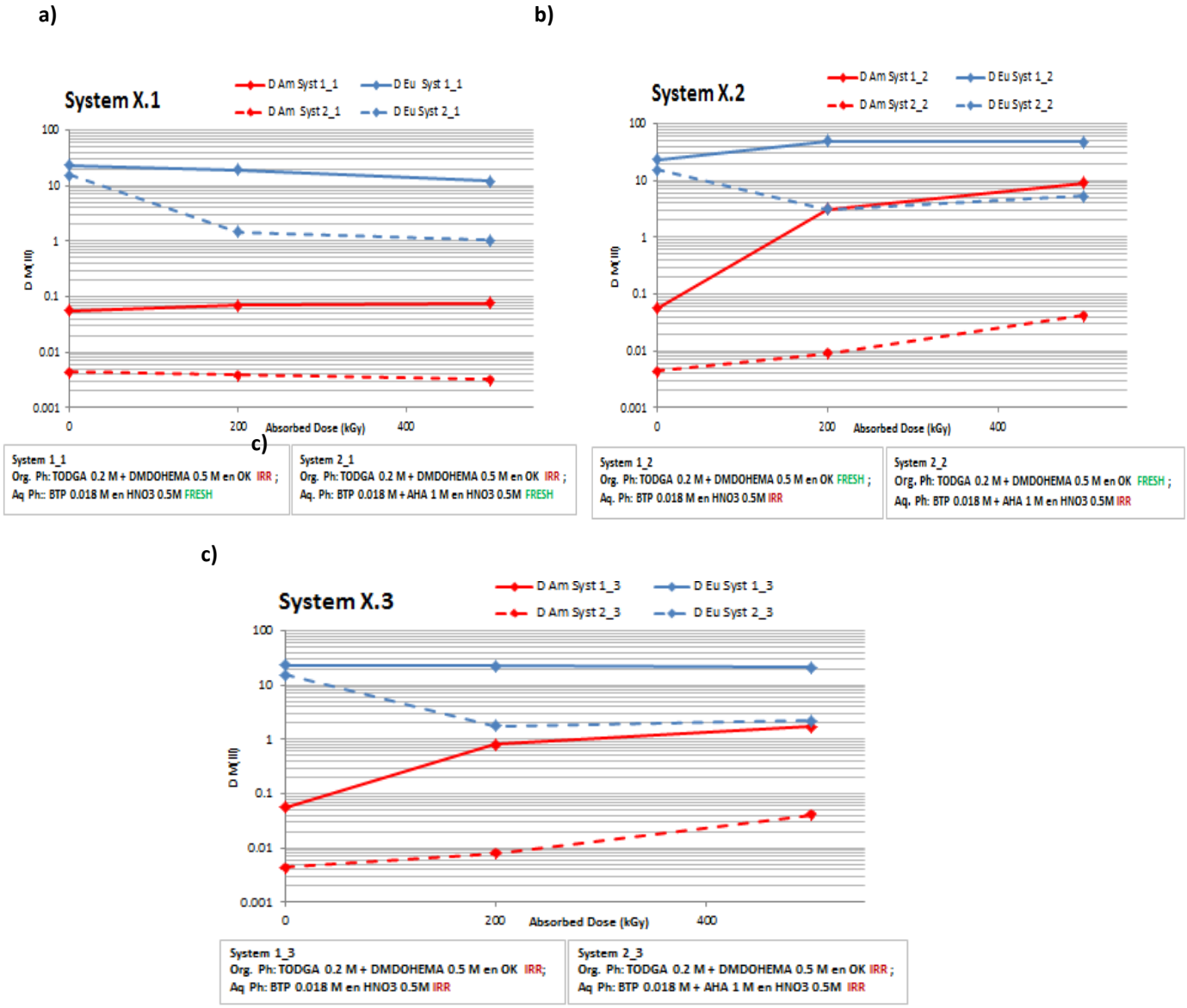

Figure 4. Am(III) and Eu(III) extraction by TODGA-DMDOHEMA/ SO_3PhBTP-AHA systems irradiated as it shown Table 2. Spiked with ^{241}Am(III) + ^{152}Eu(III) (1000 Bq each).

Figure 4c shows the extraction capacity after the irradiation of samples corresponding to *System* 1_3 and *System* 2_3. In this case, both phases were irradiated together and have not been replaced for the extraction experiments. Once again, the presence of AHA (*System* 2_3) gives place to different D_{Eu} and D_{Am} values that only can be explained of a mixture of different factors that have to be studied in more detail.

This project has received funding from the EURATOM research and training programme 2014–2018 under grant agreement No. 755171. The content of this deliverable reflects only the authors' view. The European Commission is not responsible for any use that may be made of the information it contains.

It can be said that *System* 1_3 (TODGA-DMDOHEMA/SO_3-Ph-BTP, Figure 4c) shows a similar trend than observed for TODGA/SO_3-Ph-BTP system [41]. Extraction systems keep better the performance after irradiation as function of the organic phase in contact (no-organic-phase < Ok < TODGA-DMDOHEMA). Therefore, all data obtained until now point out toward it is the contact between phases and not the O_2 which provides such protection. Nevertheless, for a better understanding of all factors involved, quantitative studies about the composition of both phases are needed.

First, it was full characterized the degraded organic phases. Quantification by HPLC-MS of remaining TODGA and DMDOHEMA concentrations in organic phases is summarised in Figure 5. TODGA and DMDOHEMA concentration decreases as function of dose as it can be expected, without any relevant difference between systems studied. Therefore, the variation of the performance previously observed should be attributed only to different SO_3-Ph-BTP remaining concentration or the presence of AHA.

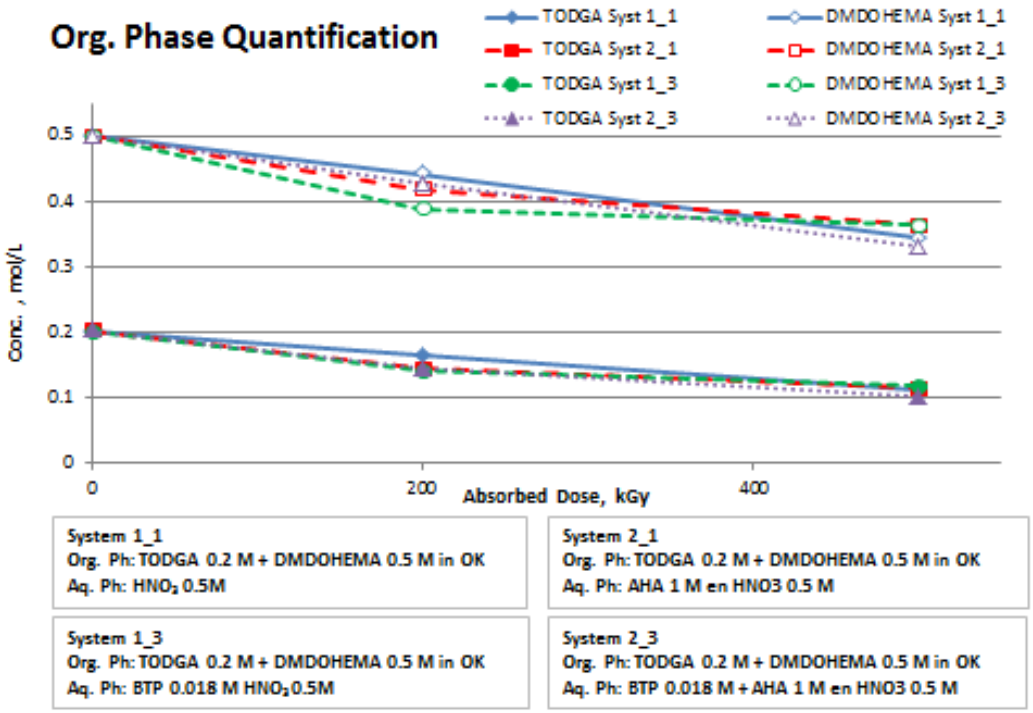

Figure 5. TODGA and DMDOHEMA concentration in the organic phase of System 1 (Systems 1_1 and 1_3) and System 2 (Systems 2_1 and 2_3) after irradiation experiments.

Figure 5 shows the qualitative analysis by HPLC-MS of fresh and irradiated Euro-GANEX solvents under the different irradiation conditions: in presence of HNO_3 (system 1_1); in presence of HNO_3 and AHA (system 2_1); in presence of HNO_3 and BTP (system 1_3); and in presence of HNO_3, BTP and AHA (system 2_3). As expected, the same 9 DCs from TODGA and 4 from DMDOHEMA have been found after irradiation, in agreement with previous works [23]. Their structures are presented in Figure 7. Once again, DC proportion points out to it is not the presence of different aqueous phases which modified degradation pathways, but the oxygen amount [46].

This project has received funding from the EURATOM research and training programme 2014–2018 under grant agreement No. 755171. The content of this deliverable reflects only the authors' view. The European Commission is not responsible for any use that may be made of the information it contains.

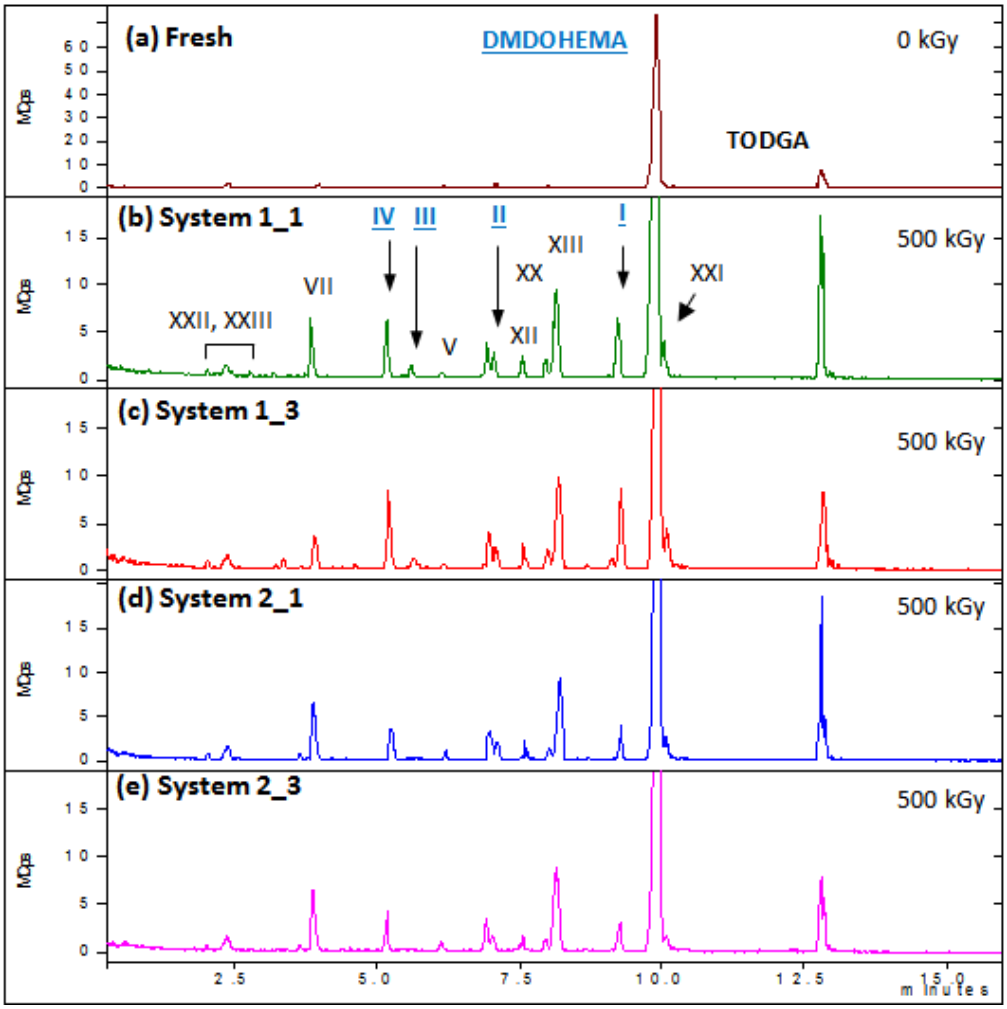

Figure 6. HPLC-MS chromatograms of fresh and irradiated Euro-GANEX solvent: a) fresh solvent as reference material, b) 500 kGy in presence of HNO_3 (system 1_1); 500kGy in presence of HNO_3 and BTP (system 1_3); 500 kGy in presence of HNO_3 and AHA (system 2_1); and 500 kGy in presence of HNO_3, BTP and AHA (system 2_3).

Only the main TODGA DCs were quantified due to those DMDOHEMA DCs are not available yet. Figure 8 shows the quantification of main TODGA DCs formed (DCs: V, VII, XII, XIII, XX and XXI) up to 200 and 500 kGy and under all conditions studied (system 1_1, 1_3, 2_1 and 2_3, see Table 1). In general, the rupture of weakest bonds of TODGA (C-O and N-C) gives place to DCs XII, XIII and XXI or VII and their proportion do not change drastically despite the different aqueous phases in contact.

If we compare the results in absence of AHA, it means HNO_3 with or without BTP (system 1_1 and system 1_3), a slight increase in the concentration of most of the DCs except VII is observed. And, if we compare the irradiations in absence of BTP, it means HNO_3 with or without AHA (system 1_1 versus system 2_1), the main difference is the decrease in XXI concentration. These two results agree with the result obtained for the full system (system 2_3: TODGA-DMDOHEMA/SO_3-Ph-BTP-AHA). Although some of these DCs show Ln and An extraction properties, at 0.5 mol/L HNO_3 only DC XXI is able to extract them [37]. Therefore, the extraction behaviour observed after 500 kGy could be attributed to changes in the concentration of extractants of both

This project has received funding from the EURATOM research and training programme 2014–2018 under grant agreement No. 755171. The content of this deliverable reflects only the authors' view. The European Commission is not responsible for any use that may be made of the information it contains.

phases; however, after a 200 kGy, it should be only attributed to change in the composition of the aqueous SO_3-Ph-BTP or AHA, since the concentration of DCs are not still significant.

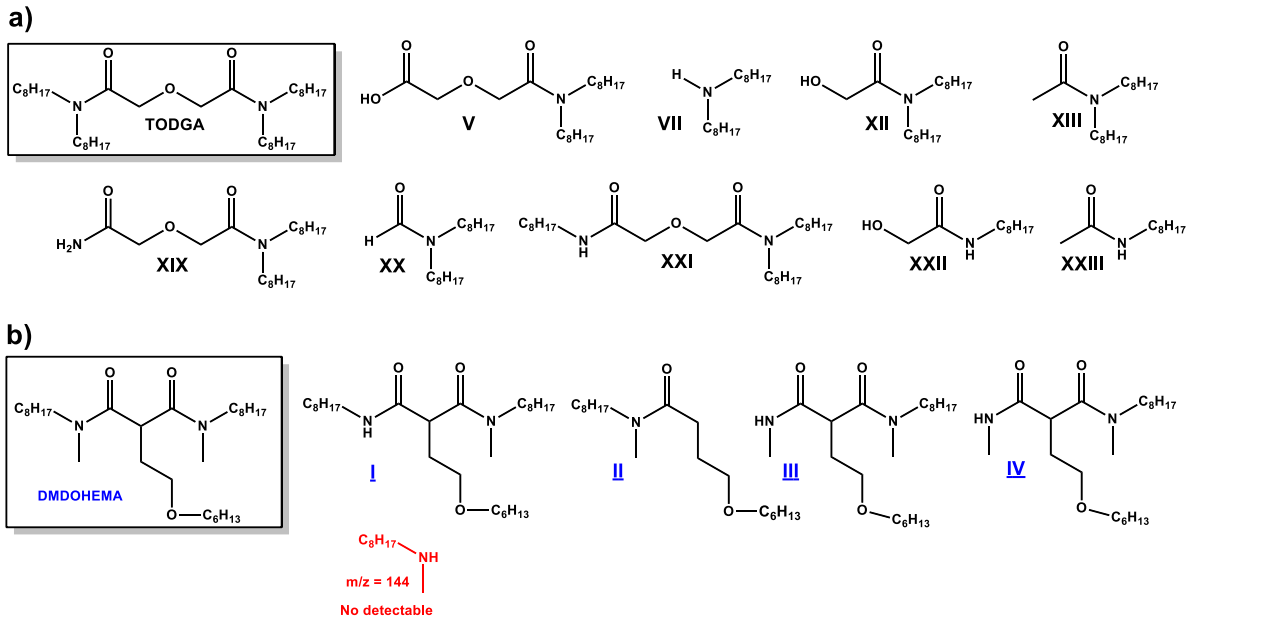

Figure 7. Structures of (a) TODGA and its main radiolytic degradation products [23-26] and (b) DMDOHEMA and its main radiolytic degradation products [27-29].

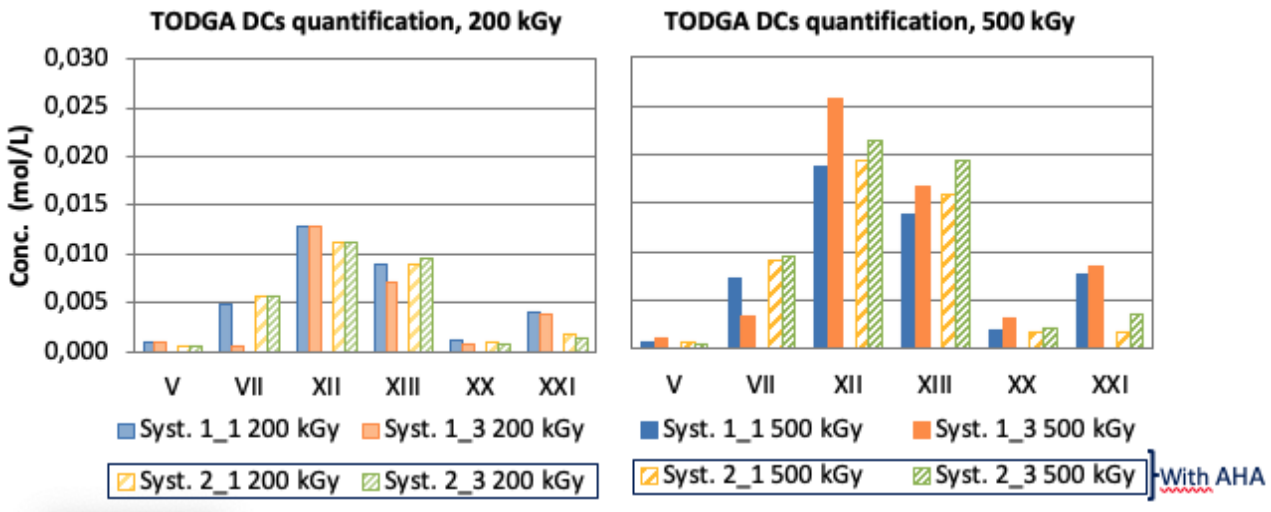

Figure 8. HPLC-MS quantitative studies of different TODGA degradation compounds for the different irradiation conditions of Euro-GANEX solvent: in presence of HNO_3 (system 1_1); in presence of HNO_3 and BTP (system 1_3); in presence of HNO_3 and AHA (system 2_1); and in presence of HNO_3, BTP and AHA (system 2_3).

Regarding the composition of the aqueous phase, it is known that AHA hydrolysis is catalyzed in acidic media giving place to acetic acid (AcOH) and hydroxylamine (HA), being kinetically insignificant in neutral media. The half-live of AHA in nitric acid solutions is enough for the residence time of centrifugal contactors. Although the

This project has received funding from the EURATOM research and training programme 2014–2018 under grant agreement No. 755171. The content of this deliverable reflects only the authors' view. The European Commission is not responsible for any use that may be made of the information it contains.

irradiation time depends on dose rate applied, most of irradiation experiments take more than 24 hours. Therefore, to understand what is happening in the aqueous phase and the D values obtained it has been evaluated the concentration of AHA as a function of time. In the moment these experiments were carried out, to quantify AHA concentration it was followed the methodology described to measurement by UV-vis the Fe(III)-AHA complex absorption around 500 nm [47], currently it has been developed a quantitative Raman methodology [44, 45]. Figure 9a shows the AHA concentration as a function of time for both aqueous phases, AHA in nitric acid and AHA + BTP in nitric acid. Although it can be observed slight differences between the two systems, the general trend is similar. After 24 h, the systems reach a steady stage, where the reduction of AHA concentration is far from being negligible and it must be considered for the understanding of stability studies. Besides, products from AHA hydrolysis could be transfer to the organic phase or modified the pH of the aq. phase. Once hydroxylamine is formed, it acts as a base ($NH_2OH + HNO_3 \rightarrow NHOHNO_3$) increasing the pH of the solution (Figure 9b). That result corroborate that all D values obtained from stability studies of systems containing AHA in the aqueous phase are strongly affected by pH, and the extraction behaviour cannot be used as an approach of the degradation of the aqueous phase.

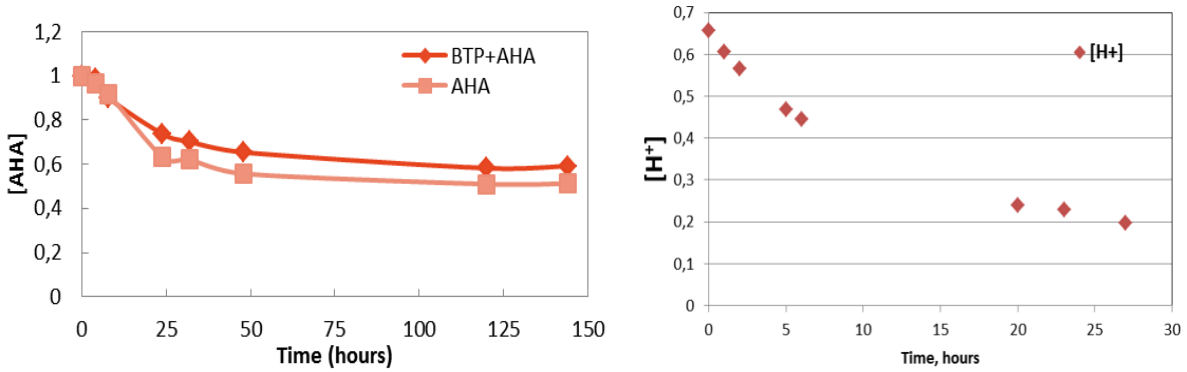

Figure 9. a) Concentrations obtained of AHA in the AHA hydrolysis process by UV-Vis; b) Proton concentration as a function of hydrolysis time of AHA (1 mol/L) in 0.5 mol/L HNO_3.

In the moment these experiments were performed, the methodology to quantify SO_3-Ph-BTP by Raman spectroscopy was not available. Therefore, for those samples without AHA in the aqueous phase (system 1_2 and system 1_3, Table 1) it has been estimated the remaining SO_3-Ph-BTP concentration as function of the dose assuming degradation products do not interfere in the extraction and taking into account the dependency of Am(III) distribution ratios on the concentration of SO_3-Ph-BTP as reported in [48]. Figure 10a shows the linear dependence of D_{Am} by the corresponding organic solvent, TODGA-DMDOHEMA in OK as a function of SO_3-Ph-BTP concentration in the aqueous phase. This linear correlation has been used for estimating the remaining SO_3-Ph-BTP concentration of system 1_2 and system 1_3. Figure 10b shows the estimated concentration of SO_3-Ph-BTP for system 1_2 and system 1_3. These data revealed an important reduction in BTP concentration after 200 kGy.

This project has received funding from the EURATOM research and training programme 2014–2018 under grant agreement No. 755171. The content of this deliverable reflects only the authors' view. The European Commission is not responsible for any use that may be made of the information it contains.

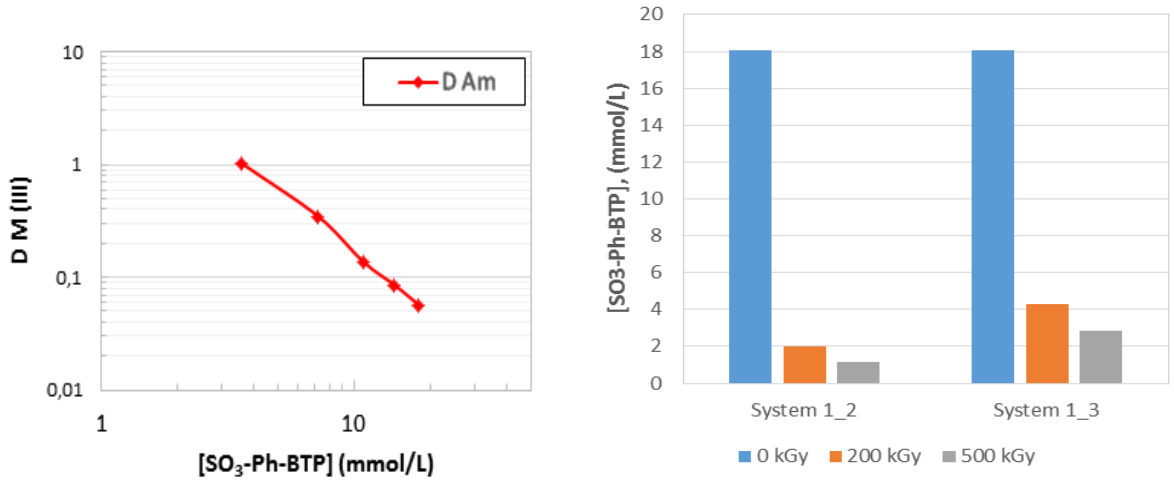

Figure 10. a) Am(III) distribution ratios of TODGA-DMDOHEMA/SO_3-Ph-BTP system as a function of SO_3-Ph-BTP concentration in the aqueous phase. Organic: 0.2 mol/L TODGA and 0.5 mol/L DMDOHEMA in OK; Aqueous: 0-18 mmol/L SO_3-Ph-BTP in 0.5 mol/L HNO_3; b) Estimated SO_3-Ph-BTP concentration as a function of dose (0-500 kGy) and the organic phase in contact for different irradiated systems: system 1_2, 18 mmol/L SO_3-Ph-BTP in 0.5 mol/L HNO_3 in contact with OK; system 1_3, 18 mmol/L SO_3-Ph-BTP in 0.5 mol/L HNO_3 in contact with 0.2 mol/L TODGA and 0.5 mol/L DMDOHEMA in OK.

This project has received funding from the EURATOM research and training programme 2014–2018 under grant agreement No. 755171. The content of this deliverable reflects only the authors' view. The European Commission is not responsible for any use that may be made of the information it contains.

IRRADATION LOOP TESTS OF EURO-GANEX PROCESS

Authors: Iván Sánchez-García, Hitos Galán, Ana Núñez, Lorena Serrano and Sofía Durán (CIEMAT).

IRRADIATION LOOP DESIGN AT NÁYADE FACILITY OF CIEMAT

During the GENIORS project, it has been designed, manufactured and set up an irradiation loop at Náyade facility of CIEMAT. The objective of the Náyade irradiation loop is to provide the possibility to perform very simple test by performing dynamic irradiation experiments where some of the most important relevant process conditions are considered. The design developed allows an easy modification of experiments and running with relatively low volumes, taking into account the different dose expected for each process steps and phases since process are simulated step by step.

The Náyade irradiation facility consists of a pool of a 1.2 m^2 by 4.5 m deep that uses water as the biological shield. At the bottom of the pool, 60 sources of ^{60}Co (15 mm diam. x 135 mm long each) with a total activity of $1.1 \cdot 10^{14}$ Bq can be distributed in six lots. The cylindrical irradiation container used provides homogeneous irradiation flux within a 60 mm diam. x 100 mm high volume.

Between the different loop designs explored, and reported in CIEMAT HYPARs, the chosen one implies the mixing of the two phases outside the Náyade pool and the introduction of them as a homogeneous mixture in the irradiation zone to be irradiated together. With this aim, the irradiations in dynamic conditions can be carried out by using two peristaltic pumps located outside of the pool (one per each phase) pumping the phases in a container. Them, both phases are mixed thanks to a T connection and pumped to the irradiation reactor inside of the Náyade pool. Different design of irradiation reactors have also been consider, but the coil shape reactor was chosen because to improve the irradiation of two phases in contact (see [49-53] and Figure 11).

The materials used for the loop must be resistant to the different conditions employed, *i.e.* contact with diluent as kerosene, nitric acid and submitted to gamma radiation. Therefore, several materials for the tubing and reactor were tested under the experimental conditions. For tubing, VITON Iso-Versinic tube has passed all resistance test and it was chosen for the experiments. For reactor materials, glass and stainless steel were chosen such material capable to resist all conditions mentioned above. The connections between the tubing and reactor was also evaluated using different materials such as plastic and stainless steel connections. Using plastic connections with the glass reactors, it was concluded that it should be checked frequently and could be a point where the system fails. Therefore a 316 stainless steel reactor (11 cm length, 10 mm outside and 8 mm inner diameters) with a screw cap of the same stainless steel for connecting the reactor with the tubing was chosen to carry out different dynamic experiments, as close as possible to a real process, considering that centrifugal contactors are made of stainless steel material. The reactor in the Náyade pool has to be inside irradiation device, which was designed and manufactured at CIEMAT and allows to introduce the tubing but it avoids the water entry. The final scheme of the irradiation loop device developed at CIEMAT is shown in Figure 11.

Following the designs described in Figure 11, it has been calculated the total volumes and residence time to estimate the absorbed dose. The minimum volume necessary per phase is 135 mL, with a residence time in the irradiation reactor of 4.95 min per hour of experiment. For that reason, it was decided to apply a higher dose rate (^{60}Co sources, 44.72 kGy/h) to be able to reach moderate high integrated dose and minimise the duration of the experiment. It is important to note that stainless steel shield a fraction of the gamma radiation. Therefore, in order to know the effective dose rate provided by ^{60}Co sources inside of the irradiation reactor, a Fricke

This project has received funding from the EURATOM research and training programme 2014–2018 under grant agreement No. 755171. The content of this deliverable reflects only the authors' view. The European Commission is not responsible for any use that may be made of the information it contains.

dosimetry using a shielding of stainless steel with the same thickness than the reactor was carried out resulting in 35.11 kGy/h. As for the test loop the phases are in continuous movement, only a fraction of the total solution (1:1 organic/aqueous phase) resides inside of the coil. During the running loop test, the flow rate was adjusted to maintain the volume ratio in the range of 0.31 L/h. Then, knowing the dose rate and taking into account the coil volume and phase residence time, the total effective dose rate is 2.89 kGy/h. The final system is shown in Figure 12.

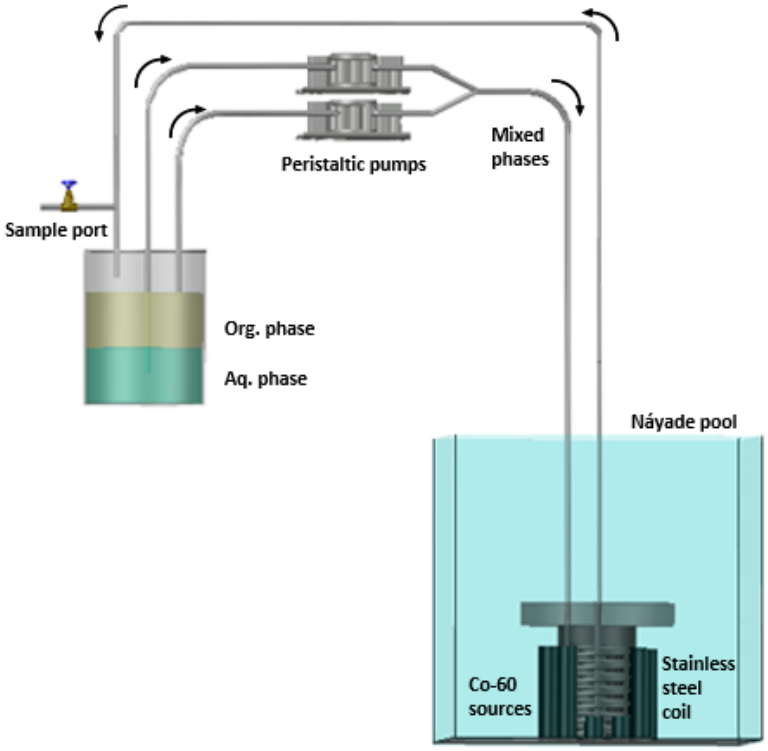

Figure 11 Schematic diagram of the irradiation test loop developed at CIEMAT.

Figure 12. Irradiation loop developed at CIEMAT.

This project has received funding from the EURATOM research and training programme 2014–2018 under grant agreement No. 755171. The content of this deliverable reflects only the authors' view. The European Commission is not responsible for any use that may be made of the information it contains.

FIRST EURO-GANEX LOOP TEST IN NÁYADE IRRADIATION FACILTY

Using the irradiation loop device described in previous section, a dynamic irradiation (loop test) was performed to simulate and study the effects over the main EURO-GANEX process steps: the lanthanide (Ln) and actinide (An) co-extraction follows-up the transuranic (TRU) stripping.

To simulate the most relevant aspects of the main EURO-GANEX steps, and based on all previous studies about the resistance of the organic and aqueous phases involved [30, 39, 41, 46], , the design of the loop should involve the irradiation of two phases in contact, taking into account their full solvent formulation, the nitric acid concentration, the renewal of oxygen content and the dose expected for each phase. With this purpose, the organic and aqueous phases is always mixed under an open atmosphere outside of the irradiator device and irradiated together inside of the irradiator reactor (coil). Considering that the organic phase will be recycled as much as possible, it will be simulated its degradation after high doses (up to around 500 kGy); however, as it is not expected the recycling of aqueous phases, the aqueous phases containing the stripping agent will not be submitted to high doses [8]. For that, two solvent systems will be irradiated, one for An + Ln co-extraction step and other for TRU stripping step (Figure 13).

In the first step, the EURO-GANEX solvent consisting of 0.2 mol/L TODGA and 0.5 mol/L DMDOHEMA in OK in contact with 5 mol/L HNO_3 was irradiated up to 500 kGy. The purpose of this irradiation is to simulate the effects over the organic phase after many cycles of extraction. CDTA was not included in the aqueous phase since the degradation of CDTA in this step has no relevance regarding Ln and An co-extraction (see previous sections) and the doses studied are very high compared with those expected for the aqueous phase, which will be always used as fresh solution.

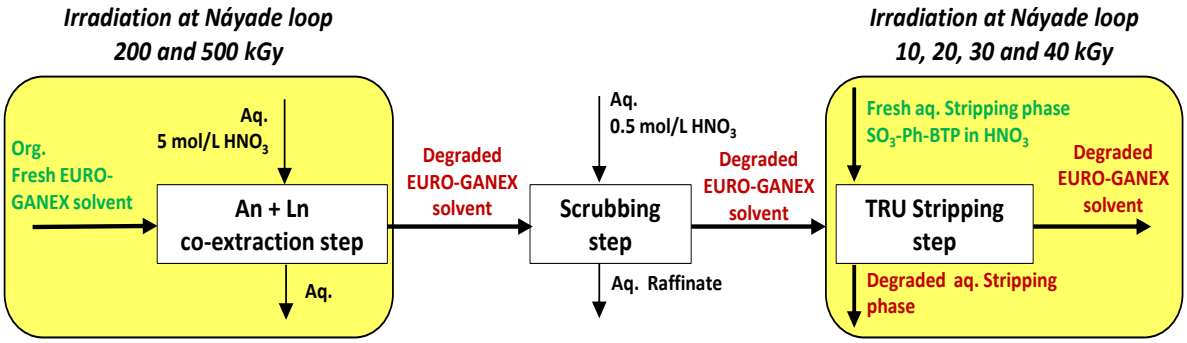

Figure 13 Scheme of the main steps of EURO-GANEX simulated by the irradiation test loop at CIEMAT.

The second system represents the stripping conditions step, and for that, the irradiated organic phase of the first system (0.2 mol/L TODGA and 0.5 mol/L DMDOHEMA in OK) was submitted to radiation again up to additional 40 kGy, but this time in contact with an aqueous phase consisting of 0.018 mol/L SO_3-Ph-BTP in 0.5 mol/L HNO_3, it is main, up to 540 kGy for organic phase and 40 kGy for the aqueous phase. Although the presence of AHA seems to increase the resistance of SO_3-Ph-BTP aqueous phases [39], it was not included in the irradiation experiment to prevent the effect of AHA hydrolysis over the extraction capacity of Ln. Based in our last works [44], AHA hydrolysis produces a $D_{Ln(III)}$ decrease as a function of AHA hydrolysis time far from negligible after 2 h. Between the two main irradiations steps described, a scrubbing step with a diluted nitric acid (0.5 mol/L) was introduced, which pretends the removal of other elements as FP co-extracted and adjust the acidity for the next

This project has received funding from the EURATOM research and training programme 2014–2018 under grant agreement No. 755171. The content of this deliverable reflects only the authors' view. The European Commission is not responsible for any use that may be made of the information it contains.

step. Figure 13 shows the scheme of the main steps of EURO-GANEX simulated by the irradiation test loop at CIEMAT.

After the two different irradiations steps it was evaluated the behaviour of the systems by performing the corresponding extraction experiments. For the An+Ln co-extraction step, the aqueous phase consisting in 5 mol/L HNO_3 used in the irradiation process was replaced by fresh 0.055 mol/L CDTA + 10%$_{vol}$ of HAR solution in 5 mol/L HNO_3 spiked with ^{241}Am and ^{152}Eu aqueous samples. For the TRU stripping step, none of the phases was changed, and the samples were spiked with ^{241}Am and ^{152}Eu to perform the extraction experiments. The composition of the organic and aqueous phases of the different steps is summarised in the Table 2.

Table 2 Composition of the organic and aqueous phases of the different steps in the irradiation test loop.

	Experiments	Solvent formulation	
		Organic phase	Aqueous phase
An+Ln co-extraction Step	a) Irradiation	**Fesh EURO-GANEX solvent** 0.2 mol/L TODGA + 0.5 mol/L DMDOHEMA in OK	**FRESH** * 5 mol/L HNO_3
	b) Extraction after the 1st irradiation	**Irradiated EURO-GANEX solvent (200, 500 kGy)** TODGA +DMDOHEMA in OK	**FRESH** 0.055 mol/L CDTA + 10 %vol HAR in 5 mol/L HNO_3
Scrubbing Step	Intermediate step between irradiations	**Irradiated EURO-GANEX solvent from the previous step (500 kGy)** TODGA +DMDOHEMA in OK	**FRESH** 0.5 mol/L HNO_3
TRU stripping Step	a) Irradiation	**Irradiated EURO-GANEX solvent from the previous step (500 kGy) + scrubbing** TODGA +DMDOHEMA in OK	**FRESH**** 0.018 mol/L SO_3-Ph-BTP in 0.5 mol/L HNO_3
	b) Extraction after the 2nd irradiation	**Irradiated EURO-GANEX solvent from the second step (540 kGy)** TODGA +DMDOHEMA in OK	**IRR (10-40 kGy)**** SO_3-Ph-BTP in 0.5 mol/L HNO_3

* CDTA is not relevant for the extraction of An and Ln in this step, for this reason it is not added during irradiation but it is in the extraction tests.
**No AHA presence

During the irradiation for the An+Ln co-extraction step, both phases suffer the typical colour changes. The organic phase varies from slightly yellow to dark yellow while the aqueous phase changes from colourless to slightly yellow, suggesting a radiolytic degradation of the solvent. The extraction behaviour observed for this step of the experiment, using CDTA and HAR solution in the aqueous phase, corroborate a normal phase separation without the formation of precipitates or third phase formation. The variation of D_{Am} and D_{Eu} values as a function of absorbed dose is shown in Figure 14. Both metals are well extracted into the organic phase although a slight decrease in both distribution ratios is observed. Still, the system is able to extract An and Ln even after a 500 kGy of absorbed dose with D>100 for both metals.

This project has received funding from the EURATOM research and training programme 2014–2018 under grant agreement No. 755171. The content of this deliverable reflects only the authors' view. The European Commission is not responsible for any use that may be made of the information it contains.

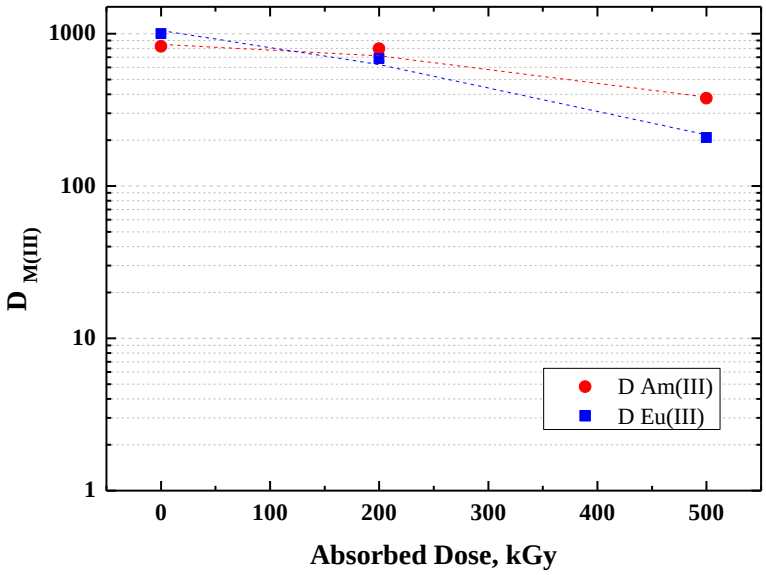

Figure 14. Distribution ratios of Am(III) and Eu(III) as a function of absorbed received dose during the first irradiation loop test of the An + Ln co-extraction step. Org. phase: Irradiated 0.2 mol/L TODGA and 0.5 mol/L DMDOHEMA in OK. Aq. Phase: Fresh 0.055 mol/L CDTA + 10%$_{vol}$ of HAR solution in 5 mol/L HNO_3 spiked with ^{241}Am and ^{152}Eu.

The variation of distribution ratios of FPs and lanthanides elements was measured by ICP-MS and it is represented as a function of absorbed dose in Figure 15. For a better comparison, experiments performed without CDTA presence have been also performed. The extraction behaviour of the irradiated and non-irradiated samples for most of the elements were unchanged, and Y and Ln showed high D values in all the cases (D > 100). The influence of the CDTA presence on the extraction of Zr and Pd is clearly observed with a significant decrease of the D_{Pd} and D_{Zr} reaching values of D < 0.01, in agreement with the literature [7, 8, 54], and this behaviour is not modified even if the organic phase is irradiated up to 500 kGy.

4 mol/L HNO_3			
Lanthanides		Fission products	
Elements	mg/L	Elements	mg/L
Ce	463	Ba	280
Eu	35	Cd	18
Gd	35	Cr	100
La	278	Cu	25
Nd	718	Mo	720
Pr	293	Ni	47.5
Sm	140	Pd	198
Y	108	Rb	68
--	--	Rh	73
--	--	Ru	408
--	--	Sn	10
--	--	Sr	180
--	--	Zr	958

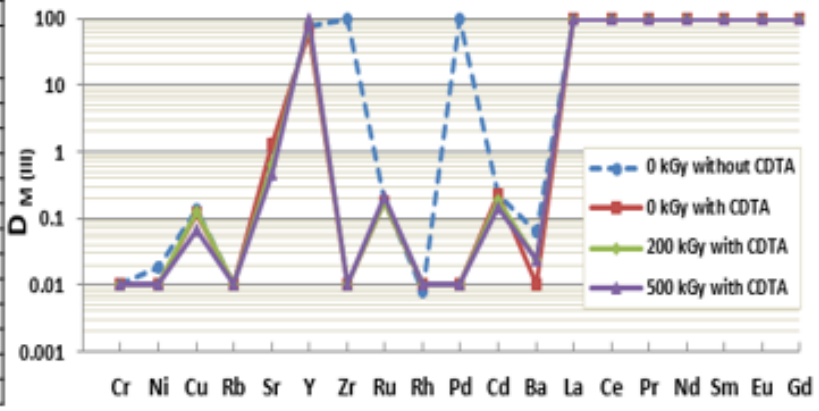

Figure 15 Ln and FP extraction by fresh and irradiated Euro-GANEX solvent (0.2 mol/L TODGA + 0.5 mol/L DMDOHEMA in OK) from 5 mol/L HNO_3 (without CDTA) and fresh 0.055 mol/L CDTA in 5 mol/L HNO_3. All aqueous phases contain 10%$_{vol}$ HAR solution.

As the reactor coil employed in the irradiation loop is made of 316 stainless steel, the possible corrosion products as a consequence of the contact with nitric acid and radiation has been studied by ICP-MS, concluding that Fe,

This project has received funding from the EURATOM research and training programme 2014–2018 under grant agreement No. 755171. The content of this deliverable reflects only the authors' view. The European Commission is not responsible for any use that may be made of the information it contains.

Cr, Ni and Mo are the most relevant stainless steel corrosion products. Figure 16 shows the evolution of their concentration in the organic and aqueous phases along the first irradiation step (An+Ln co-extraction). The concentration of all corrosion metals measured increases as a function of absorbed dose, being the most abundant Fe, Cr and Ni. Only Fe was mainly extracted into the organic phase with 2.54 mmol/L at 500 kGy, albeit there is a concentration of 0.34 mmol/L in the aqueous phase at the same absorbed dose. This is in agreement with Carrott *et al.,* [7], who explained that the main responsible of the Fe extraction is DMDOHEMA. Cr and Ni were kept in the aqueous phase reaching a concentration of 0.54 mmol/L and 0.31 mmol/L, respectively, at the highest absorbed dose (500 kGy), in agreement with Peterman *et al.,* [32] who reported ~0.30 mmol/L and ~0.36 mmol/L for Cr and Ni after ~550 kGy. Mo was found in concentrations lower than ~0.01 mmol/L in both phases.

As it was mentioned before, after the extraction and before the stripping step, it was necessary to introduce a scrubbing step with a diluted nitric acid (0.5 mol/L) (Figure 13), which still maintains the An+Ln co-extraction but is able to remove other elements co-extracted as FP or corrosion products. Figure 16 also shows the remaining concentration of corrosion products in the organic phase after 2nd scrubbing stage. The effectiveness of the scrubbing section to remove mainly Fe and Ni from the organic phase is observed, but not Cr and Mo, which remained in the organic phase in low concentration.

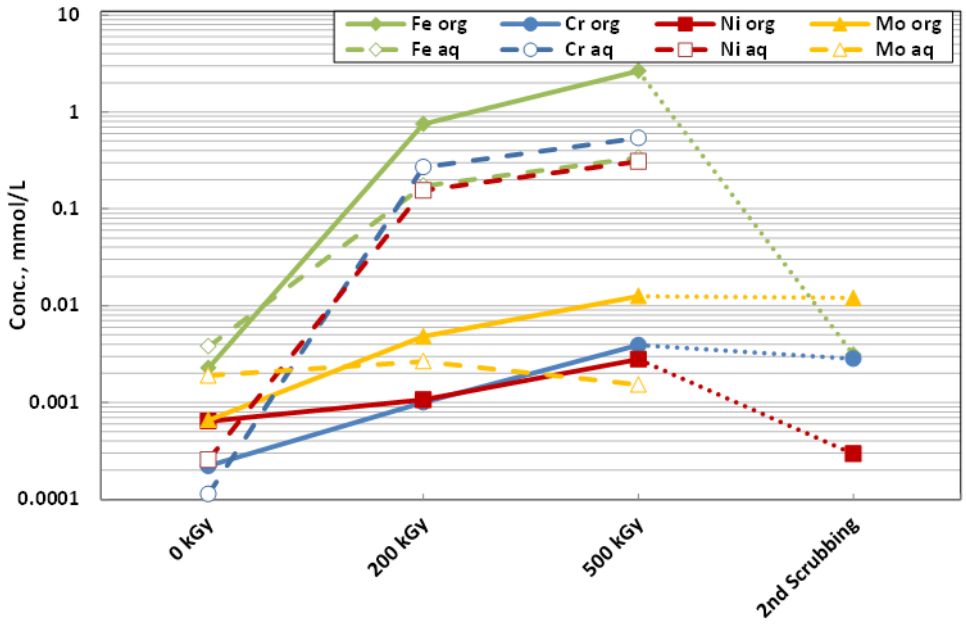

Figure 16 Evolution of the concentration of stainless steel corrosion products Fe, Cr, Ni and Mo during An+Ln co-extraction and scrubbing steps of EURO-GANEX irradiation loop.

The acid concentration of the aqueous phase along the steps studied was also checked. The proton concentration decreased from 4.65 mol/L for unirradiated HNO_3 to 3.78 mol/L for the irradiated at 500 kGy during the An+Ln co-extraction step. After the first scrubbing stage, the proton concentration was 0.89 mol/L, reaching 0.5 mol/L in the aqueous phase after the second scrubbing stage, which ensured the right acidity into the organic phase for the next TRU stripping step.

After simulating a long-term used organic phase (after 500 kGy), and the corresponding scrubbing step, the organic phase was again irradiated in contact with a new aqueous phase, consisting in 0.018 mol/L SO_3-Ph-BTP in 0.5 mol/L HNO_3, to simulate the possible effects over the global system during the TRU stripping (see Figure

This project has received funding from the EURATOM research and training programme 2014–2018 under grant agreement No. 755171. The content of this deliverable reflects only the authors' view. The European Commission is not responsible for any use that may be made of the information it contains.

13). This system was irradiated up to 10, 20, 30 and 40 additional kGy. AHA is not included in this part of the irradiation experiment to prevent its hydrolysis effect over the extraction capacity of Ln [44].

Over the course of the irradiation in the TRU stripping step, the aqueous phase consisting in SO_3-Ph-BTP darkened considerably changing its colour which is widely related to its radiolytic degradation [30, 32], from green in unirradiated samples to opaque black in irradiated samples (Figure 17).

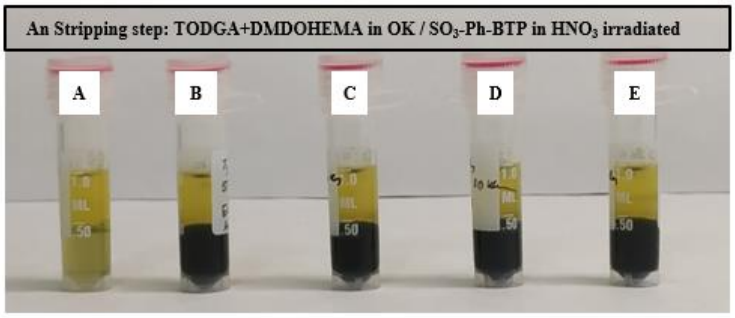

Figure 17 TRU stripping samples after different absorbed doses. Org. phase: 0.2 mol/L TODGA and 0.5 mol/L DMDOHEMA in OK irradiated at 540 kGy. Aq. phase: 0.018 mol/L SO_3-Ph-BTP in 0.5 mol/L HNO_3 irradiated at different doses: (A) 0 kGy, (B) 10 kGy, (C) 20 kGy, (D) 30 kGy and (E) 40 kGy.

The values of D_{Am} and D_{Eu} determined using samples taken from the TRU stripping test loop irradiation are presented in Figure 18. It can be observed an effect of radiolytic degradation from the first irradiation step (10 kGy), where the $D_{Am(III)}$ increase reaching values higher than 1, indicating Am is not kept in the aqueous phase and therefore is again extracted by the organic one. This means that the system loses the ability to keep the An in the aqueous phase, which is in disagreement with previous studies where the An and Ln separation was achieved up to 50 kGy in static [30], or 174 kGy in dynamic or loop test [32].

It is important to note that the first $D_{Am(III)}$ value at 0 kGy has already a high value close to 1, showing an inadequate stripping of americium in the aqueous phase by the SO_3-Ph-BTP even without radiation, which is an unexpected behaviour not observed until now.

This project has received funding from the EURATOM research and training programme 2014–2018 under grant agreement No. 755171. The content of this deliverable reflects only the authors' view. The European Commission is not responsible for any use that may be made of the information it contains.

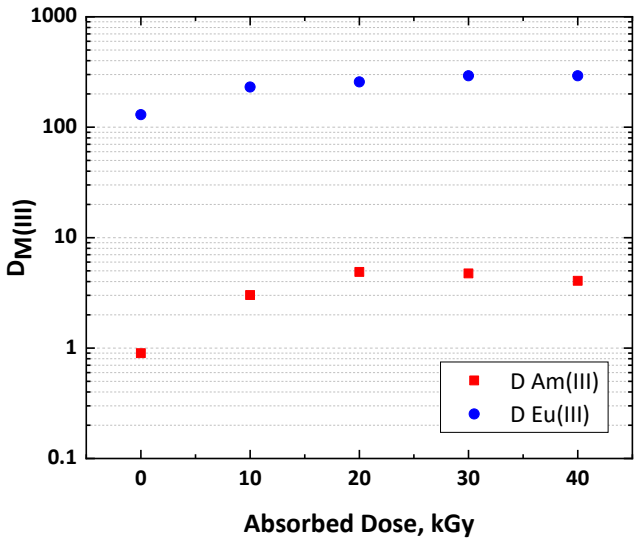

Figure 18 Distribution ratios of Am(III) and Eu(III) as a function of dose for the TRU stripping step system consisting of: Org. phase: 0.2 mol/L TODGA and 0.5 mol/L DMDOHEMA in OK irradiated at 540 kGy, and Aq. Phase: 0.018 mol/L SO_3-Ph-BTP in 0.5 mol/L HNO_3 irradiated at different doses.

For that reason, these results should not be related to the radiolytic degradation of SO_3-Ph-BTP, or not only, but also to other effects coming from the organic phase such as pH variations, corrosion metals presence or system composition variations.

The remaining concentration of corrosion metals coming from the organic phase will be added to those from the corrosions due to the new irradiation step and SO_3-Ph-BTP effect during the TRU stripping step irradiation. Figure 19 shows the evolution of their concentrations in the organic and aqueous phases along the TRU stripping step. As can be observed, the low doses applied did not produce a significant increase in corrosion metal concentration compared to the previous irradiation step. Contrary to the previous step, now Fe was found mostly in the aqueous phase, according to the study carried out by Carrott *et al.,* [7] where they reported that Fe is not extracted at low acid concentrations (up to 1 mol/L HNO_3) by the EURO-GANEX solvent. Cr and Ni were also found mainly in the aqueous phase, however, Mo was kept principally in the organic phase at a low concentration (0.01 mmol/L).

This project has received funding from the EURATOM research and training programme 2014–2018 under grant agreement No. 755171. The content of this deliverable reflects only the authors' view. The European Commission is not responsible for any use that may be made of the information it contains.

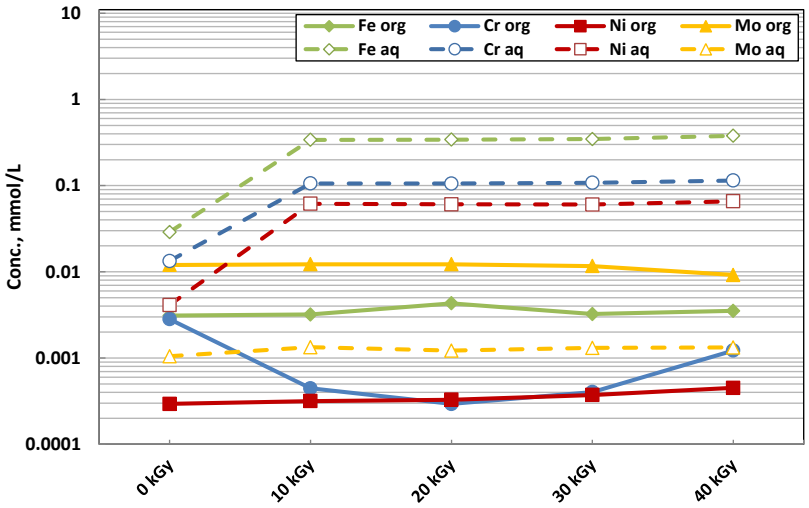

Figure 19. Evolution of the concentration of stainless steel corrosion products Fe, Cr, Ni and Mo during TRU stripping step of EURO-GANEX irradiation loop.

The presence of corrosion metals during the TRU stripping could be affecting the unexpected $D_{M(III)}$ values shown in Figure 18. Therefore, additional extraction experiments with EURO-GANEX solvent to check the TRU stripping as function of the Fe, Cr and Ni concentrations have been carried out and the results are summarised in Table 3. As the concentration of Fe, Cr and Ni increases (Exp. 2-5, Table 3), the $D_{Am(III)}$ values also increase. These results point out that the presence of these metals in the aqueous phase effectively influences the extraction capacity of the system modifying the distribution ratios, and therefore, the system performance. It should be also noted that aqueous solutions of these experiments darkened, especially when a high Fe concentration is added (Exp. 4 and 5, Table 3), similar to the irradiated TRU stripping solution obtained in the irradiation test loop. This result highlights that the colour change in the SO_3-Ph-BTP solution during the irradiation process could not only be attributed to its radiolytic degradation, but also the presence of metals such as Fe in the medium.

Table 3 Distribution ratios of An(III) and Ln(III) by fresh EURO-GANEX solvent (0.2 mol/L TODGA + 0.5 mol/L DMDOHEMA in OK) from the fresh aqueous phase consisting of 0.018 mol/L SO_3-Ph-BTP varying Fe(III), Cr(III) and Ni(II) concentrations.

Exp.	Samples composition					Distribution ratios	
	Org. phase	Aq. phase	Fe(III), mmol/L	Cr(III), mmol/L	Ni (III), mmol/L	$D_{Am(III)}$	$D_{Eu(III)}$
1	0.2 mol/L TODGA + 0.5 mol/L DMDOHEMA in OK	0.018 mol/L SO_3-Ph-BTP in 0.5 mol/L HNO_3	-	-	-	0.09	22.5
2			-	0.02	0.02	0.18	35.4
3			-	0.10	0.09	0.21	55.4
4			0.02	0.02	0.02	0.30	65.9
5			0.36	0.10	0.09	0.31	41.0

This project has received funding from the EURATOM research and training programme 2014–2018 under grant agreement No. 755171. The content of this deliverable reflects only the authors' view. The European Commission is not responsible for any use that may be made of the information it contains.

As in previous steps, the acid concentration of the aqueous phase during the TRU step was also checked and it is summarized in Table 4. The proton concentration increases from approximately 0.50 mol/L when SO_3-Ph-BTP is unirradiated, to 0.84 mol/L for all the absorbed dose studied. This significant increase in the acidity could be one of the reasons of the unexpected high $D_{Am(III)}$ values observed in Figure 18. This increase is still unknown since it would be due to the ineffective adjustment of the conditions after the first irradiation step or unexpected degradation of the aqueous phase.

Table 4 Distribution ratios of An(III) and Ln(III) by fresh EURO-GANEX solvent (0.2 mol/L TODGA + 0.5 mol/L DMDOHEMA in OK) from the fresh aqueous phase consisting of 0.018 mol/L SO_3-Ph-BTP varying Fe(III), Cr(III) and Ni(II) concentrations.

EURO-GANEX process step	Aqueous phase sample	Absorbed Dose, kGy	$[H^+]$, mol/L
TRU Stripping	0.018 mol/L SO_3-Ph-BTP in 0.5 mol/L HNO_3	0	0.48
		10	0.81
		20	0.80
		30	0.79
		40	0.84

Otherwise, the changes suffered in the composition caused by the degradation of extractants also affect the extraction capacity of the system. Therefore, although distribution ratios give us a lot of information about the systems and allow predicting their behaviour, they should not be used as the only metric for ligand degradation. Hence, to have a global picture of what is happening and a further understanding, the composition of both the organic and the aqueous phases of the corresponding An+Ln co-extraction and TRU stripping steps were investigated. The composition of the organic phase has been analysed qualitative and quantitative by HPLC-MS, while the composition of the aqueous phase was analysed by Raman spectroscopy technique, using the methodology followed in our last works [39, 41, 46].

First it has full characterised the degraded organic phase by HPLC-MS quantifying not only TODGA and DMDOHEMA but also the main degradation compounds (DCs) found. Quantification of remaining TODGA and DMDOHEMA concentrations in organic phases is summarized in Figure 20. TODGA and DMDOHEMA concentration decreases as function of dose reaching a concentration decrease of 32% (25% for the An+Ln co-extraction and 7% for the TRU stripping) and 33% respectively (25% for the An+Ln co-extraction and 8% for the TRU stripping. On the one hand, the DMDOHEMA degradation is in agreement with the previous results obtained and showed in CIEMAT_HYPAR 4 [52], while the TODGA concentration decrease is lower than the previous results [41, 46]. On the other hand, the degradation of the organic EURO-GANEX solvent in contact with SO_3-Ph-BTP aqueous phase is slightly higher that when it is irradiated in presence of 5 mol/L HNO_3 for 40 kGy.

This project has received funding from the EURATOM research and training programme 2014–2018 under grant agreement No. 755171. The content of this deliverable reflects only the authors' view. The European Commission is not responsible for any use that may be made of the information it contains.

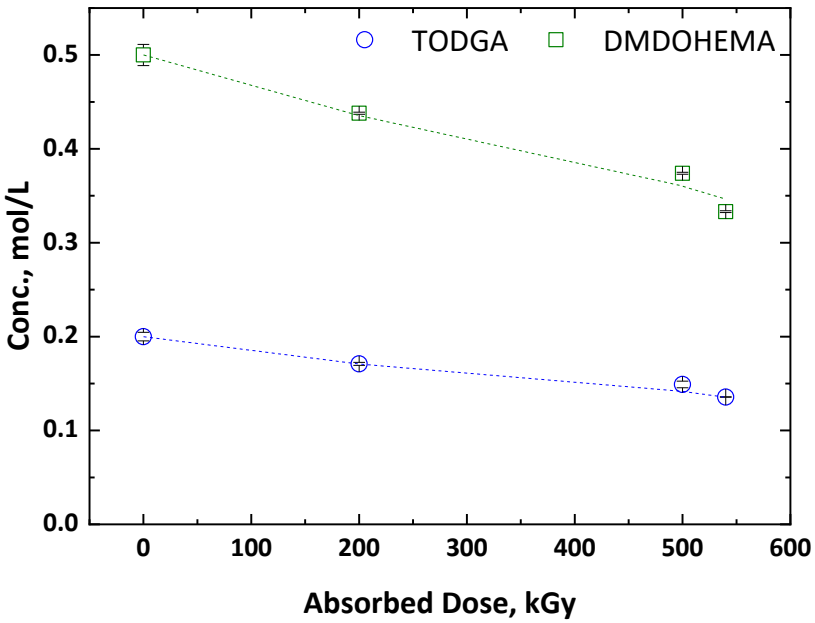

Figure 20 TODGA and DMDOHEMA concentration as a function of the dose. Fresh EURO-GANEX solvent (reference sample), irradiated at 200 and 500 kGy in contact with of 5 mol/L HNO_3, and irradiated at 500 kGy in contact with 5 mol/L HNO_3 and extra 40 kGy with 0.018 mol/L SO_3-Ph-BTP in 0.5 mol/L HNO_3.

Figure 21 and Figure 22 show the qualitative analysis of fresh and irradiated EURO-GANEX solvent at the different absorbed doses studied, and the structures of TODGA and DMDOHEMA degradation compounds, respectively As expected, the main TODGA DCs and 6 DMDOHEMA DCs have been found after irradiation, in agreement with previous works [23-28]. Moreover, three new signals have been identified as possible undescribed DCs (m/z = 383.3, r.t = 7.10 min; m/z = 400.2, r.t = 7.75 min; and m/z = 498.3, r.t = 11.55 min) which their proposed structures are also shown in Figure 22, probably as consequence of the irradiation in dynamic conditions, *i.e.* better contact between phases and the presence of higher oxygen content during the irradiation process. The appearance of new peaks is in agreement with our previous works [41, 46], where the presence of new hypothetical TODGA DCs when the irradiation occurs with more oxygen content was reported.

This project has received funding from the EURATOM research and training programme 2014–2018 under grant agreement No. 755171. The content of this deliverable reflects only the authors' view. The European Commission is not responsible for any use that may be made of the information it contains.

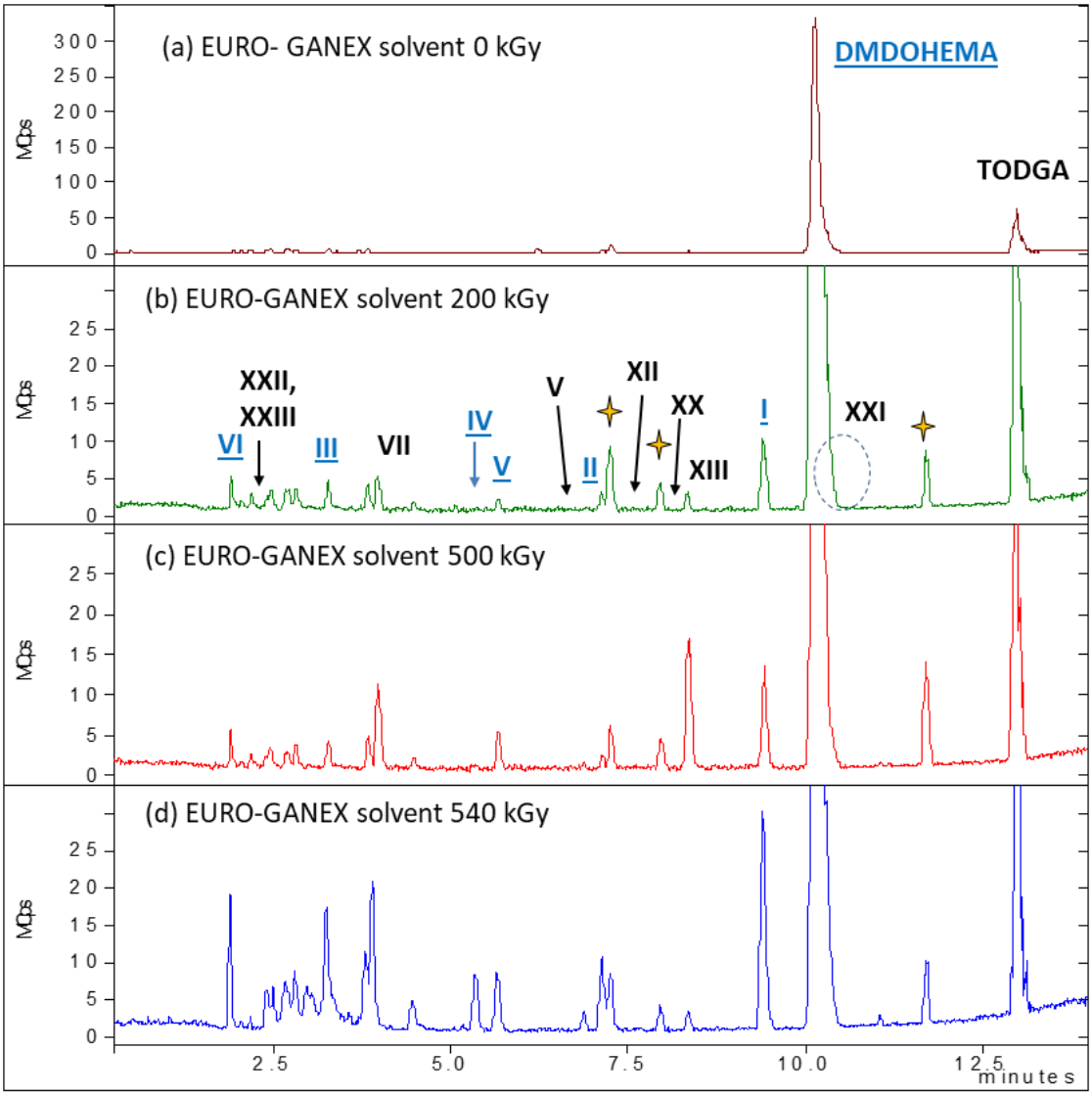

Figure 21 HPLC-MS chromatograms of EURO-GANEX solvent obtained during irradiation test loop : a) fresh EURO-GANEX solvent (reference sample); b) Irradiated EURO-GANEX at 200 kGy solvent in contact with of 5 mol/L HNO_3; c) Irradiated EURO-GANEX solvent at 500 kGy in contact with of 5 mol/L HNO_3; d) Irradiated EURO-GANEX solvent at 500 kGy in contact with of 5 mol/L HNO_3 and other 40 kGy in contact with 0.018 mol/L SO_3-Ph-BTP in 0.5 mol/L HNO_3.

This project has received funding from the EURATOM research and training programme 2014–2018 under grant agreement No. 755171. The content of this deliverable reflects only the authors' view. The European Commission is not responsible for any use that may be made of the information it contains.

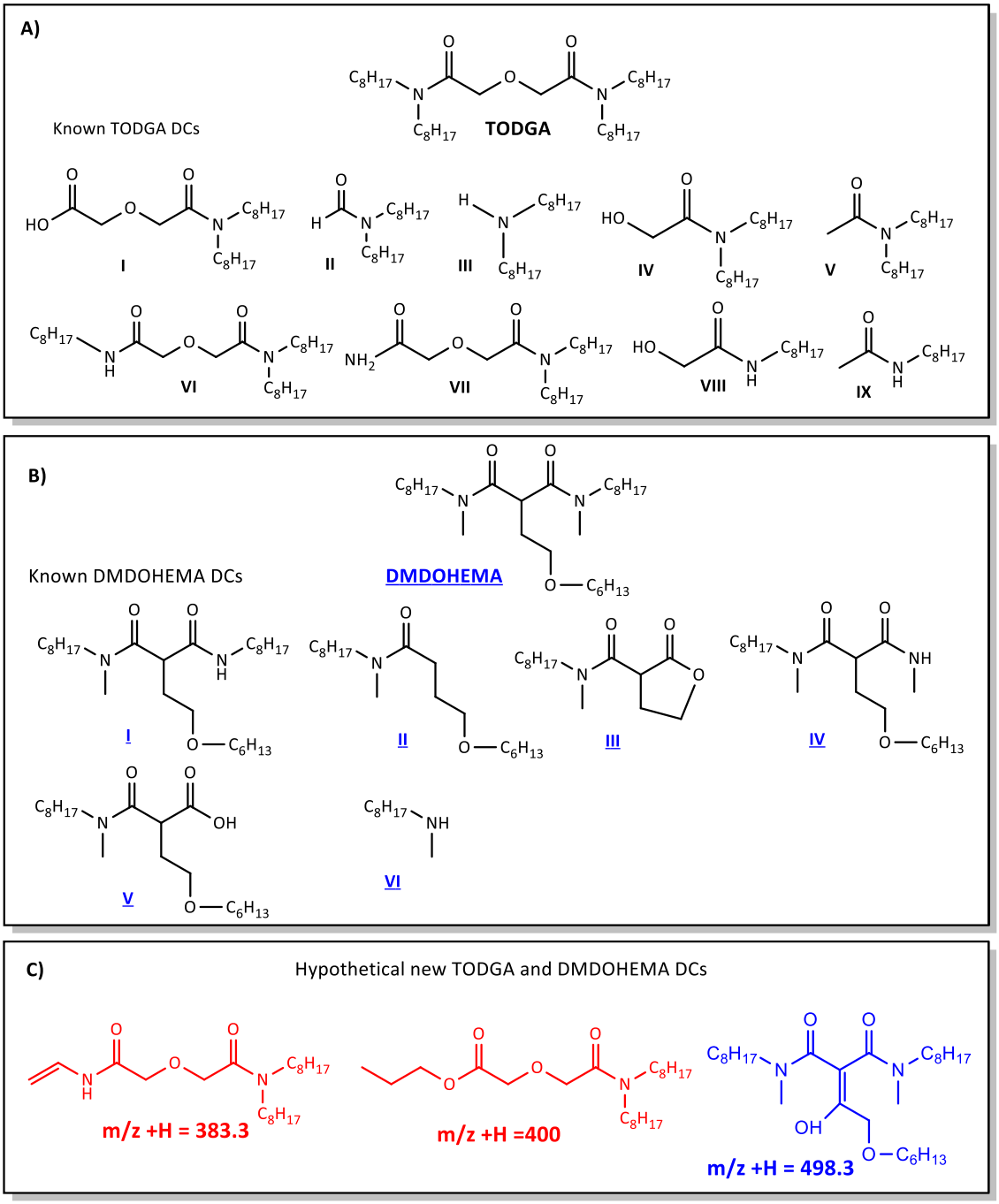

Figure 22 Structures of A) TODGA and b) DMDOHEMA, both of them with their respective degradation compounds (DCs), and C) Hypothetical structures for the new signal found by HPLC-MS.

Only the main TODGA DCs were quantified due to those corresponding to DMDOHEMA are not available to obtain theirs calibration curves. Figure 23 shows the quantification of TODGA DCs for DC V, VII, XII, XIII, and XXI by HPLC-MS for samples irradiated at 200 kGy and 500 kGy. The other DCs are not shown due to their concentrations were lower than the detection limit (<0.003 mol/L). As expected, concentrations of all DCs increase as a function to absorbed dose, as a consequence of TODGA degradation. Typically, the DCs XII, XIII and XXI are the most abundant due to the radiation effect over the weakest bonds of TODGA (C-O_{ether} and N-C) [23-

This project has received funding from the EURATOM research and training programme 2014–2018 under grant agreement No. 755171. The content of this deliverable reflects only the authors' view. The European Commission is not responsible for any use that may be made of the information it contains.

26]. However, from the results obtained in Figure 23, it can be seen that under test loop conditions, DCs XII, VII and V are the majority. The concentrations of both DCs XII and XIII should be similar due to they came from the same rupture, when TODGA is degraded by C-O_{ether} bond rupture, but in this case DC XII concentration is higher than XIII, in agreement with previous works [41, 46]. The presence of high amount of V and VII, and the low concentration of XXI, is in agreement with the previous results obtained for the TODGA based solvent when there is higher oxygen content during the irradiation [41, 46]. The variation in the proportion of TODGA DCs could be result of a change in the degradation pathways given by the higher oxygen content or better contact between phases.

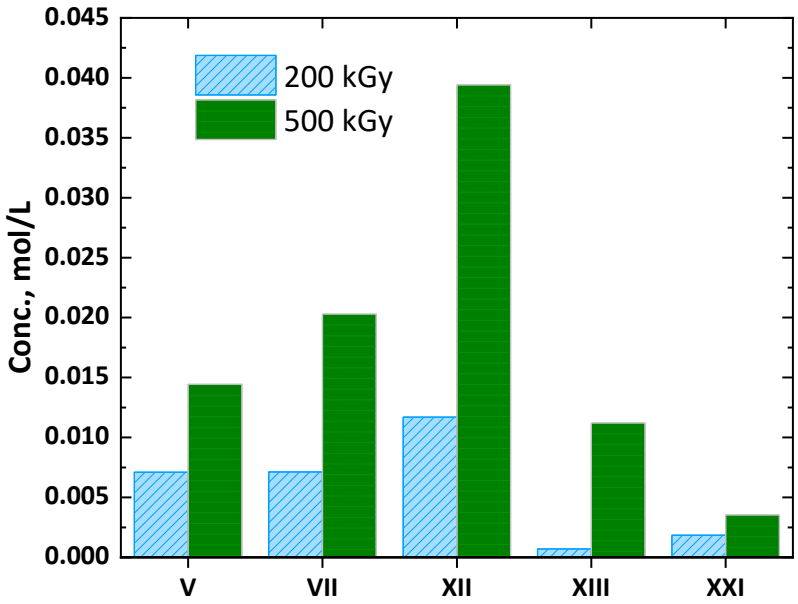

Figure 23 HPLC-MS quantitative analysis of different TODGA DCs when EURO-GANEX solvent is irradiated with 5 mol/L HNO_3 in the irradiation test loop at 200 and 500 kGy in the An+Ln co-extraction step.

The different proportion or even the presence of new DCs formed using dynamic conditions is a very important observation because their accumulations and their individual properties during the extraction process could affect the behaviour of the system in the long term.

In addition to the organic phase composition, the SO_3-Ph-BTP aqueous phase is also studied. The degradation of SO_3-Ph-BTP produced by radiolysis effect was analysed by quantitative Raman spectroscopy (QRS) following the methodology developed and previously used in one of our last works [39] and D2.1 [43].

Figure 24 shows the SO_3-Ph-BTP concentration decrease as a function of absorbed dose, *i.e.* approx. a 65% is lost at 40 kGy. These reduction in the SO_3-Ph-BTP concentration highlights that this compound is very susceptible to degradation under the studied radiation conditions, in agreement with the studies found in literature [30, 31, 39]. However, this result is in disagreement with the data obtained by Peterman *et al.,* using also an irradiation test loop [32], who reported no significant SO_3-Ph-BTP degradation up to 175 kGy, and with the previous data published in our work, [42] where it was reported a ~60% reduction at 200 kGy, obtained by using the indirect method by means of the dependence with D_{Am} with the SO_3-Ph-BTP concentration by gamma spectrometry, when two phases were irradiated together in static conditions using different irradiation conditions (air, argon and air sparging flux).

This project has received funding from the EURATOM research and training programme 2014–2018 under grant agreement No. 755171. The content of this deliverable reflects only the authors' view. The European Commission is not responsible for any use that may be made of the information it contains.

Moreover, the SO_3-Ph-BTP degradation observed for the current irradiation test loop is slightly higher than the studies where only aqueous phases were irradiated in static conditions [30, 39]. In one of them, it was quantified using the same QRS methodology obtaining a ~50% concentration decrease at 50 kGy [39]. In the other one, a loss of 50% of the concentration of SO_3-Ph-BTP was estimated at 60 kGy using the same indirect method mentioned above [30].

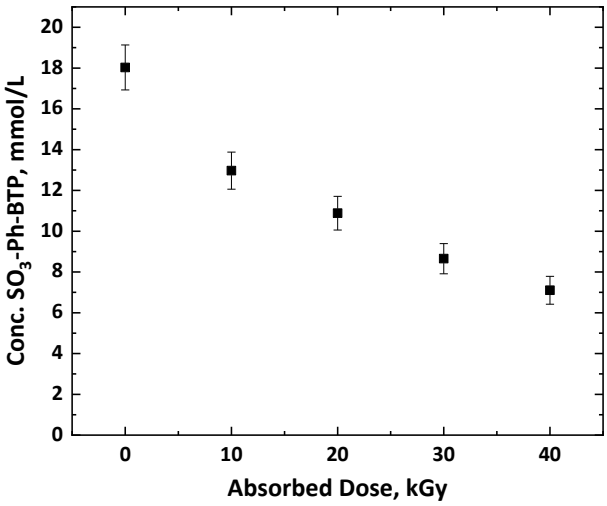

Figure 24 SO_3-Ph-BTP concentration obtained by Raman spectroscopy as a function of absorbed dose for the test irradiation loop of the TRU stripping step.

This project has received funding from the EURATOM research and training programme 2014–2018 under grant agreement No. 755171. The content of this deliverable reflects only the authors' view. The European Commission is not responsible for any use that may be made of the information it contains.

NEW EURO-GANEX SOLVENT DEGRADATION STUDIES

Authors: Andreas Wilden, Giuseppe Modolo (Juelich); Bart Verlinden and Rainier Hermans (SCK•CEN); Patrik Wessling and Andreas Geist (KIT-INE); Wim Verboom (TWE).

INTRODUCTION

The Deliverable Report, *D5.2, Impacts of solvent degradation and recycle on the EURO-GANEX process,* also compiles radiolysis studies, solvent extraction studies with irradiated solvents, and theoretical studies performed within the GENIORS project regarding NEW EURO-GANEX solvent.

The new EURO-GANEX system is an optimisation EURO-GANEX system based on the modification of the solvents employed. On the one hand, it is desirable a lower solvent complexity by using a single extractant in the organic phase. On the other hand, an An complexant which meet the CHON principle is required to replace SO_3-Ph-BTP. In that sense, TODGA and DMDOHEMA have been replaced from the organic phase formulation for the dimethyl-*N,N,N',N'*-tetradecyl-diglycolamide (cis-mTDDGA). This molecule is similar to TODGA but has several modifications such as: additional methyl substituents in the backbone and increased side-chain length. Malmbeck *et al.,* recently studied this molecule and concluded that these modifications make it a suitable extractant [55]. For the substitution of SO_3-Ph-BTP, 2,6-bis[1-(propan-1-ol)-1,2,3-triazol-4-yl)]pyridine (PyTri-Diol, or PTD) is proposed. PTD was found to have high actinide selectivity and radiochemical stability [56-58] and could therefore be suitable for application as a stripping reagent in a new EURO-GANEX process. Figure 25 shows the chemical structures of cis-mTDDGA and PTD, currently studied to be used in a new EURO-GANEX system.

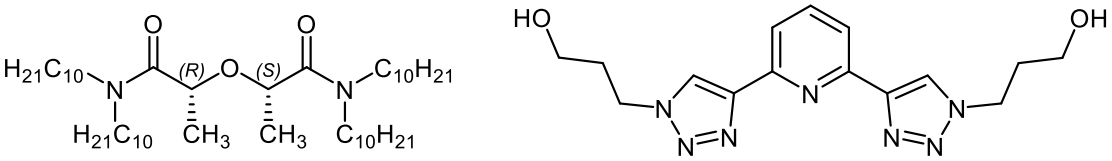

***cis*-mTDDGA** **PyTri-diol or PTD**

Figure 25. Chemical structure of cis-mTDDGA and PTD.

mTDDGA RADIOLYSIS STUDIES

The radiolytic stability of mTDDGA is under investigation for application in a new EURO-GANEX process [8]. It is an analogue of TODGA with longer alkyl side chains and additional methyl substituents in the backbone. The radiolytic stability of the double methylated TODGA, Me_2-TODGA, was studied before [59]. mTDDGA can form different diastereomers (Figure 26), of which the *cis* diastereomer is preferably used in process applications, as it is the better extractant. The same improved extraction of the *cis* diastereomer was observed for Me_2-TODGA [60]. In the radiolysis studied, a mixture of diastereomers was used, as well as the pure *cis* diastereomer.

This project has received funding from the EURATOM research and training programme 2014–2018 under grant agreement No. 755171. The content of this deliverable reflects only the authors' view. The European Commission is not responsible for any use that may be made of the information it contains.

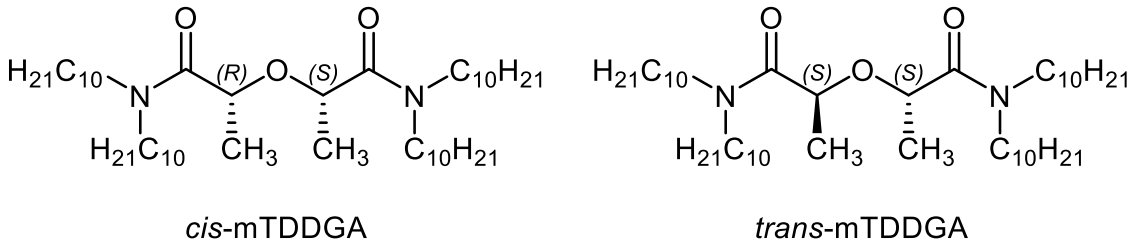

Figure 26. Chemical structure of *cis* and *trans*-mTDDGA.

QUANTIFICATION OF MTDDGA

Gamma irradiations with ^{60}Co sources were conducted at the BRIGITTE irradiation facility of SCK•CEN. Red Perspex dosimeters from Harwell were used for the determination of the dose rate at the exact positions of the samples. The average dose rate in the irradiation chamber was determined as 9.44 kGy/h at the samples' positions. For the preparation of the 0.05 M mTDDGA solutions in dodecane, the batch sent by Wim Verboom was used, with a cis to trans ratio of 3.5 to 1.

The results of the quantitative measurements with HPLC-ESI-MS/MS for mTDDGA and TODGA are shown in Figure 27.

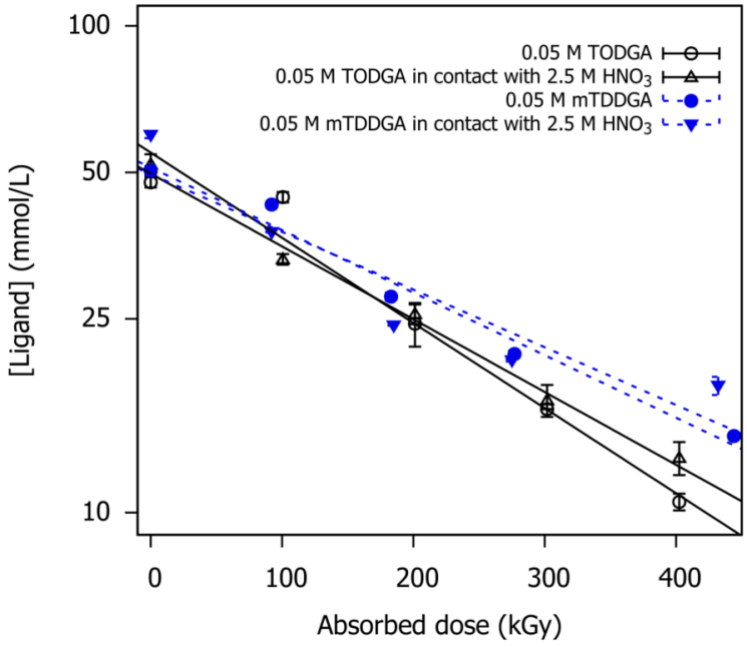

Figure 27. Diglycolamide concentrations as a function of absorbed dose. The initial concentration was 0.05 M for both ligands.

This project has received funding from the EURATOM research and training programme 2014–2018 under grant agreement No. 755171. The content of this deliverable reflects only the authors' view. The European Commission is not responsible for any use that may be made of the information it contains.

From the linear fitting of the natural logarithm of the concentration as a function of the absorbed dose, the dose constant (*d*) was derived as the slope of the resulting linear equation. The results for the calculation of the dose constants from the experimental data is shown in Table 5. The observed dose constant for 0.05 M of the reference molecule TODGA in *n*-dodecane is very similar to the one published by Zarzana *et al.*[26] (-4.1 × 10^{-6} Gy^{-1}) and Sugo *et al.*[61] (-4.5 × 10^{-6} Gy^{-1}).

Table 5. Determined dose constants and their standard errors, resulting from the linear least square regression of the natural logarithm of the measured concentrations as a function of the absorbed dose.

Sample	Dose constant *d* (× 10^{-6} Gy^{-1})	Standard error on fitting (× 10^{-6} Gy^{-1})
0.05 M TODGA	-4.0	0.4
0.05 M TODGA in contact with 2.5 M HNO_3	-3.4	0.2
0.05 M mTDDGA	-3.0	0.4
0.05 M mTDDGA in contact with 2.5 M HNO_3	-2.7	0.6

Compared to TODGA, mTDDGA shows a slightly lower dose constant. This observation is in line with what could be expected from the results of previous work of Galán *et al.* [59] in which double methylated TODGA derivates showed a lower dose constant. Here, a lower dose constant (3.0 ± 0.2)·10^{-3} kGy^{-1} was reported for the irradiation of the neat organic phase containing 0.05 M double methylated TODGA derivative. However, the increase in *d* value (to (5.3 ± 0.4)·10^{-3} kGy^{-1}) for samples in contact with 2.5 M HNO_3 solution reported here was not observed, but remained almost constant.

IDENTIFICATION OF RADIOLYSIS PRODUCTS

Solutions of mTDDGA in alkane diluents were irradiated in the BRIGITTE facility at SCK CEN, Mol, Belgium with ^{60}Co γ radiation with and without contact to an aqueous phase. The dose constant (*d*) was derived as the slope of the resulting linear equation from the linear fitting of the natural logarithm of the concentration as a function of the absorbed dose. Values of −3.0 ± 0.4 × 10^{-6} Gy^{-1} and −2.7 ± 0.6 × 10^{-6} Gy^{-1} were determined for the irradiation without contact and in contact with 2.5 mol L^{-1} HNO_3, respectively. Compared to TODGA, as it was mentioned before, mTDDGA shows a slightly lower dose constant. This observation is in line with what could be expected from the results of previous work of Galán *et al.*[59] in which double methylated TODGA derivates showed a lower dose constant.

The degradation products of mTDDGA were identified using high resolution mass spectrometry, of which the seven most important ones are shown in Figure 28. These degradation products agree very well with the degradation products identified previously for related diglycolamides.[26, 59, 62]. The degradation compounds were synthesized by TWENTE and used for a quantitative analysis of irradiated samples. The results show that the C_{ether}-O_{ether} bond breaking product (DC III, with the alcohol group) is the most abundant degradation product, independent of the chemical conditions during irradiation. The presence of an aqueous nitric acid phase suppressed the formation of the other C_{ether}-O_{ether} bond breaking product (DC II) or causes it to be practically

This project has received funding from the EURATOM research and training programme 2014–2018 under grant agreement No. 755171. The content of this deliverable reflects only the authors' view. The European Commission is not responsible for any use that may be made of the information it contains.

absent in the organic phase (e.g. by protonation and precipitation). The carboxylic acid degradation product (DC VII) does not appear in significant concentrations in the samples. For the irradiation of the neat organic phase, the concentration of didodecylamine was found to increase as a function of the absorbed dose. This was not the case when an acidic aqueous phase was present, as the amine was protonated and formed an insoluble precipitate. For the irradiation in contact with 2.5 mol L^{-1} HNO_3, the degradation products with the second highest concentration is DC I, the single de-alkylation product of mTDDGA. Evaluation of solvent extraction properties will be most interesting for DC I and DC III, because they dissolve easily in *n*-dodecane and were found in high concentrations in irradiated solvents. For TODGA and other related molecules, it was also previously shown that ether bond breaking compounds are mainly present in irradiated solvents [26, 40, 63].

Solvent extraction experiments with irradiated *cis*-mTDDGA of realistic concentrations (0.5 mol L^{-1}) showed only slightly decreasing distribution ratios for the actinides up to an absorbed dose of 450 kGy, proving the good radiolytic stability of the extractant. As it can be seen in following sections, the degradation products were found to be only weak extractants, which should not interfere too much in a process application.

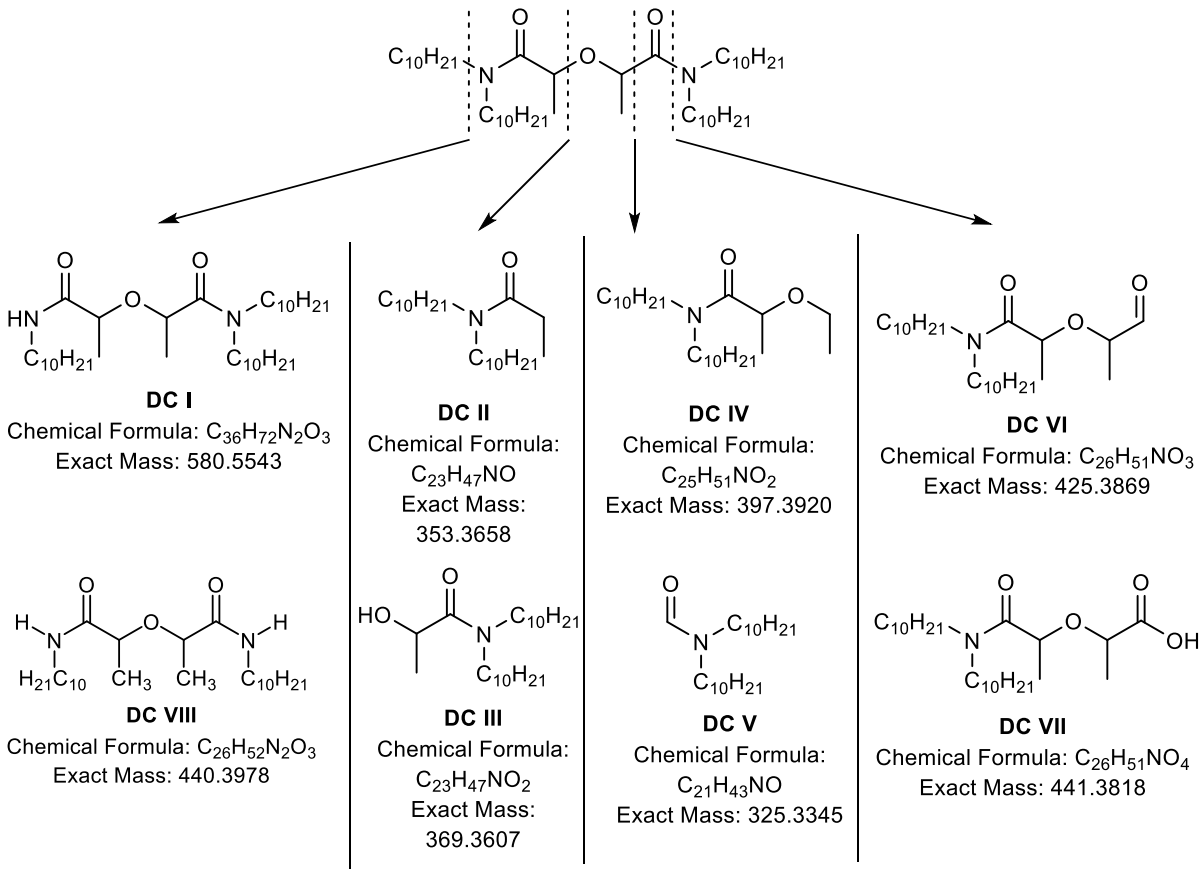

Figure 28. Identified degradation compounds of mTDDGA with their chemical formulas and monoisotopic molecular weights.

This project has received funding from the EURATOM research and training programme 2014–2018 under grant agreement No. 755171. The content of this deliverable reflects only the authors' view. The European Commission is not responsible for any use that may be made of the information it contains.

QUANTIFICATION OF DEGRADATION PRODUCTS

The previously identified radiolytic mTDDGA degradation products DC I, DC II, DC III, DC VI, DC VII, and DC VIII (see Figure 28), as well as didecylamine (DDA) were synthesized by TWENTE and used to conduct quantitative HPLC-MS analyses of irradiated samples.

Figure 29 shows the results of quantitative Electrospray Ionization High Performance Liquid Chromatography coupled with tandem Mass Spectrometry (ESI-HPLC-MS^2) analysis for the synthesized DCs and DDA in irradiated solvents of 0.05 mol L^{-1} mTDDGA in *n*-dodecane. The synthesized products were used to first optimize the measurements with multiple reaction monitoring. This allows for accurate quantification in a complex mixture, which may contain multiple species with the same *m/z* ratio in a single *m/z* separation, which interfere with the quantification, by selectively detecting specific fragments of the compound with a second mass spectrometer placed after a collision cell.

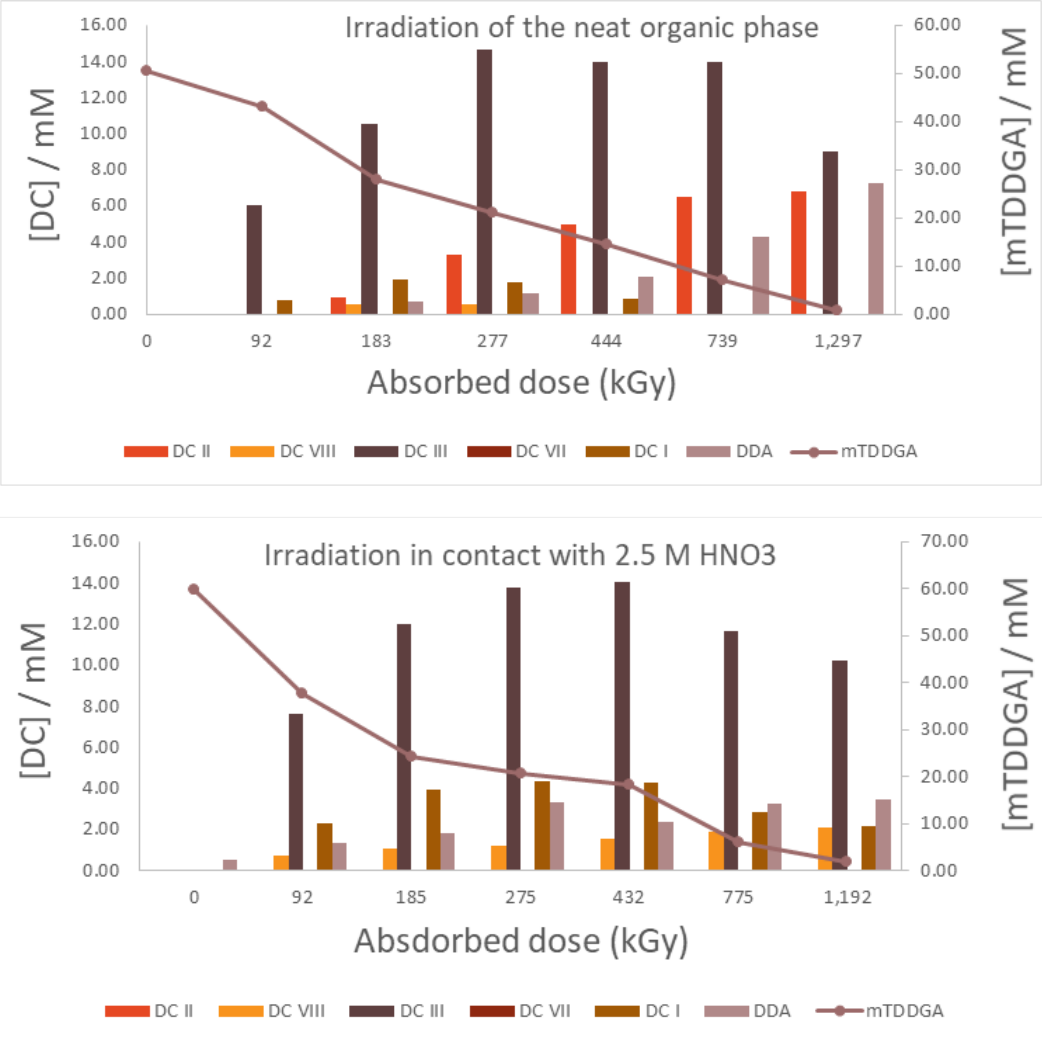

Figure 29. Quantitative analysis of the mTDDGA degradation compounds in irradiated 0.05 mol L^{-1} mTDDGA in *n*-dodecane. The mTDDGA concentration is shown for comparison.

This project has received funding from the EURATOM research and training programme 2014–2018 under grant agreement No. 755171. The content of this deliverable reflects only the authors' view. The European Commission is not responsible for any use that may be made of the information it contains.

The results show that the C_{ether}-O_{ether} bond breaking product (DC III, with the alcohol group) is the most abundant degradation product, independent of the chemical conditions during irradiation. The presence of an aqueous nitric acid phase suppressed the formation of the other C_{ether}-O_{ether} bond breaking product (DC II) or causes it to be practically absent in the organic phase (e.g. by protonation and precipitation). The carboxylic acid degradation product (DC VII) does not appear in significant concentrations in the samples. For the irradiation of the neat organic phase, the concentration of the amine DDA was found to increase as a function of the absorbed dose. This was not the case when an acidic aqueous phase was present, probably because of partial protonation of the amine. For the irradiation in contact with 2.5 mol L^{-1} HNO_3, the degradation products with the second highest concentration is DC I, the single de-alkylation product of mTDDGA. Evaluation of solvent extraction properties will be most interesting for DC I and DC III, because they dissolve easily in *n*-dodecane and were found in high concentrations in irradiated solvents. For TODGA and other related molecules, it was also previously shown that ether bond breaking compounds are mainly present in irradiated solvents [26, 40, 63].

ANALYSIS OF PRECIPITATE FORMED BY IRRADIATION OF mTDDGA

Samples of mTDDGA (0.05 mol L^{-1} mTDDGA in *n*-dodecane) irradiated in contact with 2.5 mol L^{-1} HNO_3 typically contained a precipitation, as visible in Figure 30. For two of these samples (named BV158 and BV159), the precipitate was separated and analysed.

Figure 30. Samples (BV158 and BV159) of 0.05 mol L^{-1} mTDDGA in *n*-dodecane irradiated to 454 kGy and 445 kGy in contact with 2.5 mol L^{-1} NHO_3.

For the BV158 vial, the clear organic phase was separated first. Then, the interphase containing the precipitate was transferred on a paper filter. The precipitate was slightly washed with *n*-dodecane and finally dissolved in methanol. For the BV159 vial, the interphase (mainly organic solvent) was transferred to a separate vial. This phase was consequentially washed with methanol which caused the precipitation to dissolve in the methanol phase, which was analysed.

The analyses of the dissolved precipitation solutions showed to contain mainly didecylamine. Apparently, when contacted with a nitric acid solution the amine is partly protonated and the protonated amine is not soluble in *n*-dodecane or EXXSOL D80.

This project has received funding from the EURATOM research and training programme 2014–2018 under grant agreement No. 755171. The content of this deliverable reflects only the authors' view. The European Commission is not responsible for any use that may be made of the information it contains.

SOLVENT EXTRACTION WITH GAMMA IRRADIATED mTDDGA SOLVENTS

To evaluate the effect of gamma irradiation on the studied solvent extraction system, solutions of 0.5 mol L^{-1} *cis*-mTDDGA in EXXSOL D80 were irradiated up to 445 kGy with a ^{60}Co source in contact with 5 mol L^{-1} HNO_3. The absorbed doses were determined by measurement of the local dose rate at the samples' position (2 repetitions) with Perspex dosimetry. The samples were phase separated for own solvent extraction studies and aliquots of the organic phases were sent to KIT for Pu loading experiments (see following sections).

At KIT, the irradiated *cis*-mTDDGA solvent (0.5 mol L^{-1} in EXXSOL D80, irradiated in contact with 5 mol L^{-1} nitric acid) was contacted with a Pu(IV) solution containing 36.2 g L^{-1} Pu(IV), after receiving up to 445 kGy absorbed dose. Table 6 shows the organic phase concentrations as a function of the absorbed dose. Due to high dilution factors necessary for ICP-MS measurements there is added uncertainty on the data in Table 6. However, even after irradiation up to the maximum dose of 445 kGy, there was still no visible precipitation (Figure 31) and the *cis*-mTDDGA solvent remains its Pu extracting capabilities. This gives an indication that some of the degradation compounds are able to extract Pu(IV).

Table 6. Concentration of Pu in the irradiated organic phases of 0.5 mol L^{-1} *cis* mTDDGA in EXXSOL D80, determined by measurements after back extraction (in two steps) with 4 mol L^{-1} AHA in 0.3 mol L^{-1} HNO_3, and by calculation based on measurements of the aqueous phase.

Absorbed dose (kGy)	$[Pu]_{org}$ (g/L)	$[Pu]_{org}$ (based on aq. phase) (g/L)
0	33.6	36.2
92	28.8	N/A
222	32.5	N/A
445	36.2	36.2

Figure 31. Vials with the irradiated (0, 92, 222 and 445 kGy) organic phases of 0.5 mol L^{-1} *cis*-mTDDGA in EXXSOL D80 after 1 h shaking in contact with 36.2 g L^{-1} Pu(IV) solution with $[HNO_3]$ = 5 mol L^{-1}.

In Figure 32, distribution ratios of Am, Pu, Cm, Eu and Np are shown as a function of absorbed dose. Only a slight decrease in distribution ratios was found for irradiation up to 445 kGy. Most remarkable is that the irradiated

This project has received funding from the EURATOM research and training programme 2014–2018 under grant agreement No. 755171. The content of this deliverable reflects only the authors' view. The European Commission is not responsible for any use that may be made of the information it contains.

solvent extracts neptunium significantly better than the fresh solvent, probably due to oxidation of the initial Np(V) by oxidative radicals formed during radiolysis. Similar behaviour was observed previously and during the EURO-GANEX development [6, 8, 64-66].

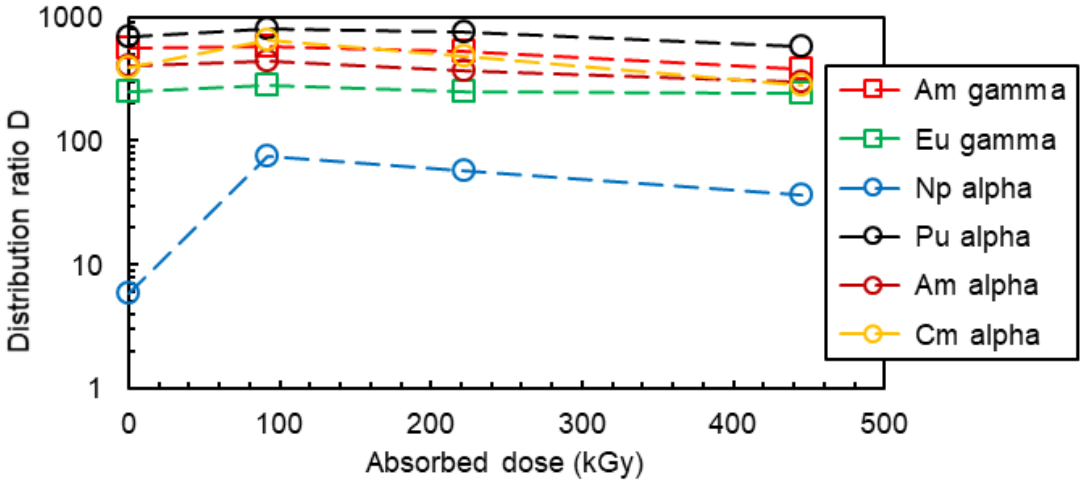

Figure 32. Extraction of Am, Pu, Cm, Eu and Np as a function of the absorbed dose for the organic phase irradiated in contact with 5 mol L^{-1} HNO_3. Initial org. 0.5 mol L^{-1} *cis*-mTDDGA in Exxsol D80, aq phase: 5 mol L^{-1} HNO_3, [Ln], [Y] = $1 \cdot 10^{-5}$ mol L^{-1}, 2.78 kBq ^{152}Eu, 2.81 kBq ^{241}Am, 1.51 kBq ^{244}Cm, 3.23 kBq ^{239}Pu; 0.74 kBq ^{237}Np, O/A ratio = 1, 25°C, 60 min., 2500 rpm.

Figure 33 shows the distribution ratios of the inactive elements as a function of absorbed dose. The lanthanide distribution ratios slightly increase during the first 100 kGy of irradiation and slightly decrease again, like the actinide distribution ratios. This can be an indication that formed degradation compounds have extracting properties as well. This trend was also visible in Figure 32, however less pronounced because of the very high distribution ratios. The Ln extraction pattern does not change with dose and holmium is the lanthanide with the highest distribution ratio, independent of dose.

The extraction of Zr and Ru seems to decrease with increasing dose. Masking of Zr and Pd should be possible with CDTA, as has been shown for TODGA based solvents [67], and should be tested in the future for mTDDGA. It should be noted that the mass balance for Zr, Mo and Pd during ICP-MS measurements was not consistent. There might be the formation of a small amount of precipitate which cannot be observed visually. The possible formation of precipitates in an important issue in process development and will be addressed in the future. Maybe a replacement for CDTA as a masking agent is needed.

This project has received funding from the EURATOM research and training programme 2014–2018 under grant agreement No. 755171. The content of this deliverable reflects only the authors' view. The European Commission is not responsible for any use that may be made of the information it contains.

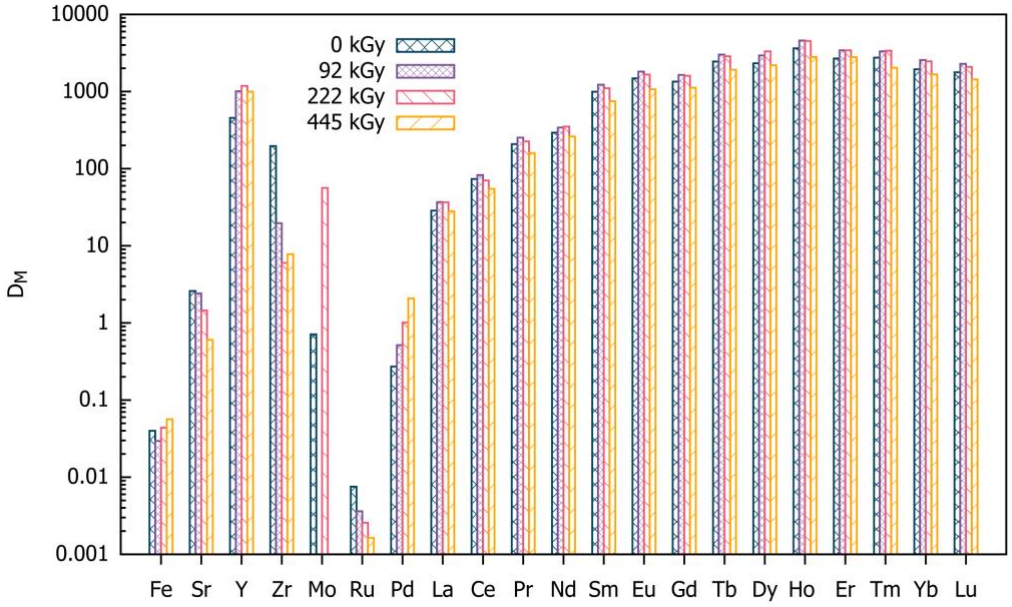

Figure 33. Extraction of inactive elements as a function of the absorbed dose for the organic phase irradiated in contact with 5 mol L^{-1} HNO_3. Initial org. 0.5 mol L^{-1} *cis*-mTDDGA in Exxsol D80, aq phase: 5 mol L^{-1} HNO_3, [Ln], [Y] = $1 \cdot 10^{-5}$ mol L^{-1}, 2.78 kBq ^{152}Eu, 2.81 kBq ^{241}Am, 1.51 kBq ^{244}Cm, 3.23 kBq ^{239}Pu; 0.74 kBq ^{237}Np, O/A ratio = 1, 25°C, 60 min., 2500 rpm.

PU(IV) LOADING INTO ALPHA-IRRADIATED DGA SOLVENTS

To study the stability of the Pu(IV) loading capacity against α radiolysis both the TODGA/DIPB system [68] and the *cis*-mTDDGA/Exxsol D80 system [55] were loaded with Pu(IV), and the organic Pu(IV) concentration was monitored over a period of 5 months.

8.3 g/L Pu(IV) (in case of TODGA/DIPB) and 36 g/L Pu(IV) (in case of *cis*-mTDDGA/Exxsol D80) were extracted from 5 mol/L HNO_3 into 0.5 mol/L of the respective solvent. The organic phases were kept with and without contact to the aqueous phase. Also, the pure solvent samples were kept in contact with 5 mol/L HNO_3 to study the degradation of the solvent by HNO_3.

Figure 34 and Figure 35 show the samples over a period of 5 months in which case doses of 279 kGy (TODGA/DIPB) and 1058 kGy (*cis*-mTDDGA/Exxsol D80) were accumulated.

This project has received funding from the EURATOM research and training programme 2014–2018 under grant agreement No. 755171. The content of this deliverable reflects only the authors' view. The European Commission is not responsible for any use that may be made of the information it contains.

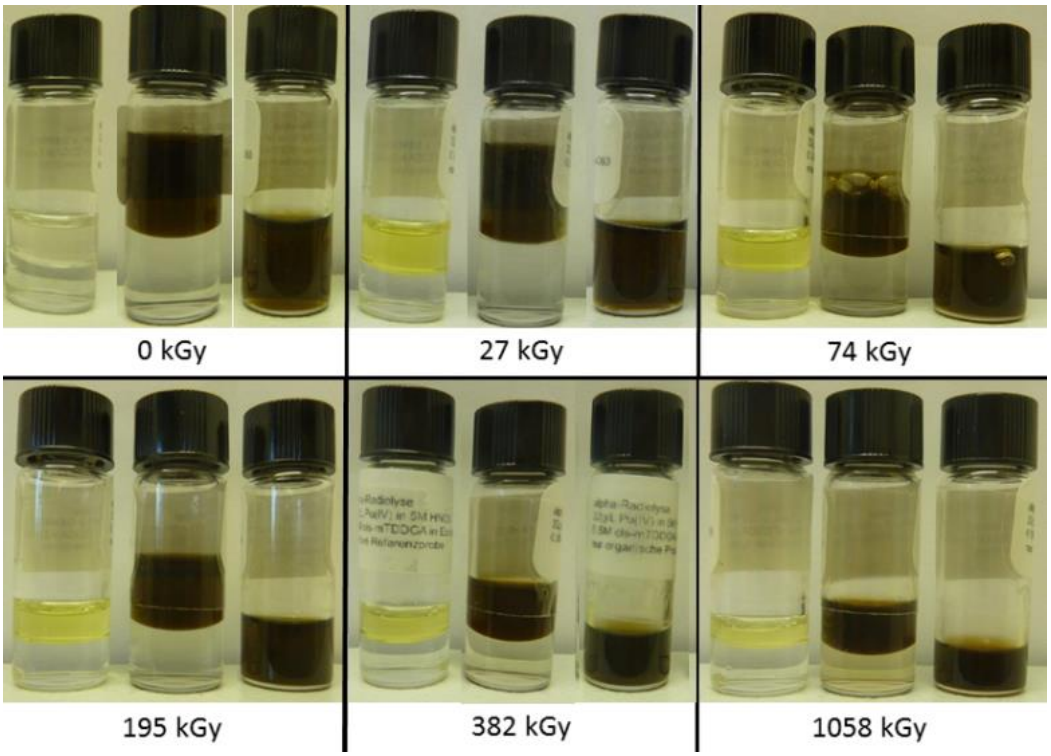

Figure 34. Pu(IV) samples after the extraction with 0.5 mol/L *cis*-mTDDGA dissolved in Exxsol D80 as a function of the accumulated α dose. Left to right: inactive reference, with and without contact to aqueous phase. 3 g/L Pu; Dose rate, 6.7 kGy/d; 5 mol/L HNO_3.

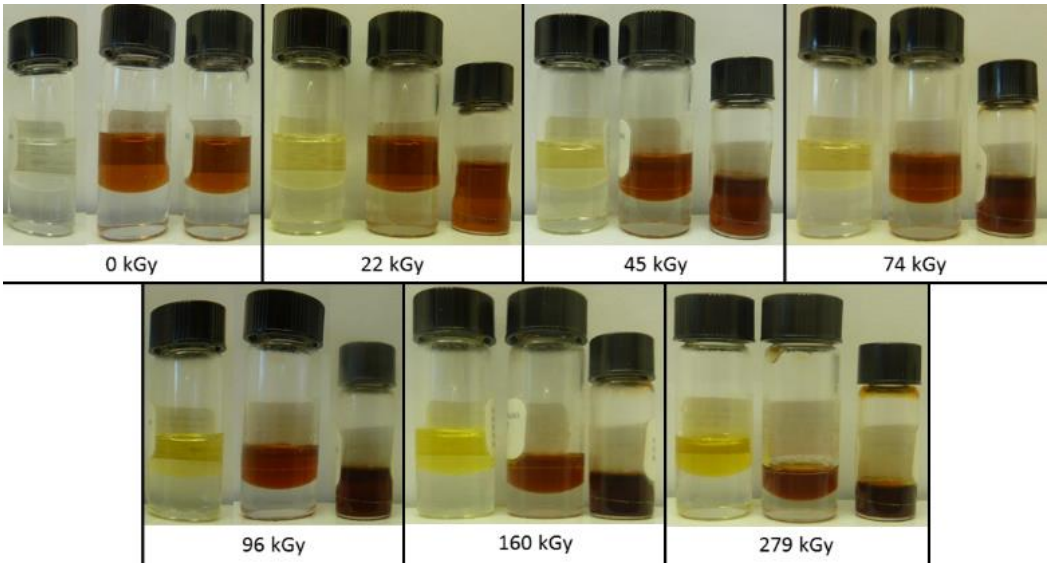

Figure 35. Pu(IV) samples after the extraction with 0.5 mol/L TODGA dissolved in DIPB as a function of the accumulated α dose. Left to right: inactive reference, with and without contact to aqueous phase. 8.3 g/L Pu; Dose rate: 1.6 kGy/d; 5 mol/L HNO_3.

This project has received funding from the EURATOM research and training programme 2014–2018 under grant agreement No. 755171. The content of this deliverable reflects only the authors' view. The European Commission is not responsible for any use that may be made of the information it contains.

Figure 36 shows the organic Pu(IV) concentration as a function of the accumulated dose for both TODGA/DIPB and *cis*-mTDDGA/Exxsol D80. A constant Pu(IV) concentration is observed for both systems, proofing the robustness of the Pu(IV) loading against α-radiolysis.

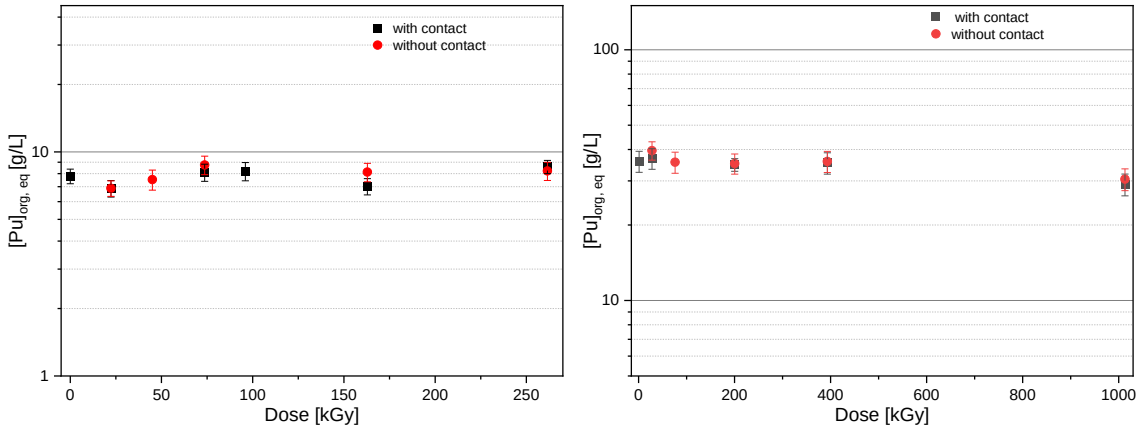

Figure 36. Equilibrium organic Pu concentration as a function of the absorbed α dose after extraction with 0.5 mol/L TODGA in DIPB (left) and 0.5 mol/L *cis*-mTDDGA in Exxsol D80.

A final check was performed after 10 months (2322 kGy for *cis*-mTDDGA/Exxsol D80, 563 kGy for TODGA/DIPB). The samples both in contact and without contact showed precipitation.

EXTRACTION PROPERTIES OF DEGRADATION COMPOUNDS

Five degradation compounds were synthesized by the University of Twente. Extraction experiments with 3 of these (RE1911, RE1913, and RE1915, Figure 37) in EXXSOL D80 were conducted, since the other two showed solubility issues. Besides 3 screening experiments, the other extractions were conducted at SCK CEN in the context of the master thesis of Rainier Hermans. Extraction conditions were kept similar: 1 h contact time, 10^{-5} mol L^{-1} metal concentrations and about 1 kBq of each radioactive tracer was added. The initial oxidation states were Np(V) and Pu(IV) for the Np and Pu tracer, respectively.

This project has received funding from the EURATOM research and training programme 2014–2018 under grant agreement No. 755171. The content of this deliverable reflects only the authors' view. The European Commission is not responsible for any use that may be made of the information it contains.

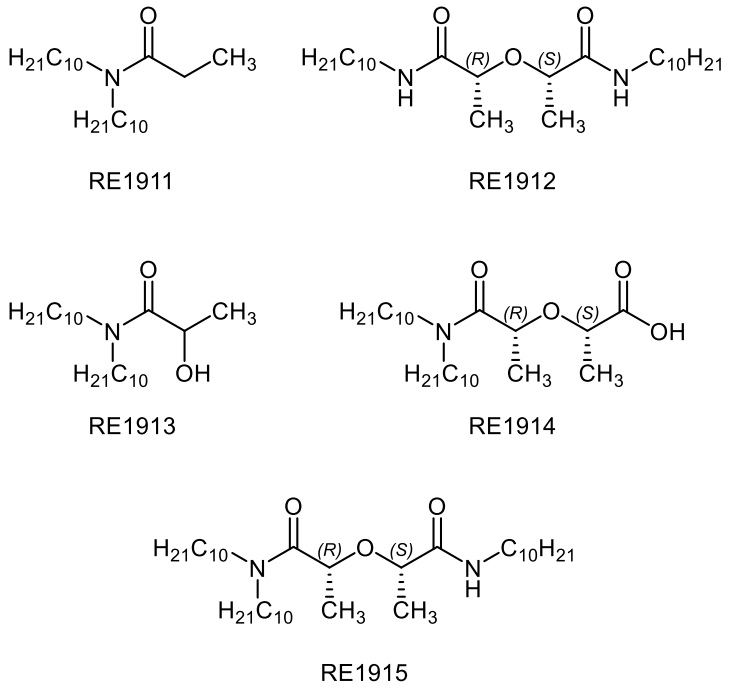

Figure 37. Degradation compounds of *cis* mTDDGA, synthesized by University of Twente.

RESULTS OF BATCH EXTRACTION EXPERIMENTS WITH RE1911

Already after the first screening experiment, it became clear that this compound is probably not a very strong metal complexant. At 0.16 mol L^{-1} DC concentration and 5 mol L^{-1} HNO_3, only slight extraction of ^{239}Pu was observed (D = 0.4). The distribution ratio for Pd was the only other one higher than 0.1 and was determined to be 5.7. Nevertheless, series of extraction experiments were conducted (nitric acid dependency and ligand concentration dependency).

In Figure 38, the distribution ratios for Pu and Np are plotted as a function of the nitric acid concentration. For the other tracers, D ratios were below 0.001 or below the detection limit of the α/γ spectrometer. Distribution ratios remain far below 1.

This project has received funding from the EURATOM research and training programme 2014–2018 under grant agreement No. 755171. The content of this deliverable reflects only the authors' view. The European Commission is not responsible for any use that may be made of the information it contains.

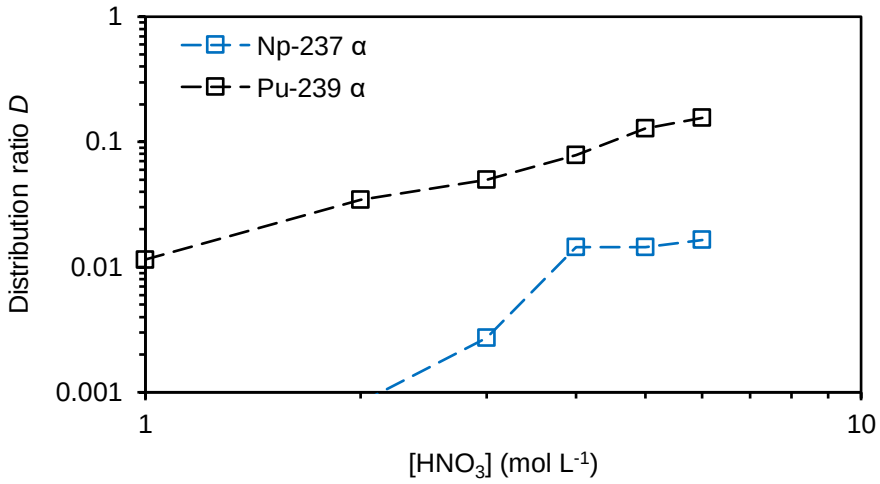

Figure 38. Np and Pu distribution ratios (alpha spectrometry) as a function of the initial nitric acid concentration of the aqueous phase: RE1911 = 0.1 mol L^{-1}, 1 h, [M] = 10^{-5} mol L^{-1}, 25 °C, A/O = 1, 1 kBq of ^{152}Eu, ^{237}Np, ^{239}Pu, ^{241}Am, ^{244}Cm.

In Figure 39, distribution ratios for the radiotracer elements are shown as a function of increasing ligand concentration. At high concentrations of this RE1913, there is some extraction of Pu observed. However, the distribution ratios are still very low, as expected from the initial screening experiment. The slopes of the log([L])/log(*D*) plots are 2.3 ± 0.04 (R^2 = 0.999) and 2.4 ± 0.1 (R^2 = 0.988) for Pu and Np, respectively, indicating mainly 2:1 complexation. This is similar to other extracting amides [69].

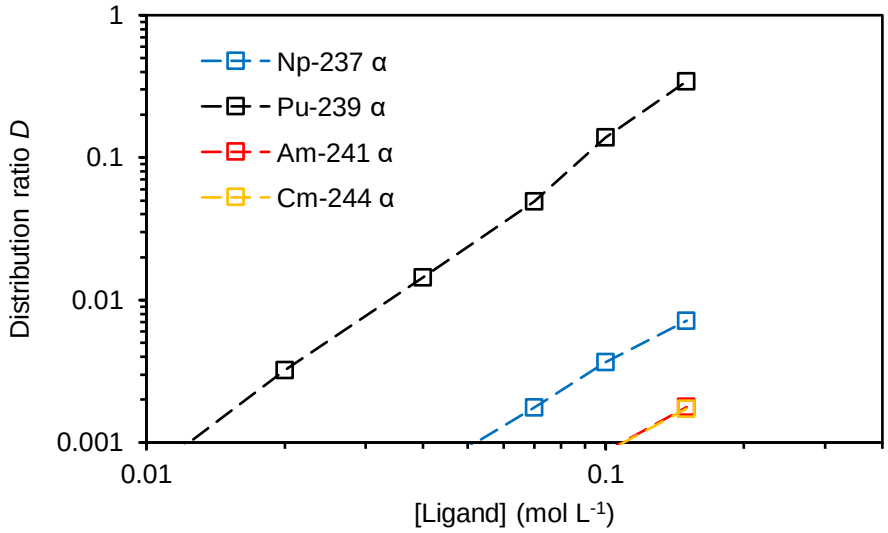

Figure 39. Distribution ratios of radiotracer elements by α spectrometry as a function of the RE1911 concentration: [HNO_3] = 5 mol L^{-1}, 1 h, [M] = 10^{-5} mol L^{-1}, 25 °C, A/O = 1, 1 kBq of ^{152}Eu, ^{237}Np, ^{239}Pu, ^{241}Am, ^{244}Cm.

This project has received funding from the EURATOM research and training programme 2014–2018 under grant agreement No. 755171. The content of this deliverable reflects only the authors' view. The European Commission is not responsible for any use that may be made of the information it contains.

For this degradation compound, the effect on the extraction behavior of an irradiated mTDDGA solvent would probably be limited since there is only significant extraction at very high ligand and nitric acid concentrations. The extraction of Pu should not be a problem since this is what is required in the EURO-GANEX process.

RESULTS OF BATCH EXTRACTION EXPERIMENTS WITH RE1913

Extraction by RE1913 mainly affected Pu distribution. At high acidities distribution ratios were over 100. The other An and Ln reach a maximum of about 1. Distribution ratios of the radioactive tracers are represented in Figure 40.

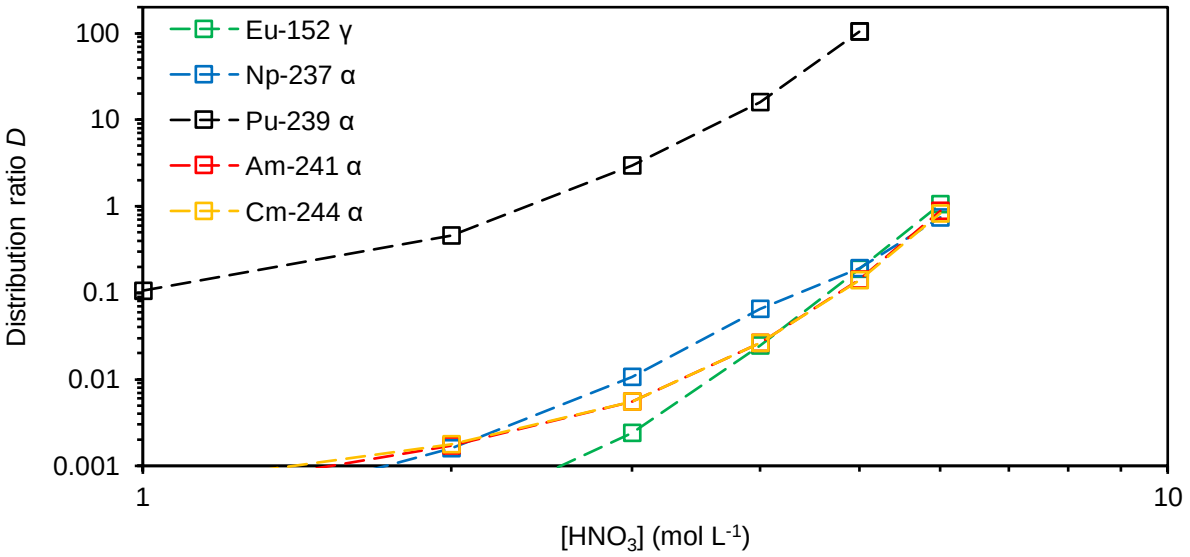

Figure 40. Distribution ratios of radiotracer elements by α and γ spectrometry as a function of the initial nitric acid concentration of the aqueous phase: RE1913 = 0.1 mol L^{-1}, 1 h, [M] = 10^{-5} mol L^{-1}, 25 °C, A/O = 1, 1 kBq of ^{152}Eu, ^{237}Np, ^{239}Pu, ^{241}Am, ^{244}Cm.

Also, in the data of the ligand dependency experiment (Figure 41), there is high selectivity for plutonium. An overlap of the alpha spectrum between ^{241}Am and ^{239}Pu in samples with a high separation factor between these two elements made accurate determination of the distribution ratio impossible. For this reason, distribution ratios for Pu were obtained from a separate experiment were only Pu and Np trace solutions were added.

This project has received funding from the EURATOM research and training programme 2014–2018 under grant agreement No. 755171. The content of this deliverable reflects only the authors' view. The European Commission is not responsible for any use that may be made of the information it contains.

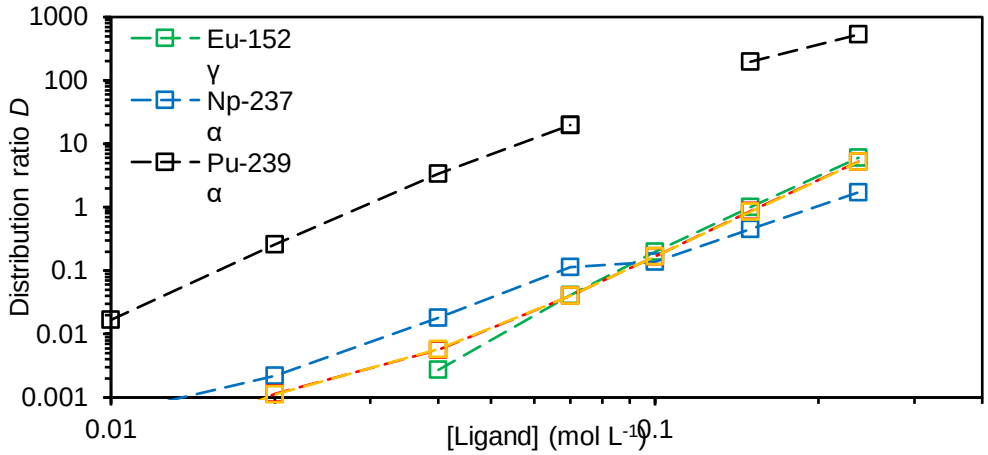

Figure 41. Distribution ratios of radiotracer elements by α and γ spectrometry as a function of the RE1913 concentration: [HNO_3] = 5 mol L^{-1}, 1 h, [M] = 10^{-5} mol L^{-1}, 25 °C, A/O = 1, 1 kBq of ^{152}Eu, ^{237}Np, ^{239}Pu, ^{241}Am, ^{244}Cm.

The ICP-MS data of the samples makes it possible to determine distribution ratios of the non-active elements as well. The results are shown in Figure 42. An important remark is that for these samples the mass balance for Mo is 20% lower. Also, for Pd mass balances are below 50%. For the lanthanides, distribution ratios max out at about 1. Probably the most problematic fission product seems to be Zr, with distribution ratios above 50 at nitric concentrations above 2 mol L^{-1} HNO_3.

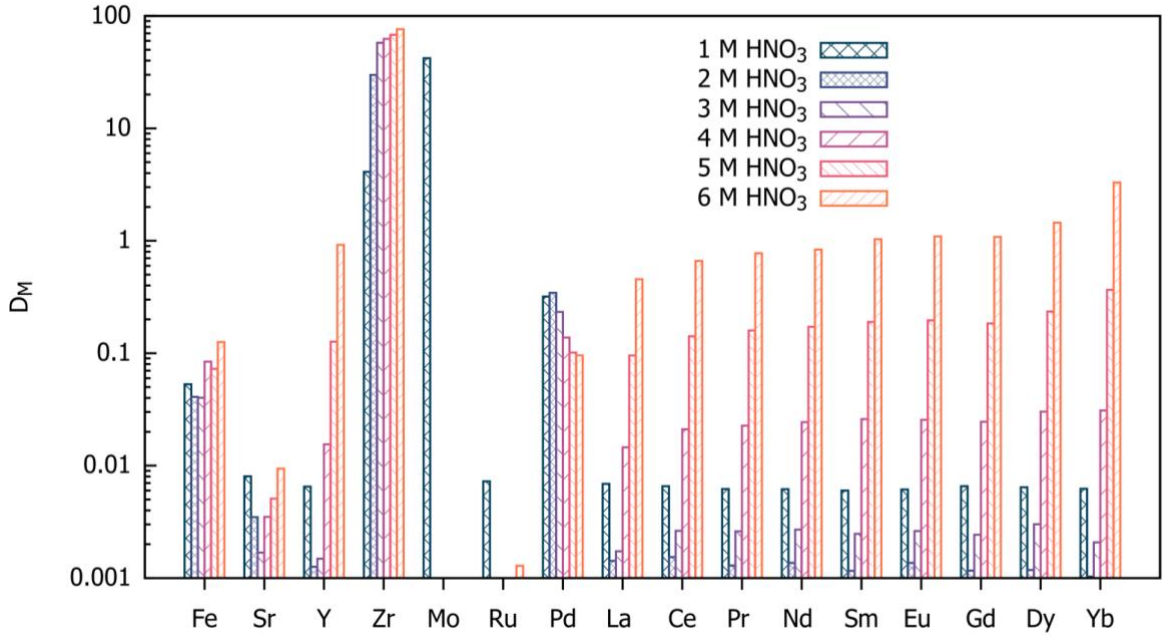

Figure 42. Distribution ratios of fission/corrosion products and lanthanides by ICP-MS as a function of the initial nitric acid concentration of the aqueous phase: RE1913 = 0.1 mol L^{-1}, 1 h, [M] = 10^{-5} mol L^{-1}, 25 °C, A/O = 1, 1 kBq of ^{152}Eu, ^{237}Np, ^{239}Pu, ^{241}Am, ^{244}Cm.

This project has received funding from the EURATOM research and training programme 2014–2018 under grant agreement No. 755171. The content of this deliverable reflects only the authors' view. The European Commission is not responsible for any use that may be made of the information it contains.

In Figure 43, the concentration of RE1913 was varied at a constant HNO_3 concentration. Distribution ratios of Mo quickly increases as the ligand concentration increases, but then suddenly drops below 0.001. Also, mass balances drop significantly (below 50%), strongly indicating towards the formation of some kind of precipitation. Palladium is also extracted, but only reaching a distribution ratio of 1 at the highest DC concentration. In general, lanthanide extraction increases as the DC concentration increases, but only reaching above 1 for the highest DC concentration(s). Higher lanthanides seem to be more extracted, in contrast to the mTDDGA itself which reaches a maximum at Ho.

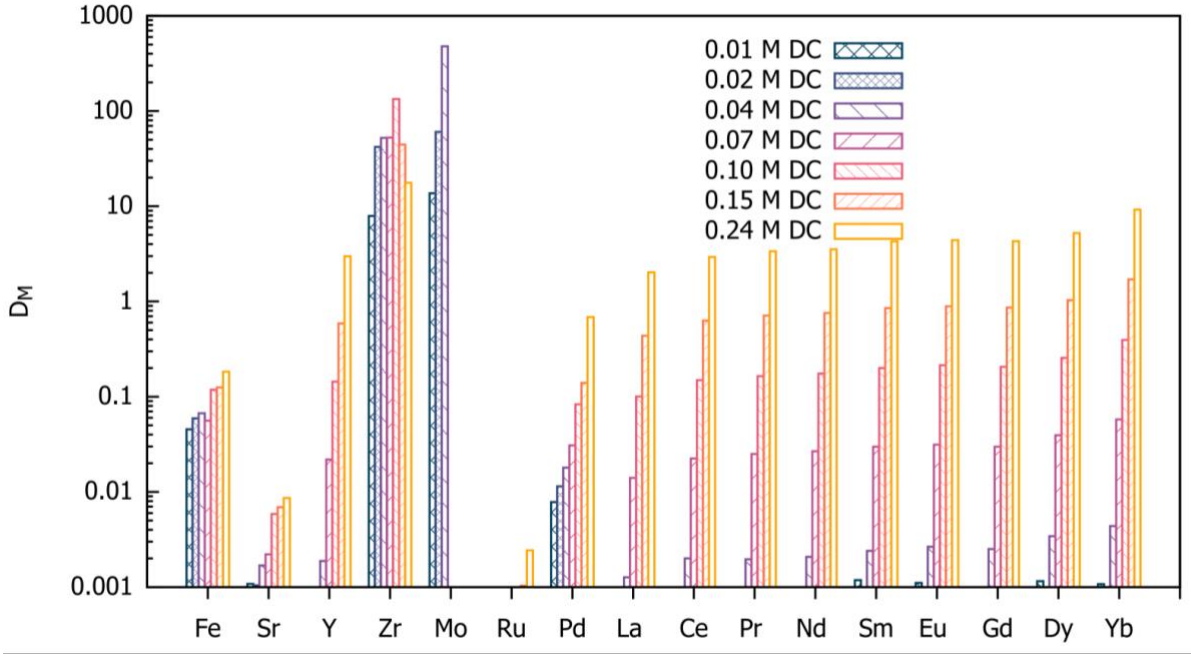

Figure 43. Distribution ratios of fission/corrosion products and lanthanides by ICP-MS as a function of the RE1913 concentration in the organic phase: [HNO_3] = 5 mol L^{-1}, 1 h, [M] = 10^{-5} mol L^{-1}, 25 °C, A/O = 1, 1 kBq of ^{152}Eu, ^{237}Np, ^{239}Pu, ^{241}Am, ^{244}Cm.

In general, this degradation compound of mTDDGA mainly extracts Pu. Issues for fission products might arise for Mo (precipitation) and Zr (extraction). However, these effects might be limited in the presence of masking agents such as CDTA.

RESULTS OF BATCH EXTRACTION EXPERIMENTS WITH RE1915

This degradation compound still has the original diglycolamide backbone as the core of its structure; however, it lost an alkyl chain which probably has consequences for its (and its complexes') solubility in the organic phases. Throughout the experimental series with increasing nitric acid concentrations, the formation of a precipitation was increasingly observed, starting from 4 mol L^{-1} HNO_3. This could be a reason for the observation of a drop in the distribution ratios for all Ln and An in Figures 44 and 45, except for Pu and Np (for which the increasing nitric acid concentration probably also affects their oxidation state). For the fission products, especially the distribution

This project has received funding from the EURATOM research and training programme 2014–2018 under grant agreement No. 755171. The content of this deliverable reflects only the authors' view. The European Commission is not responsible for any use that may be made of the information it contains.

ratio of Pd seems elevated (well above 10). However, for this element the mass balance was extremely low (<10%), which strongly indicates the formation of precipitation. Pu is best extracted element, with distribution ratios of about one order of magnitude larger than for the other actinides. Slope analyses indicate towards 3:1 complexes with trivalent actinides (Am slope of 3.26 ± 0.16, R^2 = 0.995 and Cm slope of 3.24 ± 0.15, R^2 = 0.996).

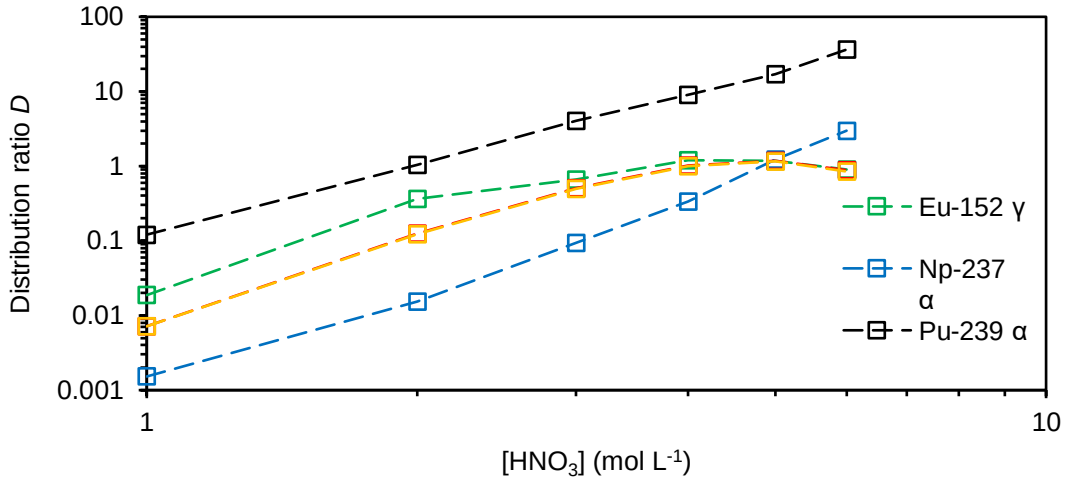

Figure 44. Distribution ratios of radiotracer elements by α and γ spectrometry as a function of the initial nitric acid concentration of the aqueous phase: RE1915 = 0.1 mol L^{-1}, 1 h, [M] = 10^{-5} mol L^{-1}, 25 °C, A/O = 1, 1 kBq of ^{152}Eu, ^{237}Np, ^{239}Pu, ^{241}Am, ^{244}Cm.

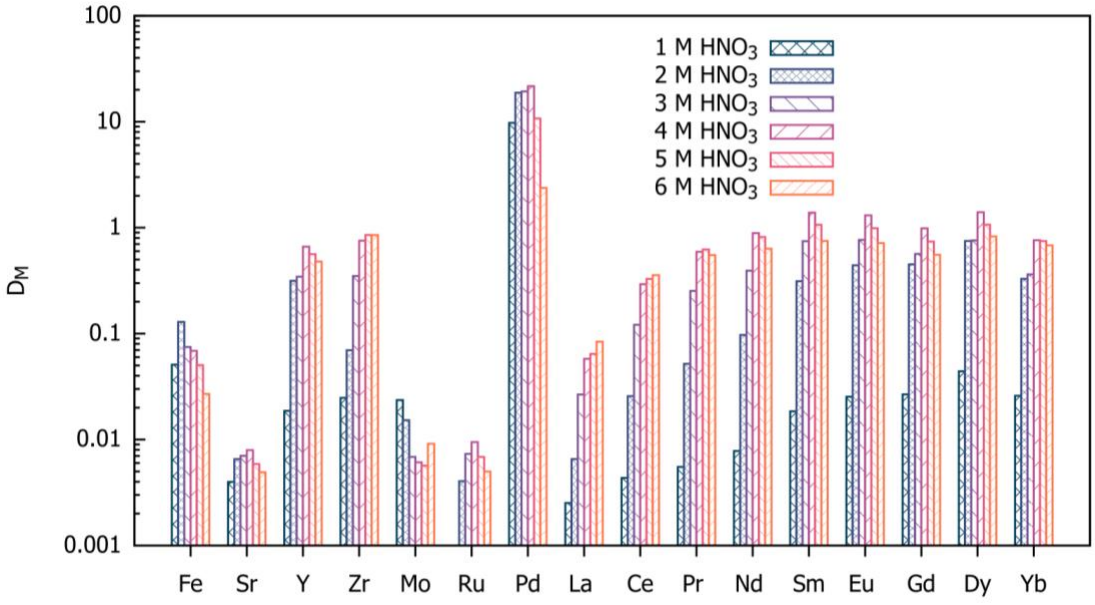

Figure 45. Distribution ratios of fission/corrosion products and lanthanides by ICP-MS as a function of the initial nitric acid concentration of the aqueous phase: RE1915 = 0.1 mol L^{-1}, 1 h, [M] = 10^{-5} mol L^{-1}, 25 °C, A/O = 1, 1 kBq of ^{152}Eu, ^{237}Np, ^{239}Pu, ^{241}Am, ^{244}Cm.

This project has received funding from the EURATOM research and training programme 2014–2018 under grant agreement No. 755171. The content of this deliverable reflects only the authors' view. The European Commission is not responsible for any use that may be made of the information it contains.

Extraction increased as the concentration of RE1915 in the organic phase increased, as shown for the radioactive elements (Figure 46) as for the inactive elements (Figure 47). However, at higher concentrations than 0.1 mol L^{-1}, there is a clear kink in the curves visible. This is also the point at which precipitation was visually observed at the interphases. Interestingly, the only elements which are almost not affected are Pu and Np.

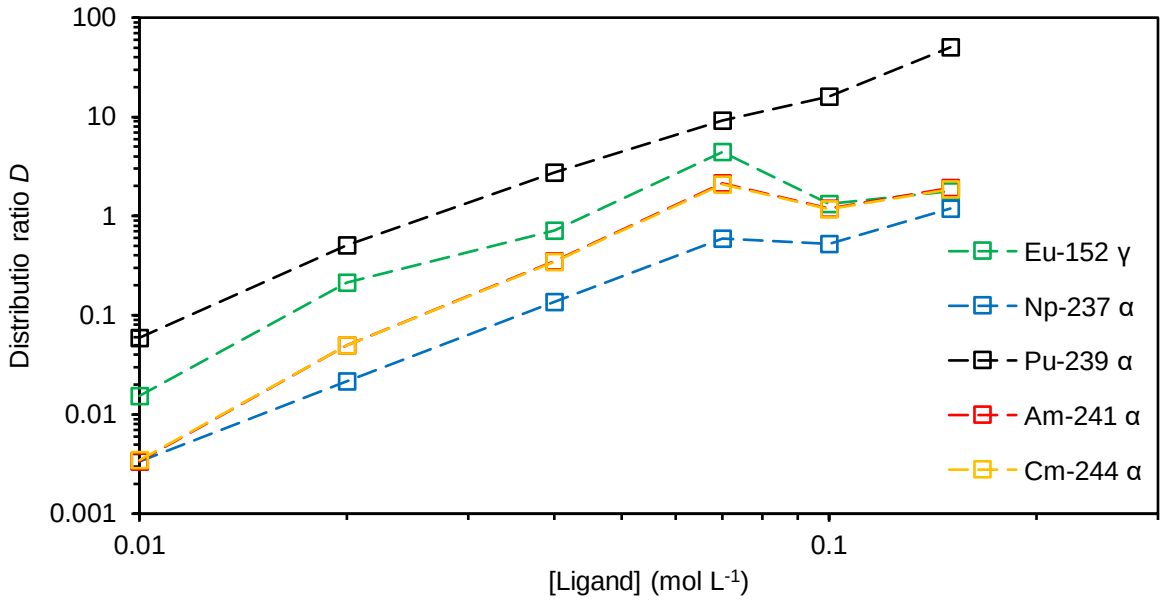

Figure 46. Distribution ratios of radiotracer elements by α and γ spectrometry as a function of the RE1915 concentration: [HNO_3] = 5 mol L^{-1}, 1 h, [M] = 10^{-5} mol L^{-1}, 25 °C, A/O = 1, 1 kBq of ^{152}Eu, ^{237}Np, ^{239}Pu, ^{241}Am, ^{244}Cm.

This project has received funding from the EURATOM research and training programme 2014–2018 under grant agreement No. 755171. The content of this deliverable reflects only the authors' view. The European Commission is not responsible for any use that may be made of the information it contains.

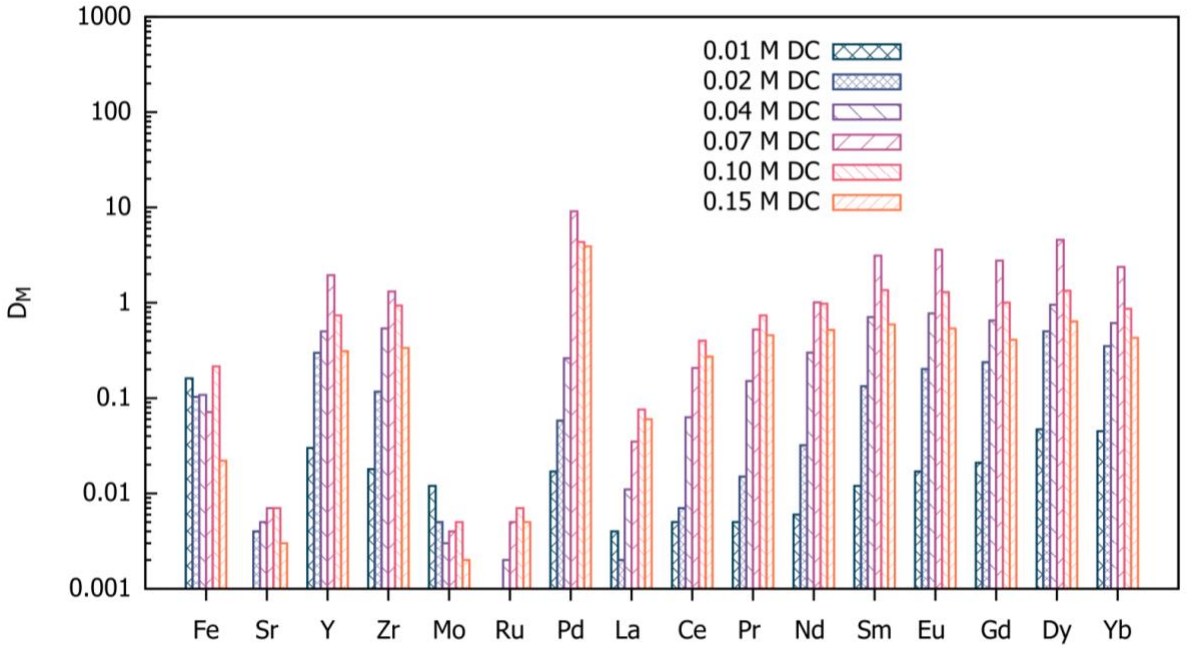

Figure 47. Distribution ratios of fission/corrosion products and lanthanides by ICP-MS as a function of the RE1915 concentration in the organic phase: [HNO_3] = 5 mol L^{-1}, 1 h, [M] = 10^{-5} mol L^{-1}, 25 °C, A/O = 1, 1 kBq of ^{152}Eu, ^{237}Np, ^{239}Pu, ^{241}Am, ^{244}Cm.

THEORETICAL STUDIES

First principle studies employing DFT calculations and radical Fukui functions were used to study the radiolysis of diglycolamides on a fundamental level. A manuscript presenting the results was submitted for publication [70]. The abstract from this paper is cited below:

"*Understanding the degradation mechanisms of organic compounds in an extreme radiolysis induced environment is important for designing efficient organic extractants for the separation of radionuclides from used nuclear fuel. In this paper, we present an in-depth computational-chemistry-based molecular level analysis of the radiolytic degradation of diglycolamides, with a focus on structural and thermodynamic aspects of the process. The most vulnerable parts of the organic ligands prone to attack and degradation by radicals are identified via electron density and bond strength analysis. We propose a combination of B88 and PBE exchange correlation functionals for the computationally efficient and accurate estimation of bond dissociation energies. A plausible degradation path is obtained by accounting for the impact of solvation on the thermodynamic quantities, including solvation entropy effects. This degradation mechanism is consistent with experimentally observed degradation products.*"

This project has received funding from the EURATOM research and training programme 2014–2018 under grant agreement No. 755171. The content of this deliverable reflects only the authors' view. The European Commission is not responsible for any use that may be made of the information it contains.

IRRADIATION LOOP TESTS OF NEW EURO-GANEX PROCESS

Authors: Iván Sánchez-García, Hitos Galán, Lorena Serrano and Sofía Durán (CIEMAT); X. Heres, S. Costenoble, S. Broussard, J. Sinot, L. Guillerme, J. Vincent, C. Sorel, M.C. Charbonnel (CEA).

INTRODUCTION

Along GENIORS project it has been designed and carried out an irradiation loops comparative study (CEA, INL, POLIMI, UNIPR, Julich, KIT-INE) which involves two irradiation facilities within GENIORS project (Marcel-CEA and Náyade-CIEMAT facilities) and the irradiation loop developed at INL-USA. The work presented in this section involved the studies done for evaluating the resistance of the new-EURO GANEX systems by using two of this irradiation loops, Náyade and Marcel Irradiation loops.

For the three loop tests of the comparative study, the main common features were previously fixed during the "LOOP" WEB MEETING (7 August 2020) according to the lasts experimental results of Julich laboratory [5]:

1. In a first step, the organic phase will be irradiated in contact with HNO_3 (concentration according to the preliminary flow-sheet) up to an integrated dose of ≈ 500 kGy. The aqueous phase may contain $Nd(NO_3)_3$ to allow on-line monitoring by absorption spectrometry.
2. In a second step, the irradiated organic phase will be contacted with the PTD solution, further irradiating to a representative dose to the actinide stripping section of a process test. A rough estimation of this dose will be made by KIT. Pre and post irradiation samples of organic and aqueous phases will be analysed using the methods available at the laboratories performing the tests. Furthermore, distribution ratios (Pu(IV), Am(III), Eu(III), important FP) will be determined using these samples.
3. Aqueous feed must contain 1 mmol/L of some metals such as Sr, La, Nd, and Eu. In general, spiked experiments were carried out for extraction tests and no scrubbing steps will be performed.
4. Organic solvent (0.4 mol/L cis-mTDDGA in *n*-dodecane, dd) be supplied by INL and PTD by UNIPR, for all labs. The concentration of PTD in 2.1 mol/L HNO_3 will depend on the type of irradiation experiment, but always distribution ratio measurements will be done using 0.4 mol/L of PTD, according to Julich laboratory studies.

This project has received funding from the EURATOM research and training programme 2014–2018 under grant agreement No. 755171. The content of this deliverable reflects only the authors' view. The European Commission is not responsible for any use that may be made of the information it contains.

NEW EURO-GANEX LOOP TEST AT NÁYADE IRRADIATION FACILTY

Náyade irradiation loop described in section before (see Figure 11; section *Irradiation loop design at Náyade facility of CIEMAT*) has been configured to simulate the two main steps of new EURO-GANEX process, i.e. An + Ln co-extraction and TRU stripping steps, as it was done with EURO-GANEX test. For that, a high accumulated dose over the organic solvent in contact with nitric acid was supplied, simulating the recycling of the organic phase; but a relatively low dose over the aqueous phase containing PTD was supplied, since it is not expected its recycling. PTD aqueous phase was irradiated in contact with the organic phase previously irradiated in the first step. A schematic representation of the main steps of the irradiation loop set-up, the composition of the phases during the different irradiation steps and the corresponding extraction experiments is shown in Figure 48 and Table 7.

For the first step (An + Ln co-extraction), it was carried out the irradiation up to an effective dose of 500 kGy of 0.4 mol/L cis-mTDDGA in dd in contact with 4.5 mol/L HNO_3 containing 1 mmol/L of SrO, $La(NO_3)_3$, Nd_2O_3, and $Eu(NO_3)_3 \cdot 6H_2O$. Along this first irradiation step the extraction assessment was carried by sampling both phases and spiking with ^{241}Am and ^{152}Eu as analogous of actinides and lanthanides, respectively. As the irradiation reactor (coil) is composed of 316 stainless steel (see HYPAR 7 CIEMAT [71]), main corrosion metals (Fe, Ni, Cr and Mo) were also considered. The corresponding distribution ratio were measured by gamma spectrometry and the ICP-MS techniques.

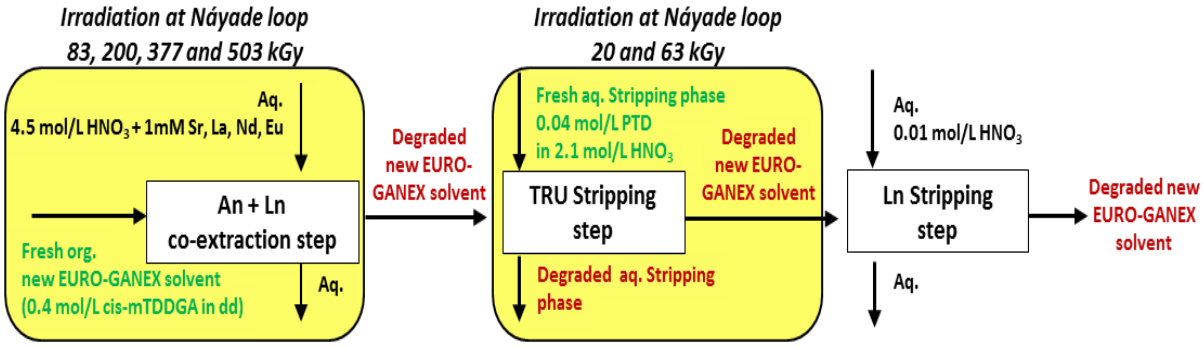

Figure 48. Scheme of the main steps of new EURO-GANEX process simulated at Náyade irradiation loop test.

For the second step, the TRU stripping, the degraded organic solvent was irradiated again up to additional effective 63 kGy but now in contact with an aqueous phase containing PTD in 2.1 mol/L HNO_3. According the last results of JUELICH laboratory [72], for distribution measurements, 0.4 mol/L PTD in 2.1 mol/L HNO_3 was fixed as the optimal composition of the aqueous phase. However, due to the impossibility to cover the PTD requirements for dynamic irradiation experiments, it was decided to uses aqueous phases consisting in 0.04 mol/L PTD in 2.1 mol/L HNO_3 just for irradiation and replace them for aqueous phase consisting in 0.4 mol/L PTD for the assessment of the extraction behaviour. The objective of irradiating 0.4 mol/L cis-mTDDGA in dd in contact with 0.04 mol/L PTD in 2.1 mol/L HNO_3 is to verify whether hydrodynamic problems could occur during this step. Therefore, to complete the study with the corresponding extraction assessment after irradiation it was necessary to perform an additional irradiation in static conditions. For that, 0.4 mol/L PTD in 2.1 mol/L HNO_3 was irradiated in static conditions up to 150 kGy, in contact with 0.4 mol/L m-TDDGA pre-equilibrated with 4.5 mol/L HNO_3.

This project has received funding from the EURATOM research and training programme 2014–2018 under grant agreement No. 755171. The content of this deliverable reflects only the authors' view. The European Commission is not responsible for any use that may be made of the information it contains.

Table 7. Composition of the organic and aqueous phases in the different steps of the irradiation test loop and the following extraction experiments.

Experiments		Solvent formulation	
		Organic phase	Aqueous phase
An+Ln co-extraction Step	a) Before Irradiation	Fresh new EURO-GANEX solvent	Fresh 4.5 mol/L HNO_3 + 1 mM Sr^{2+}, La^{3+}, Nd^{3+}, and Eu^{3+}
	1st Dynamic Irradiation (83, 200, 377 and 503 kGy)		
	b) Extraction after irradiation	Irradiated new EURO-GANEX solvent (83, 200, 377 and 503 kGy)	Irradiated (83, 200, 377 and 503 kGy) 4.5 mol/L HNO_3 + 1 mM Sr^{2+}, La^{3+}, Nd^{3+}, and Eu^{3+}
TRU stripping Step	a) Before Irradiation	Irradiated new EURO-GANEX solvent from the previous step (503 kGy)	Fresh PTD in 2.1 mol/L HNO_3
	2nd Dynamic Irradiation (20, 63 kGy)		
		Irradiated new EURO-GANEX solvent from the second step (566 kGy)	Fresh **0.04 mol/L PTD** in 2.1 mol/L HNO_3
	3rd Irradiation (Static irradiation: 20, 50, 100 and 150 kGy)		
		Pre-equilibrated fresh new EURO-GANEX solvent	Fresh **0.4 mol/L PTD** in 2.1 mol/L HNO_3
	b) Extraction after irradiation	Irradiated new EURO-GANEX solvent from the second step (566 kGy)	Irradiated Aq. phase (20, 50, 100 and 150 kGy)
Ln stripping Step	• Extraction	Irradiated new EURO-GANEX solvent from the 1st and 2nd dynamic irradiations	0.01 mol/L HNO_3

Therefore, following the simplified scheme shows in Figure 48, the CIEMAT loop test implied the following steps:

- *1º Dynamic irradiation up to 503 kGy*: Org. Ph: 0.4 mol/L m-TDDGA in dd; Aq. Ph: 4.5 mol/L HNO_3 + 1 mmol/L Eu, La, Nd, Sr.
  - Extraction assessment of Ln/An/FP/Corrosion metals: Irradiated Org. Ph: 0.4 mol/L m-TDDGA in dd; Irradiated Aq. Ph: 4.5 mol/L HNO_3 + 1 mmol/L Eu, La, Nd, Sr spiked with ^{241}Am + ^{152}Eu.
  - Assessment of TRU stripping: Irradiated and loaded Org. Ph; fresh Aq. Ph: 0.4 mol/L PTD in 2.1 mol/L HNO_3.
  - Assessment of Ln stripping: Org. Ph from TRU stripping; Aq. Ph: 0.01 mol/L HNO_3.
- *2º Dynamic irradiation up to 63 kGy*: Org. Ph: Irradiated and loaded 503 kGy from 1º irradiation; Aq. Ph: 0.04 mol/L PTD in 2.1 mol/L HNO_3.
- *3º Static irradiation with the nominal PTD concentration up to 150 kGy*: Org. Ph: 0.4 mol/L cis-mTDDGA in dd pre-equilibrated with 4.5 mol/L HNO_3; Aq. Ph: 0.4 mol/L PTD in 2.1 mol/L HNO_3.

This project has received funding from the EURATOM research and training programme 2014–2018 under grant agreement No. 755171. The content of this deliverable reflects only the authors' view. The European Commission is not responsible for any use that may be made of the information it contains.

- Assessment of TRU stripping: Irradiated and loaded Org phase from 2nd irradiation; irradiated Aq. phase from 3rd irradiation: 0.4 mol/L PTD in 2.1 mol/L HNO_3.

PHYSICO-CHEMICAL PROPERTIES OF IRRADIATED SAMPLES

After the first irradiation step (An + Ln co-extraction, Figure 48), organic phase suffered the typical colour changes from slightly yellow to dark yellow while the aqueous phase practically unchanged its colour (Figure 49A). For an absorbed doses up to 200 kGy, a turbidity and small precipitate in the organic phase can be observed, as it is shown Figure 49B for the sample irradiated at 377 kGy. For the extraction experiments, an homogenised organic sample for was employed.

Figure 49. A) Samples of the first irradiation step. Org. phase: 0.4 mol/L m-TDDGA in dd, Aq. phase: 4.5 mol/L HNO_3, with an accumulated dose of 0 kGy, 83 kGy, 200 kGy, 377 kGy and 503 kGy. B) Turbidity and small precipitate in the organic phase at 377 kGy.

Over the course of the second dynamic irradiation step (TRU stripping, Figure 48), the aqueous phase consisting in PTD changed its colour from slight yellow to dark yellow. These colour change should be related to its degradation. Moreover, in the final organic phase (irradiated at 563 kGy) a white precipitate was observed after a few days. Figure 50 shows the colour changes and the precipitate obtained in this organic phase. Therefore, mass balances of the metals should be carefully checked during the extraction results.

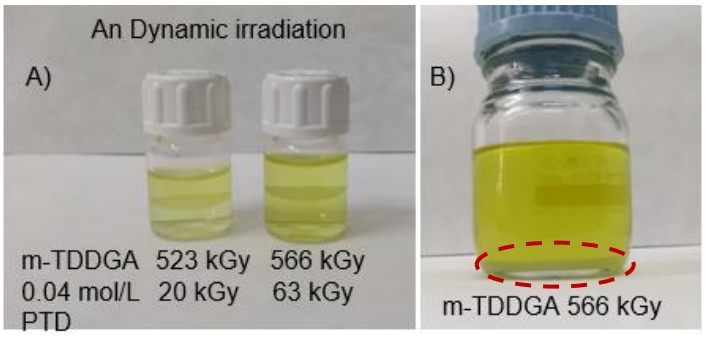

Figure 50. A) Samples of the second dynamic irradiation step. Org. phase: 0.4 mol/L cis-mTDDGA in dd, Aq. phase: 0.04 mol/L PTD in 2.1 mol/L HNO_3, with an accumulated dose of 20 kGy and 63 kGy. B) Sample of irradiated organic phase at 563 kGy containing a white precipitate.

This project has received funding from the EURATOM research and training programme 2014–2018 under grant agreement No. 755171. The content of this deliverable reflects only the authors' view. The European Commission is not responsible for any use that may be made of the information it contains.

As it was mentioned before, for TRU stripping assessment were considered the results reported by Wilden *et al.,* who showed an ineffective separation between An and Ln using 0.04 mol/L PTD [72], therefore, the irradiated 0.4 mol/L PTD in 2.1 mol/L HNO_3 in static conditions and in contact with 0.4 mol/L cis-mTDDGA pre-equilibrated with 4.5 mol/L HNO_3 was needed. The aqueous phase resulting from this irradiation was used for TRU stripping assessment (see Table 7). Figure 51 shows the colour changes observed during this static irradiation. No precipitates or third phases were observed now. That results would mean that the white precipitate observed after the 2nd dynamic irradiation comes from cis-mTDDGA degradation after a high dose.

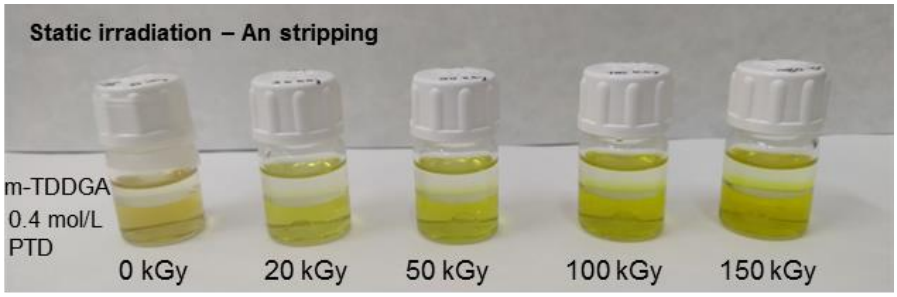

Figure 51. Samples of the static irradiation simulating the TRU stripping step. Org. phase: 0.4 mol/L m-TDDGA in dd pre-equilibrated with 4.5 mol/L HNO_3, Aq. phase: 0.4 mol/L PTD in 2.1 mol/L HNO_3, with an accumulated dose of 0 kGy, 20 kGy, 50 kGy, 100 kGy and 150 kGy.

In order to analyse the precipitate found in organic phase just after the dynamic irradiation at 566 kGy, a sample of this organic phase was filtered. The solid obtained was not completely dried, and it appeared that it might contain traces of the organic solution. This solid was dissolved in nitric acid and analysed by ICP-MS and HPLC-MS. HPLC-MS measurements are still in progress. The results obtained by ICP-MS showed a relevant concentration of La (~150 mg/L), Nd (~565 mg/L) and Eu (~384 mg/L).

All solubility problems observed after irradiation have to be considered for the deepest studies, but also, although it is not expected a low temperature during process operation, organic solvent solubility must be checked since some issues were observed when samples were refrigerated. The normal procedure after irradiation involves the refrigeration (at 5ºC) of all samples before be analysed. During this period, a white precipitate in the aqueous phase was found in some samples (Figure 52). Unexpectedly, the higher amount of precipitate was observed in the unirradiated sample containing 0.4 mol/L cis-mTDDGA in dd in contact with 0.4 mol/L PTD in 2.1 mol/L HNO_3. The precipitates despaired at room temperature and the volume of the organic phase increases.

This project has received funding from the EURATOM research and training programme 2014–2018 under grant agreement No. 755171. The content of this deliverable reflects only the authors' view. The European Commission is not responsible for any use that may be made of the information it contains.

Figure 52. Precipitated observed in the refrigerated samples.

EXTRACTION EXPERIMENTS CORRESPONDING TO AN+LN CO-EXTRACTION STEP

The D values variation of Am and Eu observed as a function of the dose for this first irradiation step is shown in Figure 53. As expected, Ln(III) and An(III) were well extracted into the organic phase even after a 503 kGy of absorbed dose although a slight decrease in the D values is observed for both families of elements.

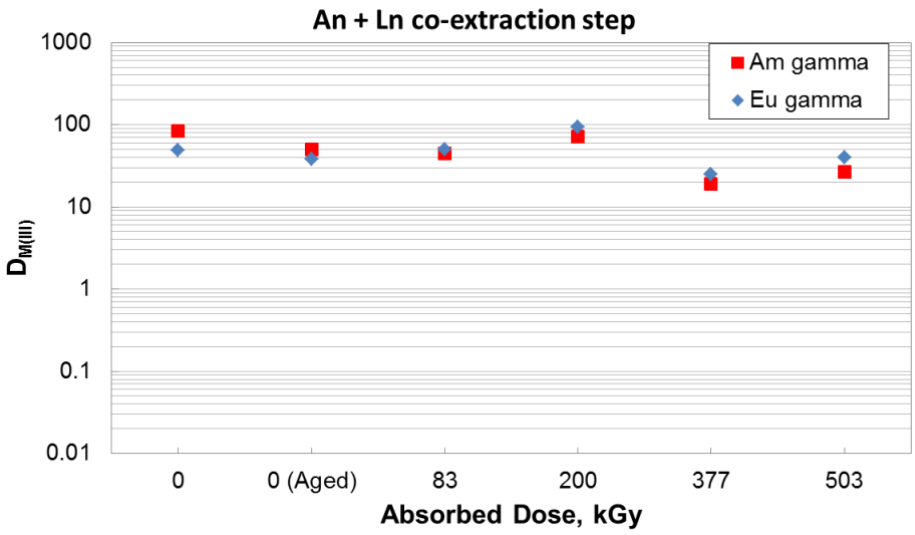

Figure 53. Distribution ratios of Am(III) and Eu(III) as a function of absorbed dose for the first step of irradiation (An + Ln co-extraction, Figure 48). Org. phase: Irradiated 0.4 mol/L cis-mTDDGA in dd. Aq. phase: Irradiated 4.5 mol/L HNO_3 with 1 mmol/L of Sr, La, Nd, and Eu and spiked with ^{241}Am and ^{152}Eu.

Figure 54 shows the results obtained by ICP-MS for the extraction of Sr, La, Nd and Eu analysed as function of the dose. All metals were well extracted into the organic phase (D>1) for the unirradiated samples, *i.e.* cis-mTDDGA extracts Ln and An, but also coextracts Sr. As absorbed dose increased, the coextraction of Sr was significantly affected after 500 kGy. Distribution ratios for Ln elements decreased as a function of absorbed but

This project has received funding from the EURATOM research and training programme 2014–2018 under grant agreement No. 755171. The content of this deliverable reflects only the authors' view. The European Commission is not responsible for any use that may be made of the information it contains.

it remains higher than 1. All these results are coherent and in agreement with the studies reported by Julich reports [73, 74]. Although the D_{Eu} values obtained for ICP-MS and gamma techniques are not in a perfect agreement, the trends are similar.

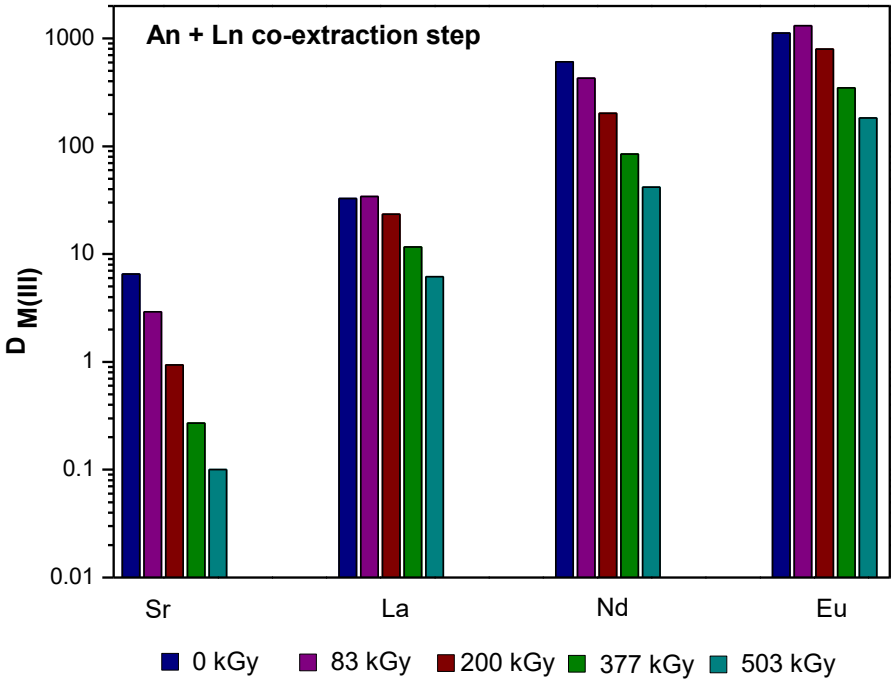

Figure 54. Distribution ratios of the inactive Sr(II), La(III), Nd(III) and Eu(III) as a function of the absorbed dose for the first step of irradiation (An + Ln co.extraction). Org. phase: Irradiated 0.4 mol/L m-TDDGA in dd. Aq. phase: Irradiated 4.5 mol/L HNO_3 with 1 mmol/L of Sr, La, Nd and Eu and spiked with ^{241}Am and ^{152}Eu

The acid concentration of the aqueous phase along the irradiation was also checked. The proton concentration decreased from 4.23 mol/L for unirradiated HNO_3 to 3.52 mol/L for the irradiated at 503 kGy during the An+Ln co-extraction step.

As it was done in the previous experiment of EURO-GANEX, the metals Fe, Ni, Cr and Mo were evaluated during the process since the irradiation reactor (coil) is composed of 316 stainless steel. Figure 55 shows the evolution of the Fe, Ni and Cr concentrations in some organic and aqueous phases along the first irradiation step (An + Ln co-extraction). The concentration of Cr and Ni in the organic phase were lower than 0.001 mmol/L as well Mo in both phases. Therefore, these data were not included in Figure 55. The concentration of corrosion metals represented increases as a function of absorbed dose, being the most abundant Fe, Cr and Ni. These metals are mainly found in the aqueous phase with a concentration of ~1.31 mmol/L, ~0.33 mmol/L and ~0.18 mmol/L, respectively. Only a low concentration of Fe (~0.01 mmol/L) was found in the organic phase after irradiation process.

This project has received funding from the EURATOM research and training programme 2014–2018 under grant agreement No. 755171. The content of this deliverable reflects only the authors' view. The European Commission is not responsible for any use that may be made of the information it contains.

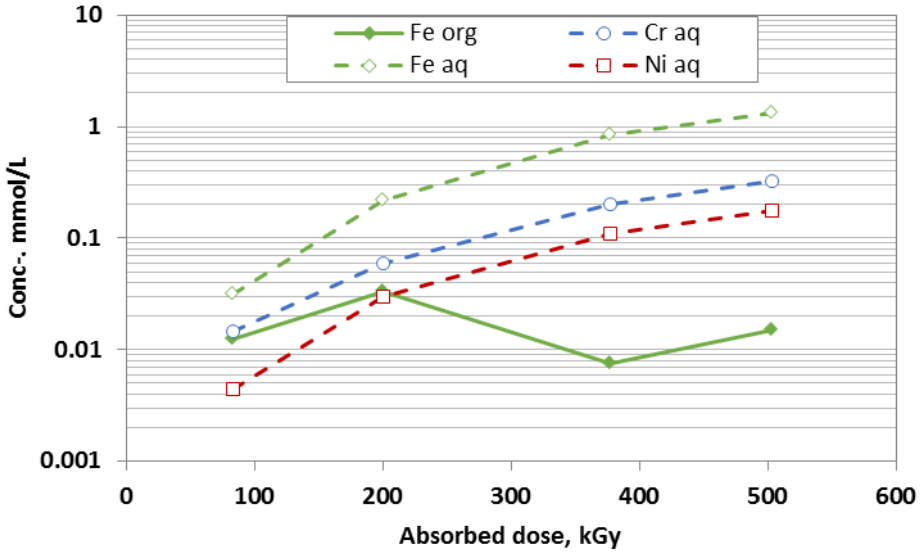

Figure 55. Evolution of the concentration of stainless steel corrosion products Fe, Cr, Ni and Mo during An+Ln co-extraction step of new EURO-GANEX irradiation loop.

EXTRACTION EXPERIMENTS CORRESPONDING TO TRU AND LN STRIPPING STEP

Figure 56 shows the distribution ratios of Eu and Am as a function of absorbed dose for the TRU extraction performance of the loop test. The organic phase employed is always 0.4 cis-mTDDGA after 563 kGy and the aqueous phase corresponds to fresh and irradiated 0.4 mol/L PTD in 2.1 mol/L HNO_3 up to 150 kGy in static conditions (see initial description of the experiment). Results show a general efficient separation between An and Ln. Moreover, it seems that the system maintains a good stability against radiation, as Mossini *et al.,* reported for initial PTD degradation studies [57], and Juelich reported in GENIORS HYPAR 5 and 6 for cis-mTDDGA degradation [73, 74].

This project has received funding from the EURATOM research and training programme 2014–2018 under grant agreement No. 755171. The content of this deliverable reflects only the authors' view. The European Commission is not responsible for any use that may be made of the information it contains.

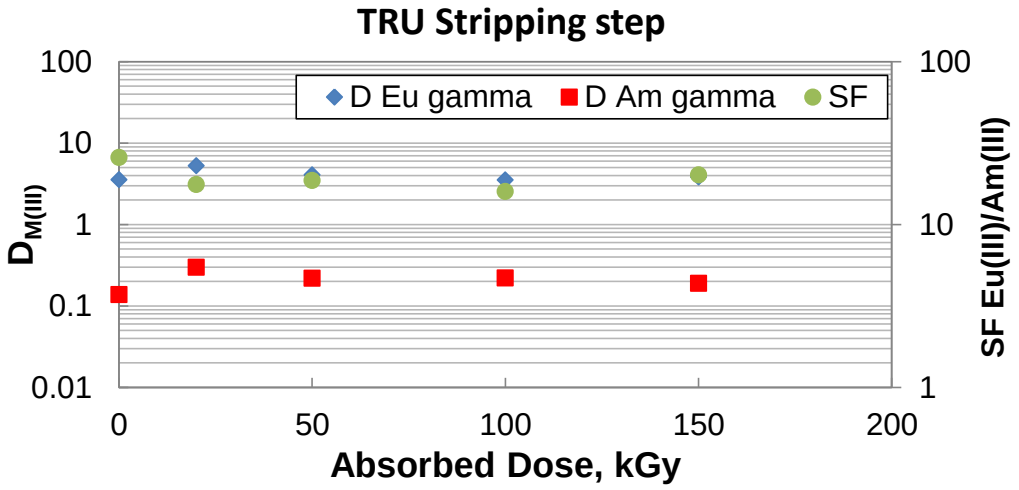

Figure 56. Distribution ratios of Am(III) and Eu(III) as a function of absorbed dose for the second step of irradiation (TRU stripping, Figure 48). Org. Phase : Irradiated 0.4 mol/L m-TDDGA in dd at 563 kGy. Aq. Phase : Irradiated 0.4 mol/L PTD in 2.1 mol/L HNO_3 up to 150 kGy and spiked with ^{241}Am and ^{152}Eu. The initial concentrations in the first step were 1 mmol/L of Sr, La, Nd, and Eu.

Figure 57 shows the results obtained by ICP-MS for the extraction of La, Nd and Eu metals corresponding to the TRU stripping step of loop test. Sr remained in the aqueous phase after the An+Ln co-extraction loop step, consequently, during the TRU stripping step Sr is not detected. Nd and Eu were extracted into the organic phase, but La mainly back-extracted in the aqueous phase. The separation of Am from the lanthanides is governed by the least extractable lanthanide, La. Therefore, in these conditions, the $SF_{La/Am}$ values (calculated for $D_{La\ ICP\text{-}MS}/D_{Am\ gamma}$ (showed in Figure 56)) kept between 4-5 for independently of the observed dose. These results are in agreement with those obtained by Wilden *et al.,* who reported a $SF_{La/Am}$=4.8, but with a D_{La} value of 0.56 [72]. However, it should be noted that the mass balance for La, during ICP-MS measurements was more problematic than the other elements. The presence of the white precipitate mentioned in sections before could explain this result. The possible formation of precipitates is an important issue in process development and must be addressed in the future.

This project has received funding from the EURATOM research and training programme 2014–2018 under grant agreement No. 755171. The content of this deliverable reflects only the authors' view. The European Commission is not responsible for any use that may be made of the information it contains.

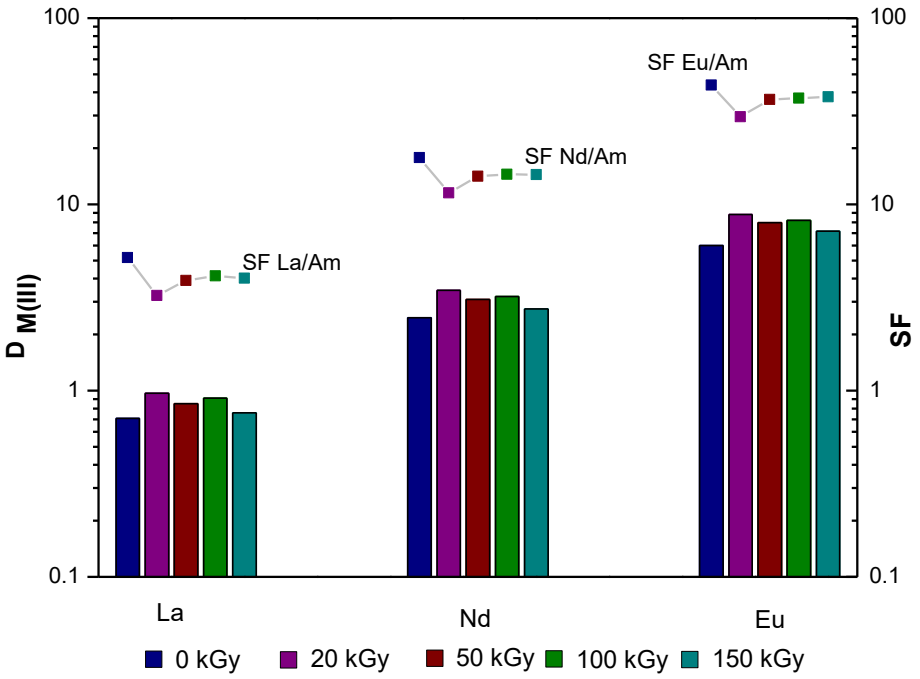

Figure 57. Distribution ratios of the inactive elements La(III), Nd(III) and Eu(III) as a function of the absorbed dose for the second step of irradiation (TRU stripping, Figure 48). Org. Phase: Irradiated 0.4 mol/L m-TDDGA in dd at 563 kGy. Aq. Phase: Irradiated 0.4 mol/L PTD in 2.1 mol/L HNO_3 up to 150 kGy spiked with ^{241}Am and ^{152}Eu. The initial concentrations in the first step were 1 mmol/L of Sr, La, Nd, and Eu.

The acid concentration in the aqueous phase after the extraction assessments was also checked, being practically unchanged after the absorbed doses received (150 kGy in static conditions, and 63 kGy in dynamic conditions).

In order to evaluate the corrosion metals during the irradiation process in this step (TRU stripping), the final organic (cis-mTDDGA 566 kGy) and aqueous (0.04 mol/L PTD in 2.1 mol/L HNO_3) phases were analysed by ICP-MS. The metals Fe, Cr and Ni were detected only in the aqueous phase with a concentration of ~0.109 mmol/L, ~0.021 mmol/L and ~0.012 mmol/L, respectively. In the organic phase, the concentration obtained were lower than ~0.002 mmol/L for these metals, and Mo concentrations were lower than 0.0002 mmol/L in both phases. This is probably related to the acidity employed in this step, as occurs in the EURO-GANEX process results.

Taking into account the metal concentrations obtained in the irradiated organic phase at 566 kGy, during the extraction in contact with fresh and irradiated 0.4 mol/L PTD in 2.1 mol/L HNO_3, a lower concentration of these metals is presented in the aqueous phase.

Additionally, the irradiated organic phase during the An+Ln co-extraction was put in contact with fresh 0.4 mol/L PTD in 2.1 mol/L HNO_3 (named An Stripping 1.1), and then replaced by 0.01 mol/L HNO_3 in order to simulate the sequence of TRU and Ln stripping steps. The aim of this experiment is to evaluate the affects over TRU and Ln stripping performance due to the degradation of the organic solvent *i.e.* the formation of cis-mTDDGA DCs. Table 8 shows the composition of both phases during this experiment (An Stripping 1.1 + Ln Stripping).

This project has received funding from the EURATOM research and training programme 2014–2018 under grant agreement No. 755171. The content of this deliverable reflects only the authors' view. The European Commission is not responsible for any use that may be made of the information it contains.

Table 8. Composition of the organic and aqueous phases during the An Stripping 1.1 and Ln Stripping experiments.

Step	Org ph.	Aq ph.: An Stripping	Aq. ph.: Ln Stripping
An Stripping 1.1 + Ln Stripping 1.1	cis-mTDDGA 0 kGy cis-mTDDGA 83.8 kGy cis-mTDDGA 200 kGy cis-mTDDGA 377.28 kGy cis-mTDDGA 503 kGy	PTD 0.4 mol/L 0 kGy in 2.1 mol/L HNO_3	0.01 mol/L HNO_3

Figure 58 shows the distribution ratios for Eu and Am during the An Stripping 1.1. An unexpected value of D_{Am} (D_{Am} >1) was found when the organic phase is unirradiated. According to Wilden *et al.* results [72], when both phases are fresh this value should be less than 1, producing an effective separation of these elements. The difference observed could be related to the purity of the solvent, since similar were found during Marcel loop test. As increased the absorbed dose a better performance of the Eu/Am separation was achieved, reaching a $SF_{Eu/Am}$ = 19, since D_{Am} were more affected than D_{Eu}.

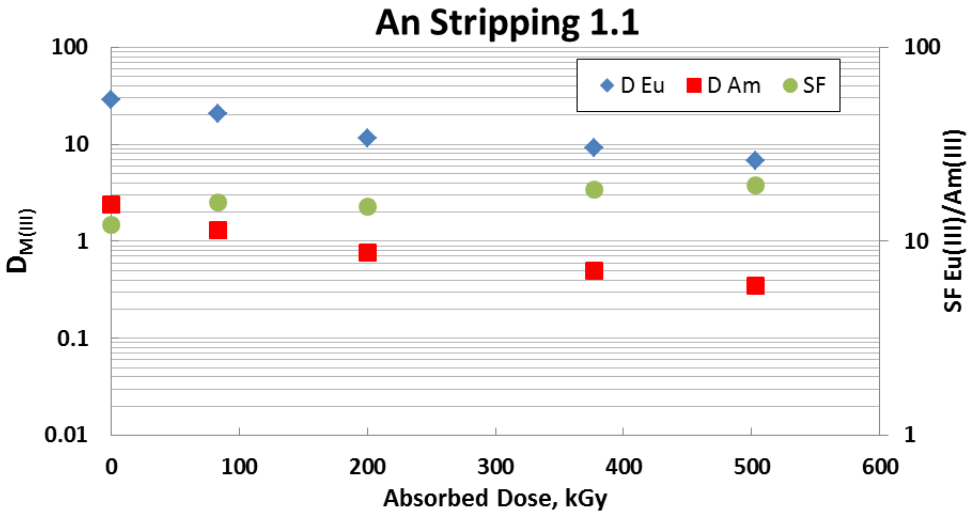

Figure 58 Distribution ratios of Am(III) and Eu(III) as a function of absorbed dose for the An stripping 1.1 experiment. Org. Phase : Fresh and Irradiated 0.4 mol/L m-TDDGA in dd up to 503 kGy. Aq. Phase : Fresh 0.4 mol/L PTD in 2.1 mol/L HNO_3 and spiked with ^{241}Am and ^{152}Eu. The initial concentrations in the first step were 1 mmol/L of Sr, La, Nd, and Eu.

Regarding the inactive elements during the An Stripping 1.1, Figure 59 shows the distribution ratios of the Sr, La, Nd and Eu as a function of absorbed dose for the organic phase obtained for ICP-MS. As in Figure 54, as cis-mTDDGA is irradiated, the Sr is mainly found in the aq. phase. All the rest of the elements are maintained in the irradiated organic phase, even in the presence of PTD solvent, as expected.

This project has received funding from the EURATOM research and training programme 2014–2018 under grant agreement No. 755171. The content of this deliverable reflects only the authors' view. The European Commission is not responsible for any use that may be made of the information it contains.

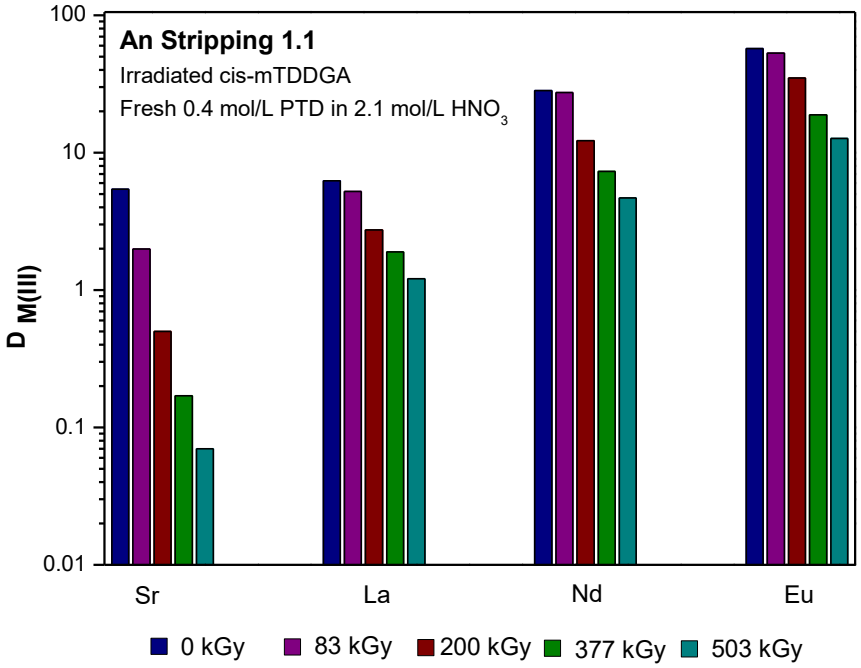

Figure 59 Distribution ratios of the inactive Sr(II), La(III), Nd(III) and Eu(III) as a function of the absorbed dose obtained by ICP-MS for the An stripping 1.1 experiment. Org. Phase : Fresh and Irradiated 0.4 mol/L m-TDDGA in dd up to 503 kGy. Aq. Phase : Fresh 0.4 mol/L PTD in 2.1 mol/L HNO_3 and spiked with ^{241}Am and ^{152}Eu. The initial concentrations in the first step were 1 mmol/L of Sr, La, Nd, and Eu.

After An stripping 1.1, the organic phase was used for the Ln stripping experiment and for that, the same evaluation for Am and Eu and inactive elements were carried out. Figure 60 shows the D_{Am} and D_{Eu} obtained for the Ln stripping. As expected, all D values are lower than 1, in agreement with the results obtained by Wilden *et al.,* [72]. However, for the trend observed, it seems to that the possible formation of cis-mTDDGA degradation compounds could influence in the extraction of Eu and Am, increasing the D values as a function of absorbed dose.

This project has received funding from the EURATOM research and training programme 2014–2018 under grant agreement No. 755171. The content of this deliverable reflects only the authors' view. The European Commission is not responsible for any use that may be made of the information it contains.

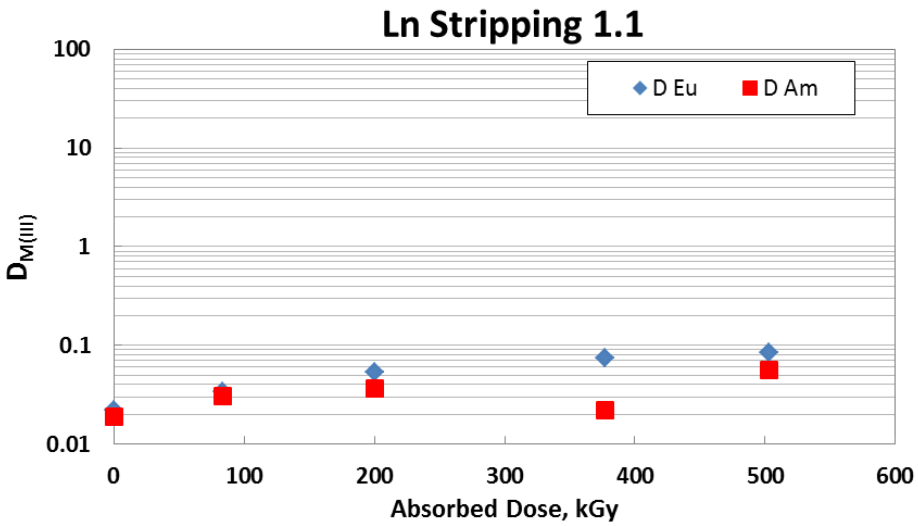

Figure 60 Distribution ratios of Am(III) and Eu(III) as a function of absorbed dose for the Ln stripping experiment. Org. Phase : Fresh and Irradiated 0.4 mol/L m-TDDGA in dd up to 503 kGy from An stripping 1.1 experiment. Aq. Phase : 0.01 mol/L HNO_3. The initial concentrations in the first step were 1 mmol/L of Sr, La, Nd, and Eu.

Figure 61 shows the distribution ratios obtained by ICP-MS for the inactive elements during the Ln stripping 1.1. As Sr is only contained in the fresh and irradiated organic phase at 83 kGy, in this figure, only Sr is observed in these absorbed doses. Concerning La, Nd and Eu, the D values are lower than 0.1 for all cases, as expected. In the case of Nd and Eu, for the samples in which the organic phase is irradiated at 377 and 503 kGy, the D_{Nd} and D_{Eu} increase slightly. This result can be related to the formation of some cis-mTDDGA DCs, which are able to extract some metals, as reported Wilden *et al.,* in the section of "results of batch extraction experiments" with different cis-mTDDGA DCs of this deliverable.

This project has received funding from the EURATOM research and training programme 2014–2018 under grant agreement No. 755171. The content of this deliverable reflects only the authors' view. The European Commission is not responsible for any use that may be made of the information it contains.

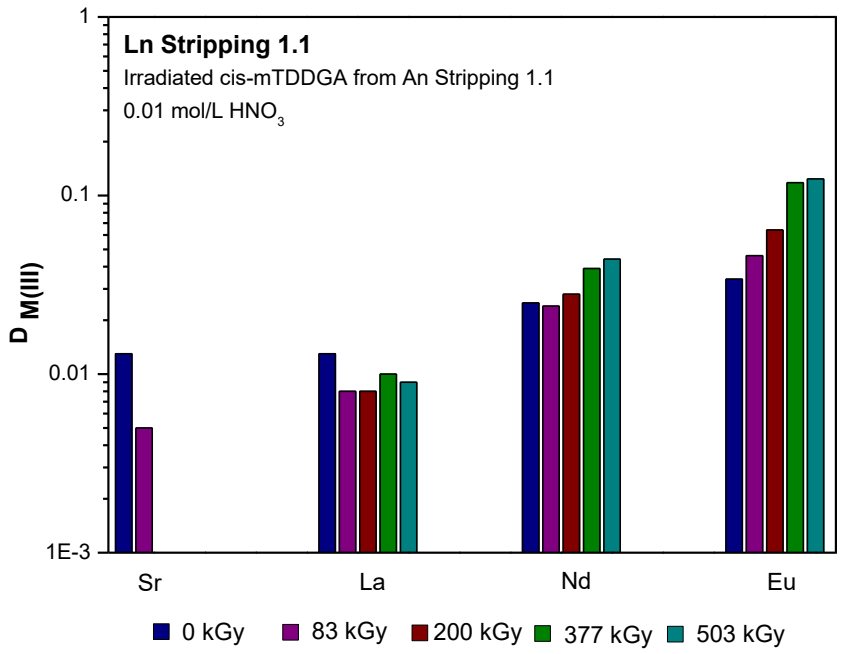

Figure 61 Distribution ratios of the inactive Sr(II), La(III), Nd(III) and Eu(III) as a function of the absorbed dose obtained by ICP-MS for the Ln stripping 1.1 experiment. Org. Phase : Fresh and Irradiated 0.4 mol/L m-TDDGA in dd up to 503 kGy from An stripping 1.1 experiment. Aq. Phase: 0.01 mol/L HNO_3. The initial concentrations in the first step were 1 mmol/L of Sr, La, Nd, and Eu.

Experiments are underway to study the possible effect of PTD DCs (employing irradiated PTD samples in the stripping) over the Ln stripping in order to understand the performance of the complete system.

QUANTIFICATION OF PTD

The quantification of PTD employed in this irradiation loop has been carried out by HPLC-MS. For that, a methodology was previously created in our equipment in order to analyse the degraded samples. The results of the quantitative measurements with HPLC-MS for irradiated PTD in static conditions up to 150 kGy are shown in Figure 62. The outcomes highlight the resistance of this molecule in the absorbed doses studied and this is in agreement with Mossini *et al.,* [57], who not detected relevant degradation after 250 kGy.

This project has received funding from the EURATOM research and training programme 2014–2018 under grant agreement No. 755171. The content of this deliverable reflects only the authors' view. The European Commission is not responsible for any use that may be made of the information it contains.

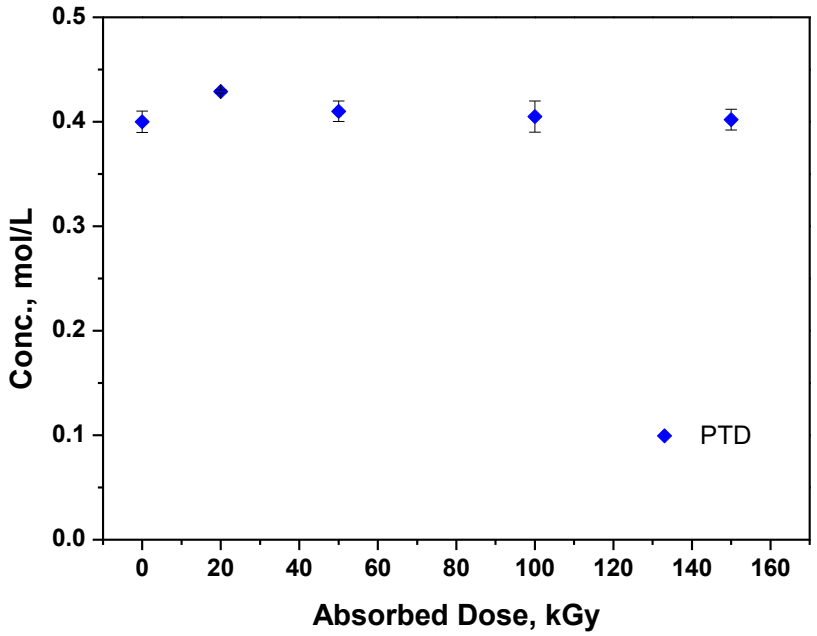

Figure 62. PTD concentration obtained by HPLC-MS as a function of absorbed dose for the new EURO-GANEX test irradiation loop of the TRU stripping step.

QUANTIFICATION OF cis-mTDDGA

The degradation of mTDDGA was quantified using the HPLC-MS methodology created at CIEMAT. Figure 63 shows the quantification obtained. As Julich reported in their HYPARS [73, 74], the degradation of mTDDGA follows a kinetic law of order 1 with respect to the monoamide concentration. With the dose rate, it is possible to express the concentration as a function of the dose integrated by the solvent following the next equation: $C = C0\ e^{-k'dos}$. By plotting the concentrations C as a function of absorbed dose (in kGy), it is possible to determine a constant k' by applying the relation: $k'\ (kGy^{-1}) = \ln(C/C0)$ / dose (kGy). This kinetic degradation constant k' allows the overall stability of extractant to be compared, independently of their concentration in solution. From the results obtained in Figure 63, the value k' is 0.0024 kGy^{-1}. This value is in perfect agreement with the obtained by Julich and reported in their HYPAR 5 (0.0027 kGy^{-1} when 0.05 mol/L mTDDGA is irradiated in contact with 2.5 mol/L HNO_3) [74]. Other way, this degradation seems to have a limited impact on the extraction performance, which could be explained by the DCs extraction properties, since some of them could maintain the original performance as was shown in previous sections.

This project has received funding from the EURATOM research and training programme 2014–2018 under grant agreement No. 755171. The content of this deliverable reflects only the authors' view. The European Commission is not responsible for any use that may be made of the information it contains.

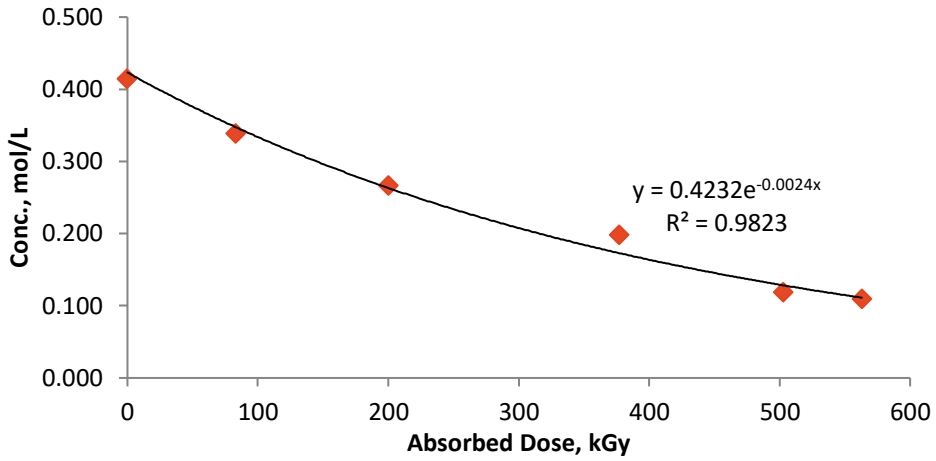

Figure 63. mTDDGA concentration as a function of the dose obtained by HPLC-MS for the New EURO-GANEX system.

The identification of the PTD DCs is currently underway as well as the identification of cis-mTDDGA DCs by HPLC-MS. Moreover, additional parameters as viscosity are currently underway in order to characterise the degraded samples.

This project has received funding from the EURATOM research and training programme 2014–2018 under grant agreement No. 755171. The content of this deliverable reflects only the authors' view. The European Commission is not responsible for any use that may be made of the information it contains.

NEW EURO-GANEX MARCEL LOOP TEST IN MARCOULE FACILITY

INTRODUCTION

In G1 facility at Marcoule center, the CEA has set up a research irradiator called MARCEL (*Advanced Radiolysis Module in Liquid-Liquid Extraction Cycles*) providing a total activity of 173 TBq thanks to four ^{137}Cs sources. This device could be coupled with PROUST (*Uranium Research and Optimization Pilot for Separation Processes*), a liquid-liquid extraction process platform with mixer-settlers or centrifugal contactors to simulate the extraction cycle part of a reprocessing plant. A MARCEL GENIORS loop test was carried out with the mTDDGA solvent during 6 weeks, continuously, in order to follow the impact of radiolysis degradation on hydrodynamics and performance behaviour of this solvent in the three main steps of a GANEX 2nd cycle type process.

In the first part of this report, the simplified model developed to design the flowsheet of this MARCEL loop test will be presented. In order to minimize solvent need, each process step is operated in only four stages. Moreover, since it is not possible to handle americium in the PROUST platform, we just add in feed solution neodymium nitrate to simulate the behaviour of rare earth family. In this process, the PTD aqueous reagent is required to perform lanthanides/actinides separation. At the beginning of the test, we injected a 0.04 mol/L PTD solution to check if there is or not hydrodynamic troubles with this aqueous phase in our mixer-settlers. Since PTD is not commercially available and Am is not in the feed solution, it was not necessary to waste this reagent during all the loop test. However, performances were assessed thanks to ^{241}Am/^{152}Eu batch experiments with irradiated solvent samples and PTD in aqueous phases. In order to check that good actinides/lanthanides separation yields could be obtained with mTDDGA solvent and PTD aqueous phase, a flowsheet with 12 stages were successfully calculated using the simplified model.

During the loop test, solvent samples were collected every 25 kGy of irradiation dose in order to characterize them and to carry out ^{241}Am/^{152}Eu batch experiments. The first week was devoted to check the proper operation of each automatic system, pump, flowmeter and scale before allowing the platform to run continuously with minimal human intervention. ICP-OES Nd measurement were performed during this first shift-work week to validate the on-line spectrophotometric measurements.

After the end of the test, every aqueous phase in mixer-settlers was collected to measure the Nd concentration profile in each step of the process. This profile was compared to the calculated one. Several irradiated solvent samples were chosen to perform ^{241}Am/^{152}Eu batch extractions for the three main steps of the process.

DESIGN OF THE FLOWSHEET OF MARCEL LOOP TEST

BACKGROUND, MODELLING

The organic phase is composed of cis-mTDDGA extractant diluted in n-dodecane. To separate americium, curium from lanthanides, Py-Tri-diol or PTD is injected in a second step [75]: lanthanides remain in the solvent whereas actinides are selectively stripped in the aqueous phase. Figure 64 gives the structural formula of these molecules.

This project has received funding from the EURATOM research and training programme 2014–2018 under grant agreement No. 755171. The content of this deliverable reflects only the authors' view. The European Commission is not responsible for any use that may be made of the information it contains.

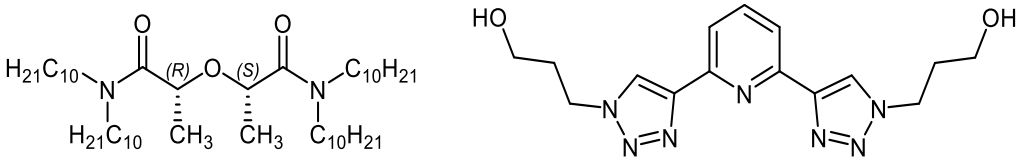

***cis*-mTDDGA** **PyTri-diol or PTD**

Figure 64 mTDDGA extractant diluted in n-dodecane in the organic phase and aqueous PTD reagent used for lanthanides/actinides separation step.

As it was mentioned at the beginning of the section, CEA, CIEMAT and Idaho National Laboratory have received the same solvent batch prepared by Santa Jansone-Popova in Oak Ridge National Laboratory (USA), and the same PTD batch prepared by Alessandro Casnati of Parma University (Italy). It would therefore be easier to compare the data obtained after irradiation in the three Institutes. This organic phase is almost the same as that used by Andreas Wilden *and al.[72]* to perform batch experiments with several fission products or actinides in trace amounts. However, Wilden's solvent came not from the same batch as ours, and the mTDDGA concentration was not measured before these experiments. Assuming that the two solvents were the same, we developed an interpolated model based on the values from Wilden's experiments.

The flowsheet of lanthanides/actinides separation consists of three main steps:

- Actinides, lanthanides co-extraction (AX) in nitric acid medium (> 4 mol/L)
- Lanthanides/actinides separation (BX) thanks to PTD reagent solubilized in moderated nitric acid medium (≈ 2 mol/L)
- Lanthanides stripping step (CX) in low nitric acid medium (0.01 mol/L < $[H^+]$ < 1 mol/L)

The goal was to design a flowsheet for GENIORS MARCEL loop test within the following operating constraints to save solvent volume:

- 4 stages par each step
- No solvent treatment
- No hydrolysis reactor

We interpolated the experimental distribution ratios without or with PTD in aqueous phase (see Figure 65, Figure 66 and Figure 67). Using these interpolations, we were able to calculate distribution ratios for the major lanthanides, americium and curium, under different conditions of acidity or PTD concentrations. The actinide/lanthanide separation can only be effective with a solution containing more than 0.4 mol/L of PTD in a nitric acid concentration higher than 2 mol/L. In the extraction step (AX), with high nitric acidity, neodymium behaves like americium and curium while Nd behaviour is quite comparable to other rare earths from fission products in the lanthanide/actinide separation step (BX). Lanthanum is the least separated from americium, but since on-line spectrophotometry could not detect this cation, we prefer to use only neodymium in the feed solution of the GENIORS MARCEL loop test to ensure to follow it during the test.

This project has received funding from the EURATOM research and training programme 2014–2018 under grant agreement No. 755171. The content of this deliverable reflects only the authors' view. The European Commission is not responsible for any use that may be made of the information it contains.

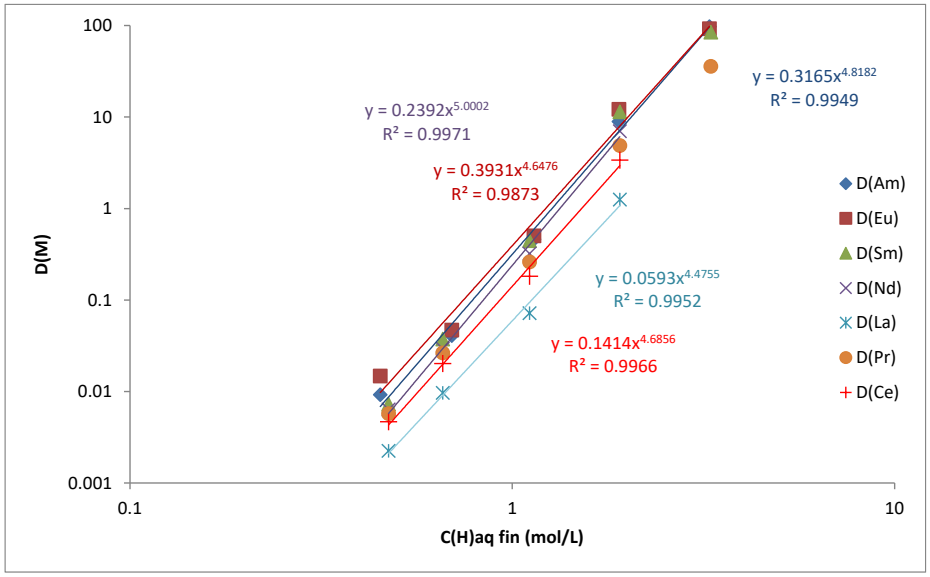

Figure 65 Experimental batch data and equations in our simplified model for trace amounts of lanthanides with cis-mTDDGA 0.4 mol/L in n-dodecane and variable nitric acid concentrations[72].

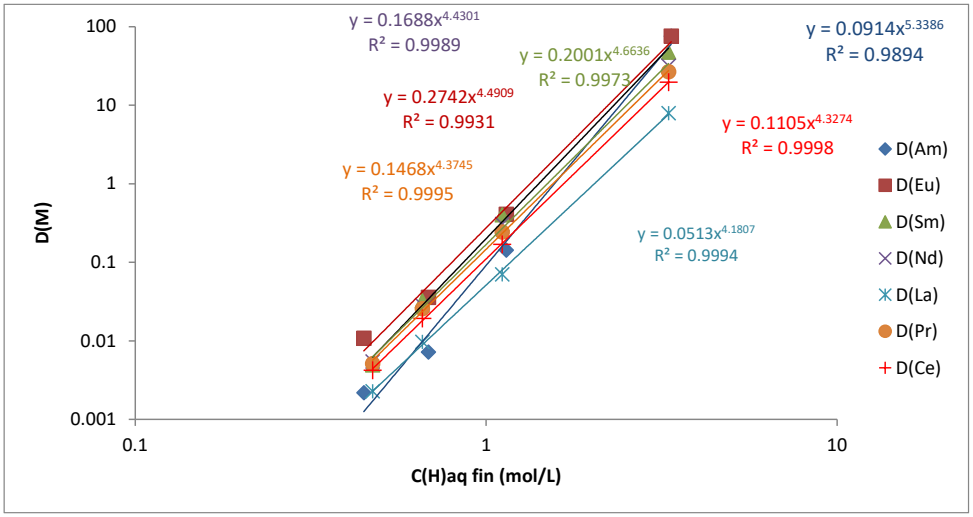

Figure 66 Experimental batch data and equations in our simplified model for trace amounts of lanthanides with cis-mTDDGA 0.4 mol/L in n-dodecane and 0.04 mol/L PTD in variable nitric acid concentrations[72].

This project has received funding from the EURATOM research and training programme 2014–2018 under grant agreement No. 755171. The content of this deliverable reflects only the authors' view. The European Commission is not responsible for any use that may be made of the information it contains.

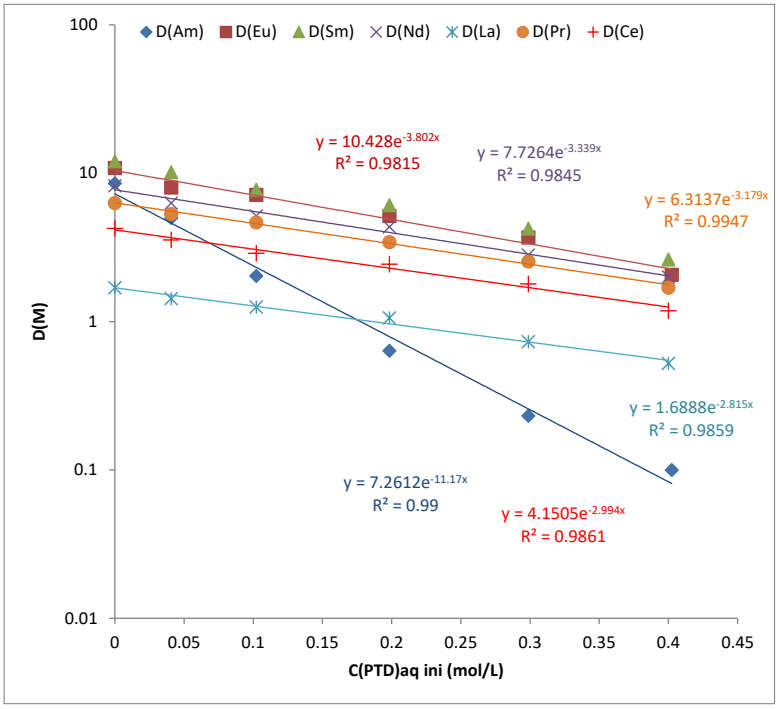

Figure 67 Experimental batch data and equations in our simplified model for traces amount of lanthanides with cis-mTDDGA 0.4 mol/L in n-dodecane and variable PTD concentrations in 2.1 mol/L nitric acid[72].

FLOWSHEET OF THE MARCEL LOOP TEST

Figure 68 gives the flowsheet of MARCEL GENIORS loop test. The italics indicate the initial values of the flowsheet that have been modified during the test due to hydrodynamic problems (see next subsection). In order not to waste the molecule, we decided to use the PTD for only 10 hours in the BX step. The objective was to verify that there was no hydrodynamic trouble caused by this aqueous molecule. Since there was no americium in the feed solution, it was not useful to set the PTD concentration to 0.4 mol/L as expected in the process. We have injected in the BX step, an aqueous solution with only 0.04 mol/L of PTD. An optimal concentration of 0.4 mol/L PTD was tested during batch experiments. We calculated that this concentration allows efficient separation of americium, curium from lanthanides. With 8 stages of Ln scrubbing (Q_{org}=15mL/h, Q_{aq}=20 mL/h) and 8 stages of An stripping (Q_{org}=15+50mL/h, Q_{aq}=20mL/h), using an aqueous phase of 0.4 mol/L PTD and 2.3 mol/L HNO_3, we could recover 99.9% of Am and Cm with less than 0.2% La, 0.01% Ce and 1.10^{-5}% Nd.

This project has received funding from the EURATOM research and training programme 2014–2018 under grant agreement No. 755171. The content of this deliverable reflects only the authors' view. The European Commission is not responsible for any use that may be made of the information it contains.

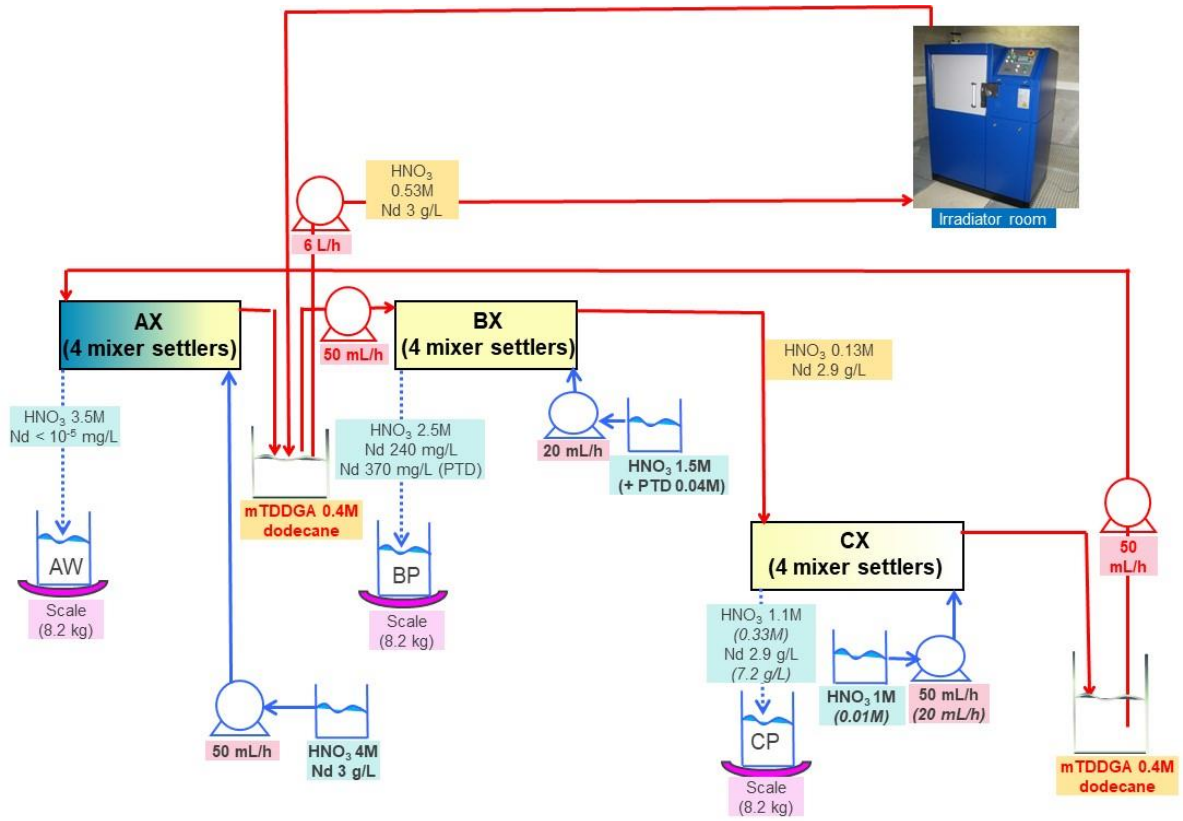

Figure 68 Modified flowsheet of the MARCEL loop test following CX hydrodynamic problem (italics indicate initial value).

The idea of this simplified flowsheet is to test hydrodynamic behaviour of the irradiated solvent in the three steps of the process. In order to better monitor the extraction behaviour of Nd, we decided to decrease the acidity of the second BX step. Hence, less neodymium is extracted and a higher concentration can be detected in the aqueous phase by on-line spectrophotometry, which facilitates the monitoring of the behaviour of this element. According to the calculated Nd concentration profile, we decided to place the spectrophotometric probes in the fourth stage of the AX and BX steps to obtain maximum accuracy; the third probe was placed in the CX outflow. Table 9 gives calculated equilibrium Nd concentrations for each step of the flowsheet. According to these calculations, more than 99.999% of the neodymium should be extracted in the organic phase in the first step. Without PTD, about 1% of extracted Nd would be stripped in BX aqueous outflow whereas 2% should be stripped with 0.04M PTD. Lastly, Nd would be quantitatively back-extracted in the third CX step (less than 0.001% in the recycled solvent). Owing to hydrodynamic problems, acidity of this last step had to be increased during the test. With 1 mol/L HNO_3 and an organic to aqueous ratio of 1, we have calculated that only few Nd should be recycled along with the solvent (about 0.3% according to the model for a non-degraded solvent).

This project has received funding from the EURATOM research and training programme 2014–2018 under grant agreement No. 755171. The content of this deliverable reflects only the authors' view. The European Commission is not responsible for any use that may be made of the information it contains.

Table 9 Calculated concentration profile for each step of the GENIORS MARCEL loop flowsheet

	AX: An-Ln Extraction				BX: An Stripping					CX: Ln Stripping				Modified CX			
	H (moL/L)	Nd (mg/L)	Flowrate (mL/h)		H (moL/L)	Nd PTD 0.04M (mg/L)	Nd (mg/L)	Flowrate (mL/h)		H (moL/L)	Nd (mg/L)	Flowrate (mL/h)		H (moL/L)	Nd (mg/L)	Flowrate (mL/h)	
Aqueous Inflow	4	**3000**	50		1.5	0	0	20		0.01	0	20		1	0	**50**	
Organic Inflow	0	0	50		0.53	**3000**	**3000**	50		0.13	**2904**	50		0.13	**2904**	50	
	Aqueous profile				Aqueous profile					Aqueous profile				Aqueous profile			
Stage	H (moL/L)	Nd (mg/L)	Flowrate (mL/h)		Stage	H (moL/L)	Nd PTD 0.04M (mg/L)	Nd (mg/L)	Flowrate (mL/h)	Stage	H (moL/L)	Nd (mg/L)	Flowrate (mL/h)	Stage	H (moL/L)	Nd (mg/L)	Flowrate (mL/h)
1	3.47	0.0000135	50		1	2.49	372	240	20	1	0.33	7260	20	1	1.06	2895	50
2	3.91	0.001	50		2	1.84	1602	1137	20	2	0.06	653	20	2	1.01	915	50
3	3.98	0.14	50		3	1.6	2925	2148	20	3	0.02	58	20	3	1.00	215	50
4	4.00	20	50		4	1.53	2562	2046	20	4	0.01	5	20	4	1.00	42	50
	Organic profile				Organic profile					Organic profile				Organic profile			
Stage	H (moL/L)	Nd (mg/L)	Flowrate (mL/h)		Stage	H (moL/L)	Nd PTD 0,04M (mg/L)	Nd (mg/L)	Flowrate (mL/h)	Stage	H (moL/L)	Nd (mg/L)	Flowrate (mL/h)	Stage	H (moL/L)	Nd (mg/L)	Flowrate (mL/h)
1	0.43	0.001	50		1	0.27	3480	3360	50	1	0.021	261	50	1	0.079	923	50
2	0.51	0.14	50		2	0.18	4020	3750	50	2	0.0037	23	50	2	0.073	225	50
3	0.53	20	50		3	0.14	3870	3720	50	3	1.1E-03	2	50	3	0.073	52	50
4	0.53	3000	50		4	0.13	2850	2904	50	4	6.8E-04	0	50	4	0.073	10	50

IMPLEMENTATION OF THE LOOP TEST

PROCESS DEVICES AND ANALYTICAL MEASUREMENTS

The liquid-liquid extraction devices consisted of PMMA mixer-settlers where the two phases flow counter-currently as shown in Figure 69.

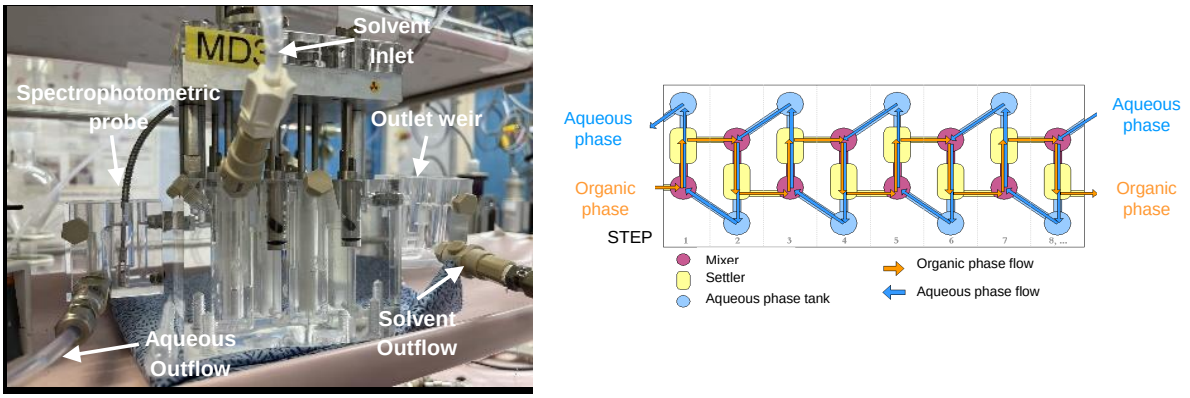

Figure 69 Picture and schematic drawing illustrating the principles of PMMA mixer-settlers.

The two phases were mixed using perforated stainless steel blades with a rotation speed of 1700 rpm. The interphases in the settling compartments were adjusted using Teflon blades located on weirs in the aqueous phase. Other weirs were installed at outlet of each battery, to regulate the flow variations and so allow on-line spectrophotometric measurements with optical probes.

All reagents and solutions were introduced thanks to the mixer-settlers by rotary piston pumps. The flow rates were controlled by a Coriolis mass flowmeter and adjusted by a specific monitoring software.

During the first week, the aqueous samples were analysed by Horiba Ultima 2 ICP-OES, to check that the on-line measurement was correct. Potentiometric titrations in saturated oxalate medium were performed on these samples to measure acid concentrations. Moreover, in order to verify that there was no evaporation of the diluent, the amide concentration of several solvent samples was analysed by potentiometry in acetic anhydride

This project has received funding from the EURATOM research and training programme 2014–2018 under grant agreement No. 755171. The content of this deliverable reflects only the authors' view. The European Commission is not responsible for any use that may be made of the information it contains.

medium, by 0.1 M solution of $HClO_4$ in anhydrous acetic acid. Amides and amines are too weak bases (pKa~9.3) for an acid-base titration in aqueous medium [76]. Furthermore, the density and viscosity of the solvent were measured by Anton Paar SVM 3000, every day for the first week and every 50 kGy for the following weeks. Prior to analyses, each solvent sample was centrifuged to ensure that it did not contain water. All input reagents were analysed by ICP-OES (Nd concentration) and potentiometric titration (acid concentration) before their use in the process.

IRRADIATION DOSE RATE

The solvent was sent into the irradiator to simulate fission products and actinides irradiation. A flow rate of 6 L/h was set instead of the main flow rate of 50 mL/h, to homogenize the liquid in the radiolysis reactor. For that loop test, we use a specific radiolysis reactor designed to reduce the volume of solvent and to maintain the same high dose of solvent irradiation inside as in the old device. The height of the reactor decreases to 2 cm instead of 4.2 cm, thus, the whole solvent is closer to the sources of cesium (147 TBq from 5 ^{137}Cs sources). Contrary to the previous one, this new reactor occupies the entire surface of the irradiator in order to get the best volume/irradiation compromise. Figure 70 shows some pictures of the new radiolysis reactor used for this GENIORS MARCEL loop test.

Figure 70 Pictures and schematic drawings of the new and former radiolysis reactors.

The dose rate in this new reactor was estimated to be 0.78 kGy/h using the Fricke method [77]. With 430 mL in this device and a solvent flowrate of 50 mL/h as proposed in the flowsheet (Figure 68), the solvent undergoes approximately 6.7 kGy/cycle. Since this test started with 1 L of solvent, a process cycle lasts 20 hours and thus every week the organic phase was exposed to a dose of 56 kGy. In the case of a plutonium-extracting solvent, in-plant processing of MOX fuel involves an irradiation dose of 28-29 KGy per week (MOX fuel cooled for 5 years with a ratio (Pu+Am)/(U+Pu+Am) of 8.2% and a burnup of 43.5 GWj/t) [78]. The MARCEL loop thus accelerates the degradation by radiolysis compared to a nuclear fuel processing plant. A similar calculation was also performed on a reagent injected in the aqueous phase of the An stripping step, such as PTD. With the same assumptions, PTD is expected to undergo about 8 kGy per cycle, which is much lower than the dose subjected to the solvent since the PTD is not expected to be recycled at this time.

This project has received funding from the EURATOM research and training programme 2014–2018 under grant agreement No. 755171. The content of this deliverable reflects only the authors' view. The European Commission is not responsible for any use that may be made of the information it contains.

PROCESS MONITORING IN AUTOMATIC MODE

In order to stop the process quickly after a malfunction and to prevent any risk of overflowing the outlet or emptying the inlet, a functional analysis has been set up in the monitoring software of the process platform. In "automatic mode", the process should stop if:

- Rotational speed feedback is outside the range (± 1000 rpm from the speed setpoint) on each mixer-settler motor for at least 5 min.
- Flowrate is outside the range (± 10mL/h from the flowrate setpoint) on each flowmeter for at least 5 min.
- Density (of aqueous phase) is greater than 1 on each flowmeter defined for at least 5 min.
- Liquid reaches its high level for 5 minutes in solvent vials.
- Output flask reaches a mass greater than a limit value for at least 5 min
- Weight is less than – 100 g on outflow scale for 5 min

During this GENIORS MARCEL test, the process was automatically stopped by the monitoring software due to flowmeter problems or an empty inlet bottle, demonstrating the effectiveness of this supervision. Figure 71 shows an example of screenshot from the monitoring software during the loop test.

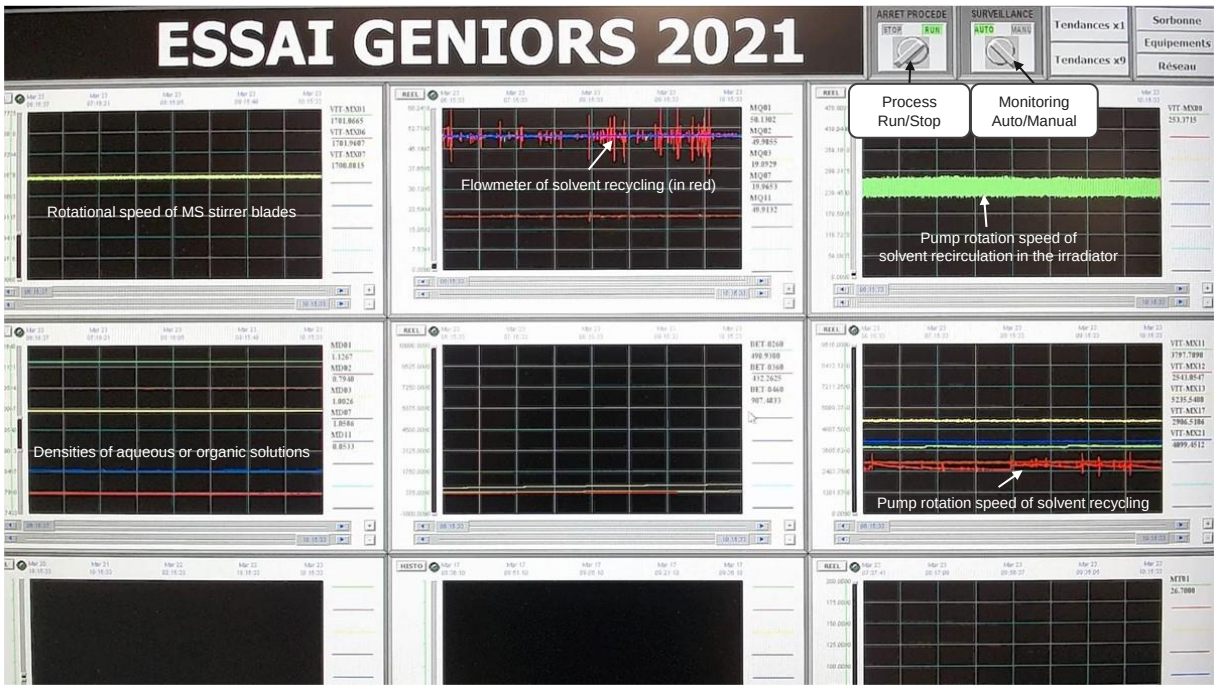

Figure 71 Example of screenshot from the monitoring software during the GENIORS loop test

ONLINE SPECTROPHOTOMETRIC MONITORING

On-line spectrophotometric monitoring was carried out using a new software, called Spectral, developed by our team. This C ++ software offers new features designed in collaboration with future users to meet their needs. The basic principle of Spectral monitoring is the creation of deconvolution models from standard solutions to

This project has received funding from the EURATOM research and training programme 2014–2018 under grant agreement No. 755171. The content of this deliverable reflects only the authors' view. The European Commission is not responsible for any use that may be made of the information it contains.

estimate the concentration of elements. These concentrations are reported in the form of curves making it possible to visualize their evolution over time. The software also allows to import spectra from benchtop spectrophotometers, in order to deconvolute them or feed the models. Multi-channel monitoring is possible thanks to the use of compact spectrophotometers, available in many wavelength and optical density ranges. Spectrophotometric probes have been designed for use in the mixer-settler system. These probes (Figure 72) are 5 mm in diameter with a 1.6 mm screw drilled for two optical fibers and a mirror. Light is carried via a first incident fibre from the light source to the probe. Then, the light passes through the solution to the mirror probe which reflects the attenuated light back through the solution again. Figure 72 shows an extraction from Spectral's absorbance database during the test.

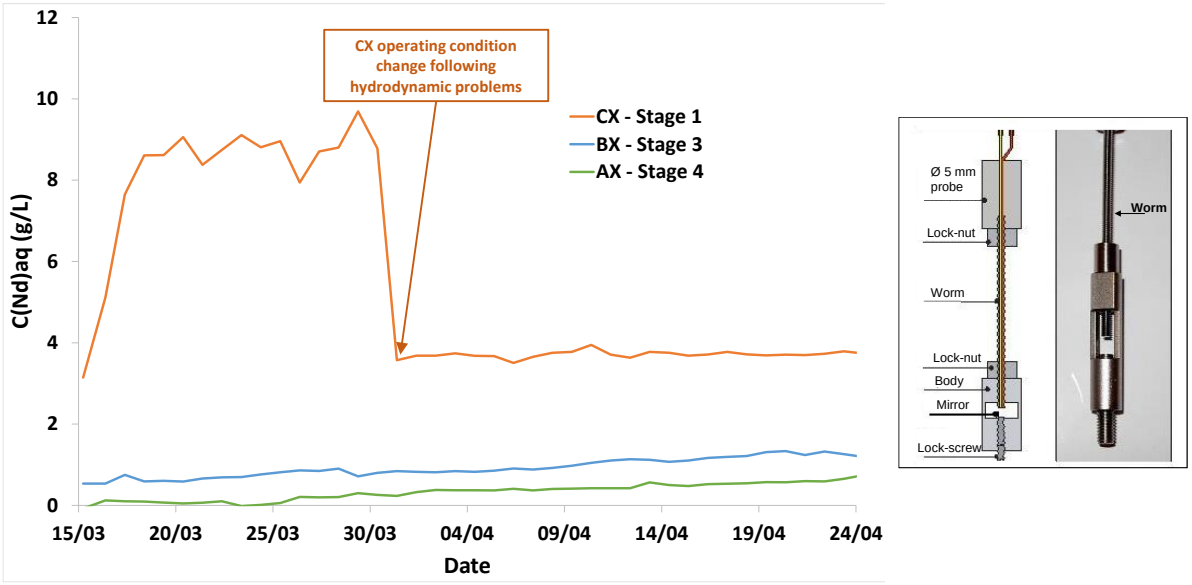

Figure 72 Online spectrophotometric monitoring during the test thanks to Spectral CEA software (database extract for CX-stage 1, BX-stage 3 and AX-stage 4). Picture of a probe used for on-line spectrophotometric measurements

OPERATION SEQUENCE AND FIRST RESULTS

SUMMARY OF KEY EVENTS DURING THE TEST

This GENIORS MARCEL loop test lasted approximately 1000 hours, with the solvent undergoing nearly 340 kGy at the end. Table 10 reports all the samples collected during the test, with the measurement values when analysis was performed. Every inlet solution was analysed by ICP-OES to get Nd concentration or by acidic potentiometric titration with NaOH 0.1 mol/L in saturated oxalate medium. In some solvent samples, Nd concentration was evaluated thanks to two successive batch extractions with 1 mol/L HNO_3 (V/V, t_{mixing}=10 min) then with water (V_{aq}=5xV_{org}, t_{mixing}=10 min). Amide concentration was measured by $HClO_4$ potentiometric titration after centrifugation.

The densities of the solvent increased during the test but in a relatively narrow proportion (2%). However, for viscosities, this increase is 20%, which was significant and required daily hydrodynamic monitoring. The potentiometric measure of solvent is not specific to mTDDGA since degradation compounds have also

This project has received funding from the EURATOM research and training programme 2014–2018 under grant agreement No. 755171. The content of this deliverable reflects only the authors' view. The European Commission is not responsible for any use that may be made of the information it contains.

amide/amine functions that could be titrated in the same way. This was a simple indication, during the first week, that no diluent was evaporated.

Figure 73 PROUST platform with its supervision and laboratory mixer-settlers

Figure 73 shows an overview of the PROUST platform with its monitoring software and an example of mixer settlers. The MARCEL irradiator is located in an adjacent room and is connected to PROUST by Teflon pipes of 23 m length and 2 mm internal diameter.

The hydrodynamic behaviour of the two-phase system did not change a lot after several irradiation cycles. Some solvent carryover of the aqueous droplets was observed from the first week. This phenomenon increased moderately during the test, requiring daily emptying of the aqueous phase present with solvent outflow of each step. However, after one week, the platform was automatically shut down following the appearance of a white gel in the last stage of Nd stripping step. The flowmeter upstream of the solvent recycling was completely blocked by this gel. After cleaning, the process was restarted but the flowmeter had to be changed one week later, due to another shutdown coming from the same hydrodynamic problem. This phenomenon was visible on the flow meter's monitoring of the recycle solvent flow rate and on the solvent pump's rotation speed (red curves in the Figure 71): unlike other flowmeters or pumps, the curves showed continuous instability during the test.

This project has received funding from the EURATOM research and training programme 2014–2018 under grant agreement No. 755171. The content of this deliverable reflects only the authors' view. The European Commission is not responsible for any use that may be made of the information it contains.

Table 10 List of samples, Nd or acidity concentrations, solvent density, viscosity or amide concentration during the test

				AX Aqueous Ouflow		BX Aqueous Ouflow		CX Aqueous Ouflow		CX Organic Ouflow			
Date	Test Duration	Solvent total dose (kGy)	Sample number	C(H+) (mol/L)	C(Nd) (mg/L)	C(H+) (mol/L)	C(Nd) (mg/L)	C(H+) (mol/L)	C(Nd) (mg/L)	Density T=23°C (g/cm^3)	Dynamic Viscosity T=23°C (mPa.s)	C(Amide) (mol/L)	C(Nd)org (mg/L)
15/03/2021 - 06:20	0:00		Irradiation On							0.7955	4.4186	0.44	
15/03/2021 - 07:10	0:50		F0	3.41									
15/03/2021 - 07:40	1:20		F1	3.38									
15/03/2021 - 08:10	1:50		F2	3.19									
15/03/2021 - 08:40	2:20		F3	3.22									
15/03/2021 - 09:10	2:50		F4	3.19									
15/03/2021 - 11:00	4:40		F5	3.28									
15/03/2021 - 14:20	8:00	1	F6	3.45	<0,1	1.58	232						
15/03/2021 - 15:55	9:35	2	F7	3.53	<0,1	1.58	267	0.38	0.824				
15/03/2021 - 17:50	11:30	2	F8	3.57	<0,1	1.62	278	0.39	1.46				
15/03/2021 - 21:10	14:50	3	F9	3.49	<0,1	1.76	286	0.37	2.46				
16/03/2021 - 02:05	19:45	5	F10	3.38	<0,1	1.97	260	0.42	3.67	0.7938	4.2036		
16/03/2021 - 06:30	24:10	6	F11	3.31	<0,1	2.01	226	0.41	4.35				
16/03/2021 - 08:40	26:20	7	F12	n.m.	n.m.	n.m.	n.m.	n.m.	n.m.	0.7938	4.1961	0.44	
16/03/2021 - 10:00	27:40	8	F13	3.38	<0,1	1.93	266	0.40	5.086				
16/03/2021 - 14:05	31:45	9	F14	3.42	<0,1	2.08	238	0.34	4.94				
16/03/2021 - 16:00	33:40	10	F15	3.42	<0,1	2.11	226	0.41	5.66	0.7939	4.2068		
16/03/2021 - 18:00	35:40	10	F16	3.44	<0,1	2.14	226	0.45	6.72				
16/03/2021 - 21:00	38:40	11	F17	3.39	5.6	2.11	219	0.41	6.10	0.7939	4.2468	0.48	0.15
17/03/2021 - 00:00	41:40	12	F18	3.46	<0,1	2.15	214	0.43	6.62				
17/03/2021 - 03:00	44:40	13	F19	3.44	<0,1	2.17	226	0.38	6.2	0.7940	4.2838	0.46	< 0,1
17/03/2021 - 06:25	48:05	14	F20	3.33	<0,1	2.10	238	0.38	6.56				
17/03/2021 - 09:45	51:25	16	F21	3.43	<0,1	2.21	223	0.40	6.52	0.7939	4.2712	0.43	
17/03/2021 - 14:10	55:50	17	F22	3.44	<0,1	2.26	234	0.41	7.03				
17/03/2021 - 16:10	57:50	18	F23	3.46	<0,1	2.27	221	0.44	7.42	0.7940	4.2951	0.44	
17/03/2021 - 18:25	60:05	18	F24	3.46	<0,1	2.28	222	0.42	6.82				
17/03/2021 - 21:00	62:40	19	F25	3.46	<0,1	2.21	224	0.41	7.3				
18/03/2021 - 00:00	65:40	20	F26	3.46	<0,1	2.24	207	0.43	7.05				
18/03/2021 - 03:00	68:40	21	F27	3.44	<0,1	2.22	208	0.43	6.8	0.7941	4.2267	0.42	
18/03/2021 - 06:35	72:15	23	F28	3.39	<0,1	2.23	197	0.43	7.16				
18/03/2021 - 09:55	75:35	24	F29	3.42	<0,1	2.29	208	0.41	7.08	0.7941	4.296	0.42	
18/03/2021 - 14:05	79:45	25	F30	3.45	<0,1	2.28	218	0.43	7.78				
18/03/2021 - 16:15	81:55	26	F31	3.45	<0,1	2.27	219	0.45	7.82	0.7943	4.2577		
18/03/2021 - 18:00	83:40	26	F32	3.46	<0,1	2.26	220	0.42	7.26				
18/03/2021 - 21:15	86:55	27	F33	3.47	<0,1	2.26	215	0.44	8.02				
19/03/2021 - 00:00	89:40	28	F34	3.46	<0,1	2.23	222	0.42	7.66				
19/03/2021 - 03:10	92:50	29	F35	3.43	<0,1	2.23	232	0.44	7.94	0.7942	4.3092		
19/03/2021 - 06:15	95:55	31	F36	3.43	<0,1	2.27	227	0.46	8.1				
19/03/2021 - 09:25	99:05	32	F37	3.44	<0,1	2.26	209	0.42	7.33	0.7943	4.3326		
19/03/2021 - 11:40	101:20	32	F38	n.m.	n.m.	n.m.	n.m.	n.m.	7.8				
19/03/2021 - 14:10	103:50	33	F39	3.48	<0,1	2.30	210	0.43	7.59				
22/03/2021 - 09:50	171:30	56	**F40**							0.7950	4.3039		
24/03/2021 - 15:40	224:20	74	F41							0.7953	4.3677	0.43	
27/03/2021 - 17:00	297:40	98	**F42**							0.7989	4.6341		
30/03/2021 - 17:30	370:10	123	F43										138
02/04/2021 - 16:45	441:25	147	**F44**							0.7998	4.8029	0.42	
06/04/2021 - 08:40	529:20	177	F45							0.8000	4.7361		147
08/04/2021 - 18:00	586:40	198	**F46**							0.8004	4.7896		
12/04/2021 - 08:15	672:55	231	F47										
14/04/2021 - 09:15	721:55	249	**F48**										
16/04/2021 - 17:35	778:15	271	F49										
19/04/2021 - 08:45	841:25	295	**F50**										
22/04/2021 - 08:35	913:15	322	F51							0.8037	5.0481		178
24/04/2021 - 05:00	957:40	339	**End of test**										

Figure 74 shows an example of this gel or stable emulsion observed in the CX solvent outflow. Batch experiments were performed with CX aqueous phase and a solvent sample. The formation of a stable gel or emulsion was confirmed. By increasing the acidity of the medium, this phenomenon tends to decrease. It is likely to be caused by a degradation compound of mTDDGA, since during the first days of the test, no hydrodynamic problem was observed. This phenomenon could be due to a COOH, OH-amid or amine degradation product [41, 73, 79]. At higher acidity and in the presence of Nd, the COOH, OH- or amine group remains protonated or complexed with

This project has received funding from the EURATOM research and training programme 2014–2018 under grant agreement No. 755171. The content of this deliverable reflects only the authors' view. The European Commission is not responsible for any use that may be made of the information it contains.

cations, thus this degradation compound remains completely in the solvent, unlike at low acidity without Nd in the organic phase. According to A. Wilden *et al.* studies [73], the analyses of the dissolved precipitation solutions showed to contain mainly didecylamine, less soluble when protonated. However, it seems that this precipitate was not the same as the one obtained in MARCEL because the gel appeared rather at low acidity. ESI-MS or CPG-MS analyses are underway to identify the degradation compound in the gel.

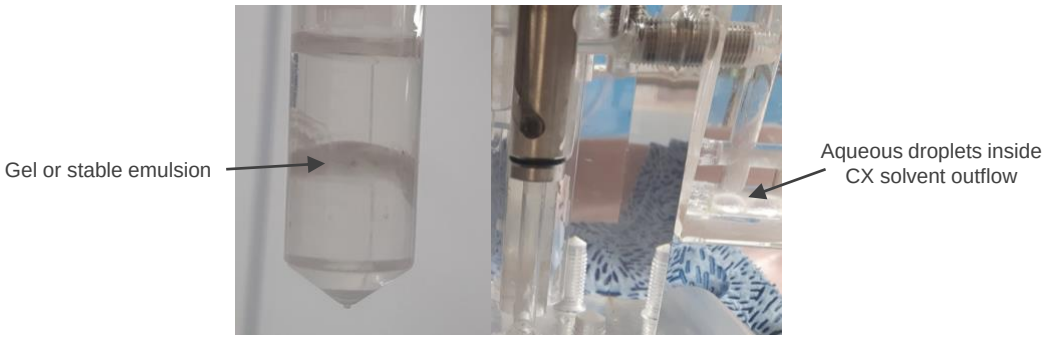

Figure 74 Photos of the gel recovered in the solvent vial and in the flowmeter upstream of the recycling.

After two weeks, the Nd stripping flowsheet was changed: instead of 0.01 mol/L, 1 mol/L HNO_3 was injected at a flowrate of 50 mL/h (20 mL/h initially). This higher flowrate explains why the Nd concentration in the CX outflow decreased after March 30 (Figure 72). With this increase in flowrate, Nd could be effectively stripped in the aqueous phase before solvent recycling. The drawback of this change was the inability to recover the neodymium produced in the CX outflow into the feed solution, since the Nd concentration is the same as in feed solution but its acidity is too low.

Thanks to this flowsheet modification, the loop test has still worked for 5 weeks but the platform was stopped twice more because of the same phenomenon. The increase in acidity did not completely eliminate the hydrodynamic problems but it did reduce the clogging of the solvent pump or flowmeter.

AQUEOUS CONCENTRATION PROFILES

After stopping the test, each stage was emptied. The aqueous phases in the settling chambers were sampled to measured Nd concentration by ICP-OES for all twelve stages. There was no PTD in An stripping step (BX). In Figure 75, are plotted the Nd concentration profiles measured at the end of the test (solid line) and those calculated with the model, based on a non-irradiated solvent (dotted line). The curves have the same shape for the An stripping step but a significant deviation is observed for the other steps. Figure 75 indicates acid concentration ranges for the 3 steps. An stripping step is carried out into a moderate acidity whereas the first one is in higher acidity and the third one in lower acidity. As mTDDGA is degraded by radiolysis during the loop test, its concentration has decreased and therefore less Nd is extracted from high nitric acidity. This should explain why there is more neodymium in the aqueous stages of the AX step since less is extracted in each mixer-settler (lower distribution ratios). This explanation is correct if we assume that the degradation compounds do not extract Nd from a high nitric acid solution. It would be correct if they extract as a cation exchanger, penalised by increased acidity. On the other hand, the presence of these acidic degradation compounds leads to less easy stripping of Nd as the acidity decreases. This should explain why the slope of the Nd concentration profile in the CX step is lower, indicating that the distribution ratios are higher than expected. In a solution of intermediate acidity, the decrease in Nd extractability by mTDDGA is complemented by the Nd extraction from the synergism between mTDDGA and degradation compounds. Therefore, the distribution ratios of Nd are close to those calculated and

This project has received funding from the EURATOM research and training programme 2014–2018 under grant agreement No. 755171. The content of this deliverable reflects only the authors' view. The European Commission is not responsible for any use that may be made of the information it contains.

the concentration profiles are similar. These explanations need to be confirmed by identification and quantification of the degradation compounds in MARCEL solvent samples.

Despite the degradation of the solvent by radiolysis, sufficient neodymium could be extracted and back-extracted to avoid losses in the extraction raffinate or organic recycling of large amounts of neodymium. This confirms the large operating margins offered by the mTDDGA solvent in the flowsheet.

Another important point is to investigate whether the degradation could decrease the separation factor between actinides and lanthanides. This could be studied by batch experiments with solvent samples, collected during the loop test.

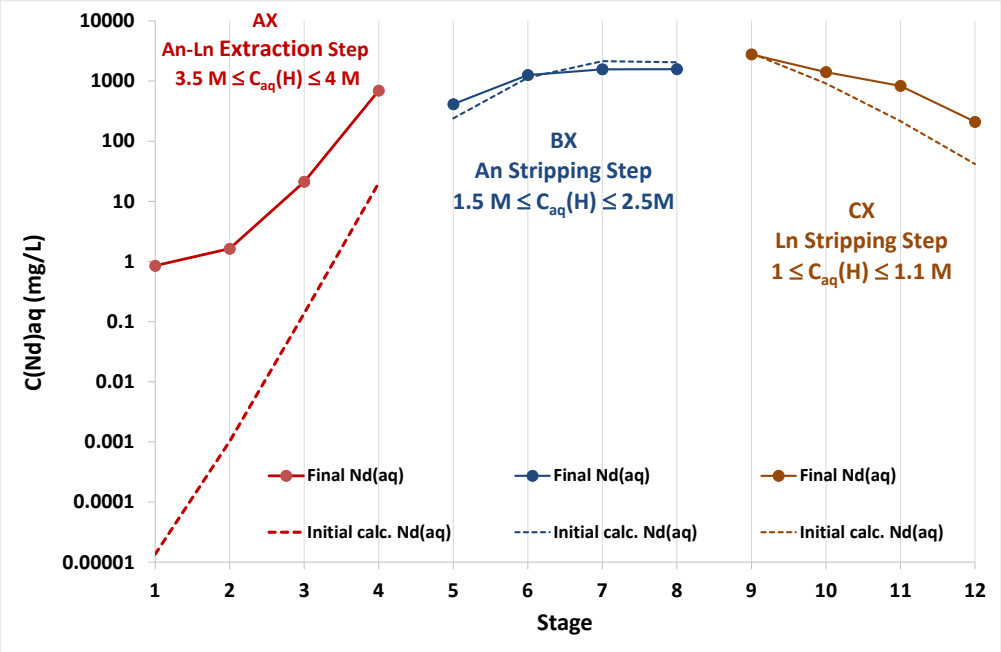

Figure 75 Aqueous Nd concentration profiles at the end of the test, comparison to the initial calculated profile (without PTD in BX step)

BATCH EXPERIMENTS WITH SOLVENT SAMPLES

Batch experiments have been performed with 8 solvent samples: initial, F40 (56 KGy), F42 (98 KGy), F44 (147 KGy), F46 (198 KGy), F48 (249 KGy), F50 (295 KGy), Final S2 (339KGy) (Table 10). All solvents were contacted with 0.01 mol/L HNO_3 (V_{aq}=V_{org} - 30 min stirring) then centrifuged to strip acidity and residual neodymium. The protocol consists in performing an extraction with solvents and an aqueous phase containing trace amounts of ^{241}Am and ^{152}Eu with 4.2M HNO_3 then a back-extraction of these cations with four aqueous solutions in parallel: 0.4M PTD – 2.1M HNO_3, 0.04M PTD – 1.5M HNO_3 (irradiated at 100 kGy or not) and 0.01M HNO_3.

All batch experiments were completed by the end of May. The results are given in Table 11 and in Figure 76. The distribution coefficients $D_{Am,Eu}$ are calculated as the ratio of the total organic to aqueous cation concentrations. The separation factor SF(Eu/Am) is the ratio of the distribution coefficients, useful for assessing the metal selectivity provided by the system.

This project has received funding from the EURATOM research and training programme 2014–2018 under grant agreement No. 755171. The content of this deliverable reflects only the authors' view. The European Commission is not responsible for any use that may be made of the information it contains.

$D_{Am,Eu}$ obtained with the initial mTDDGA solvent are similar to those from CIEMAT with the same solvent batch. However, they are very different from those obtained with another batch of solvent, from which the simplified model was built (see first chapter). With PTD, the SF(Eu/Am) are almost the same as expected. This means that there is no problem with PTD in the aqueous phase. However, $D_{Am,Eu}$ are 10 times higher than those expected for 0.4M cis-mTDDGA. This large difference could be due to the concentration of cis-mTDDGA or an impurity in our solvent and the one used by Andreas Wilden *et al*. This result may show that there can be notable differences in cation extraction depending on the quality of the mTDDGA solvent. Hence the interest in taking the same solvent for each GENIORS partner to allow a more direct comparison of the results. For performance efficiency, the separation factor seems to be the most interesting parameter to follow. The fact that the D_M are higher than expected can always be adjusted on a genuine flowsheet thanks to the nitric acidity of the aqueous phase.

Initial results confirm that 100 kGy gamma irradiation has little impact on PTD since the separation factors are almost the same as for unirradiated PTD. This confirms the stability of PTD already observed. On the other hand, mTDDGA seems to be more sensitive to radiolysis, which can lead to a drop in D_M above 100 kGy, with an acidity above 1.7 mol/L. In the case of low acidity (Ln stripping, HNO_3 0.5 mol/L), D(Am, Eu) increase very considerably with gamma dose, which remains consistent with the trend observed in the Nd concentration profile in the previous paragraph As already mentioned, this phenomenon could be attributed to a synergism between mTDDGA and degradation compounds resulting in particular from the breaking of the ether bond.

These first data show that up to a gamma dose of 339 kGy, the distribution ratios of Am and Eu are moderately affected by irradiation, which means that mTDDGA is sufficiently stable to be used in a nuclear process. In addition, solvent treatment was not performed during the loop test because no studies on this step have been performed before. It is likely that solvent treatment with alkaline reactants should improve the stability of extraction performance if it removes acidic degradation products, as tested with malonamides for DIAMEX process.

This project has received funding from the EURATOM research and training programme 2014–2018 under grant agreement No. 755171. The content of this deliverable reflects only the authors' view. The European Commission is not responsible for any use that may be made of the information it contains.

Table 11 Results obtained in batch experiments with trace amount of ^{241}Am (125 kBq/L), ^{152}Eu (97 lBq/L) (V/V, stirring time=30 min, T=25°C)

An-Ln Extraction HNO_3 4.2M	$C(HNO_3)_{eq\ aq}$ (mol/L	D(Am)	D(Eu)
Calculated	*4.2*	*325*	*319*
0 KGy	4.2	297	739
56 KGy	4.2	296	776
98 KGy	4.2	237	576
147 KGy	4.2	255	639
198 KGy	4.1	247	605
249 KGy	4.2	238	580
295 KGy	4.2	215	518
339 KGy	4.2	210	554
Ln Stripping HNO_3 0.01M	$C(HNO_3)_{eq\ aq}$ (mol/L	D(Am)	D(Eu)
Calculated	*0.55*	*0.018*	*0.024*
0 KGy	0.55	0.010	0.007
98 Kgy	0.50	0.019	0.018
147 KGy	0.49	0.022	0.023
249 KGy	0.47	0.033	0.037
295 KGy	0.48	0.038	0.044
339 KGy	0.50	0.039	0.046

An Stripping PTD 0.4M	$C(HNO_3)_{eq\ aq}$ (mol/L	D(Am)	D(Eu)	$SF_{Eu/Am}$
Calculated	*2.5*	*0.19*	*4.1*	*22*
0 KGy	2.5	1.7	23	14
56 KGy	2.4	1.4	21	15
98 KGy	2.5	1.4	21	15
147 KGy	2.4	1.2	18	15
198 KGy	2.5	1.2	18	15
249 KGy	2.4	1.1	18	16
295 KGy	2.4	1.1	16	15
339 KGy	2.4	1.0	15	16
An Stripping PTD 0.04M	$C(HNO_3)_{eq\ aq}$ (mol/L	D(Am)	D(Eu)	$SF_{Eu/Am}$
Calculated	*1.8*	*1.8*	*3.4*	*1.9*
0 KGy	1.8	2.9	5.6	1.9
56 KGy	1.7	2.6	5.1	2.0
98 KGy	1.7	3.0	6.0	2.0
147 KGy	1.6	2.2	4.3	2.0
198 KGy	1.7	2.8	6.1	2.2
249 KGy	1.7	2.6	6.0	2.3
295 KGy	1.7	2.4	5.2	2.1
339 KGy	1.7	2.3	5.0	2.2
An Stripping PTD 0.04M 100 KGy	$C(HNO_3)_{eq\ aq}$ (mol/L	D(Am)	D(Eu)	$SF_{Eu/Am}$
0 KGy	1.8	3.1	5.2	1.7
56 KGy	1.7	2.4	4.8	2.0
98 Kgy	1.7	2.9	5.4	1.9
147 KGy	1.7	2.2	4.0	1.8
198 KGy	1.7	2.7	5.5	2.0
249 KGy	1.7	2.5	4.8	2.0
295 KGy	1.7	2.5	5.0	2.0
339 KGy	1.7	2.3	4.7	2.0

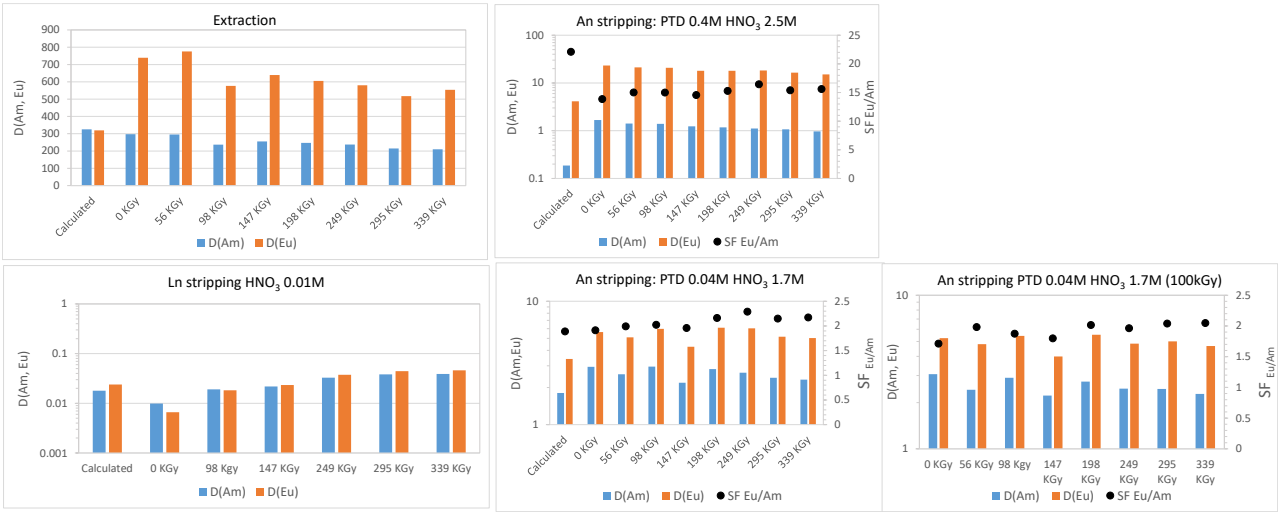

Figure 76 Results obtained in batch experiments with trace amount of ^{241}Am (125 kBq/L), ^{152}Eu (97 lBq/L) (V/V, stirring time=30 min, T=25°C)

This project has received funding from the EURATOM research and training programme 2014–2018 under grant agreement No. 755171. The content of this deliverable reflects only the authors' view. The European Commission is not responsible for any use that may be made of the information it contains.

HPLC-MS MEASUREMENTS BY CIEMAT

CIEMAT measured by HPLC-MS our solvent samples assessed by batch experiments in the previous paragraph [80]. The degradation of mTDDGA follows a kinetic law of order 1 with respect to the monoamide concentration, i.e. the concentration follows a law of the type: $C = C0\ e^{-kt}$ where t is time, C0 is the initial concentration, C is the concentration at time t and k is a degradation kinetic constant. With the dose rate, it is possible to express the concentration as a function of the dose integrated by the solvent. (Dose = dose rate * t) $C = C0\ e^{-k'dos}$. By plotting the concentrations C as a function of dose (in kGy), it is possible to determine a constant k' by applying the relation: k' (kGy^{-1}) = ln(C/C0) / dose (kGy). This kinetic degradation constant k' allows the overall stability of extractant to be compared, independently of their concentration in solution.

Figure 77 shows the values provided by I. Sanchez *et al.* The curve allows k' to be evaluated at 0.002 kGy^{-1}. This value is somewhat higher than that obtained with monoamide extractants for which k' values between 10^{-4} and 10^{-3} kGy^{-1} have been obtained[81]. However, this degradation of mTDDGA has only a limited impact on the extraction and separation performance of americium and europium traces. This means that the main degradation products maintain the initial extraction of the cations and do not have a negative impact on the separation, which is very important for the process.

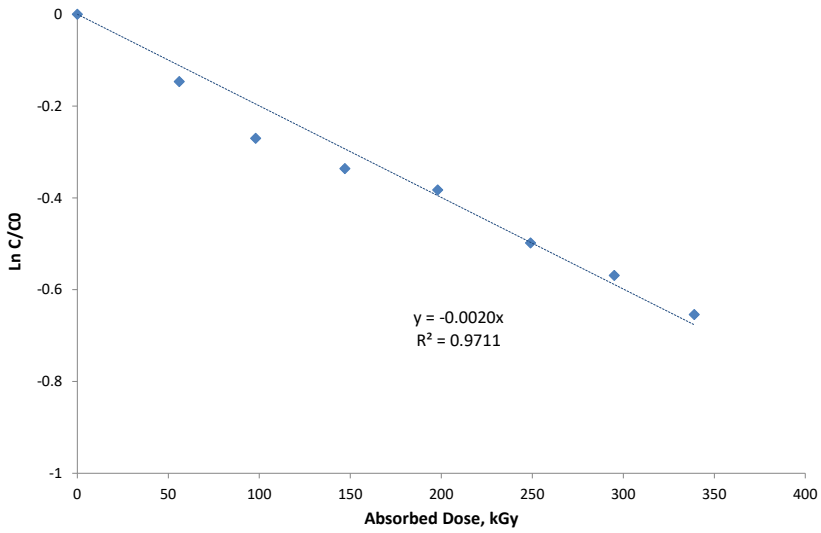

Figure 77 Ln(C/Co) curve as a function of the dose received with C, concentration of mTDDGA and C0, its initial concentration.

CHEMICALS

All used chemicals are of analytical grade. The Cis-mTDDGA was provided by Santa Jansone-Popova of Oak Ridge National Laboratory and the PTD was synthesised by Alessandro Casnati of the University of Parma.

This project has received funding from the EURATOM research and training programme 2014–2018 under grant agreement No. 755171. The content of this deliverable reflects only the authors' view. The European Commission is not responsible for any use that may be made of the information it contains.

CONCLUSIONS

This GENIORS MARCEL loop test, carried out continuously in mixer-settlers for 6 weeks, up to an irradiation dose of 341 kGy, showed that the viscosity and density of the mTDDGA solvent did not increase significantly, which is a good point for the hydrodynamic stability of this system. However, the degraded solvent has produced compounds that could clog the small orifices of the transfer or measuring devices. This phenomenon is assumed to be related to an acidic degradation compound and could be avoided if an effective solvent treatment is implemented. Analyses are underway to confirm this hypothesis. The final values of the batch experiments confirm the good stability of the extraction performance after undergoing 339 kGy. This result is promising because this dose corresponds to a 12 week plant operation for the treatment of 43.5 GWj/t MOX fuel.

PTD appears to be a radiolysis-stable aqueous reagent up to 100 kGy, which is sufficient for use in the actinide stripping step on an industrial scale, since it would only undergo 8 kGy per cycle. It appears that the use of PTD does not lead to hydrodynamic problems, making this molecule industrially usable. However, it will be necessary to think about its recycling to avoid wasting it.

A more complete flowsheet must be carried out in the future, with all stages, solvent treatment and hydrolysis steps, in order to validate its industrial ability to treat spent nuclear fuel.

This project has received funding from the EURATOM research and training programme 2014–2018 under grant agreement No. 755171. The content of this deliverable reflects only the authors' view. The European Commission is not responsible for any use that may be made of the information it contains.

CHALMEX SOLVENT DEGRADATION STUDIES

Authors: Dimytro Bavol and Bohumir Gruner (IIC); Peter Distler and Jan John (CTU); Thea Lyseid Authen and Christian Ekberg (CHALMERS)

INTRODUCTION

The Deliverable Report, *D5.2 Impacts of solvent degradation and recycle on the EURO-GANEX process,* also includes the CHALMEX process.

The initial formulation of the Chalmers-GANEX (CHALMEX) process was developed and tested in the ACSEPT project with the aim of An/Ln separation by the selective extraction of An, which offers a simpler and more elegant solution to the challenge of recovering TRU actinides as a group [9-12]. By combining the well-known TBP extractant with a biz-triazinyl ligand ($CyMe_4$-BTBP), trivalent and hexavalent An could be extracted without the co-extraction of lanthanides and fission products. Meanwhile, the chemistry and degradation of the TBP is well established after decades of use in the PUREX process, the degradation of $CyMe_4$-BTBP is less well-known. Deliverable 2.1 (Stability and safety studies of extraction systems) already reports a summary of $CyMe_4$-BTBP degradation studies and the behaviour of the CHALMEX system after irradiation. For example, the behaviour of the CHALMEX system (10 mM $CyMe_4$-BTBP in 70% FS-13 and 30% TBP) after irradiation by accelerated electrons up to 500 kGy at four different temperatures (15 – 45 °C) was studied. The model based on mass transfer (DM model, based on the so-called two-film theory of interphase diffusion) as the rate-controlling process was found to best describe extraction of Am(III) and Eu(III). Overall mass-transfer coefficients were evaluated using this model. The values of ΔH and ΔS for the extraction of Am(III) and Eu(III) from 4 M HNO_3 were determined. The study of the irradiation of the solvent in the presence of nitric acid aqueous phase confirmed its earlier observed radioprotective effect. A comparison of the theoretical values of distribution ratios after irradiating the system with accelerated electrons, calculated from the residual concentrations of the ligand, with their experimental values suggests that some of the $CyMe_4$-BTBP degradation products or adducts of $CyMe_4$-BTBP or TBP are probably able to extract the studied metals, too. In addition, the study of the influence of nitric acid concentration shed some light on the nature of the degradation products – contrary to the original ligands, that extract by solvation mechanism, the degradation products extract by ion exchange mechanism. Also, these new radiolytically formed extractants don´t exhibit significant An / Ln selectivity.

The main part of the studies related to the composition of solvents after irradiation and degradation products was also reported in D.2.1. (Stability and safety studies of extraction systems), and here is reported a summary with recent updates.

Additional extraction experiments have been performed, and reported here, for solvents exposed to both gamma radiation, heating and acid for various time periods.

Lastly, corrosion studies of the solvent have been done under long-term irradiation in a gamma-cell. The CHALMEX solvent was shown to cause corrosion on 316L SS, most likely caused by the ligand. 310SS stainless steel was also investigated, and it was confirmed that FS-13 did not initiate corrosion on either steels. One steel sample was however shown to cause pitting corrosion, most likely 10 mM CyMe4-BTBP in 100% FS-13, confirming previous results. Absolute identification of the original solvent is pending however.

This project has received funding from the EURATOM research and training programme 2014–2018 under grant agreement No. 755171. The content of this deliverable reflects only the authors' view. The European Commission is not responsible for any use that may be made of the information it contains.

PRE-SURVEY OF CYME$_4$-BTBP DEGRADATION UNDER DIFFERENT CONDITION

The main part of the studies was already published in D.2.1. of the Geniors Project. Here we present a summary with recent updates. During this project, pre-survey was focused on deeper analyses of the irradiated samples together with influence of irradiation conditions on the presence of degradation products. Firstly, the system in fluorinated diluent FS-13 called as CHALMEX process (10 mM CyMe$_4$-BTBP in 70% FS-13 and 30% TBP; 4 M HNO_3) was studied within this project (Figure 78). More specifically, the behaviour of this system at different temperatures was investigated. Comparison of the data with FS-13 and TBP diluent with the earlier data in another fluorinated solvent BK1 is presented in more detail in Ref.[82]. Below, the most recent data are presented on the behaviour of the CHALMEX system after irradiation by pulse linear electron accelerator LINAC 4-1200 (Tesla v.t. Mikroel). The mean electron energy was 4.5 MeV, pulse width 3 µs and repeating frequency 500 Hz. To get closer to real conditions during the reprocessing, the work focused on examining the properties of the systems after irradiation at different doses up to 500 kGy at four different temperatures in combination either in neat solvent (Table 12) or in contact with HNO_3 (Table 13). All irradiations of the samples were done by our partner in CTU. For irradiated systems, the residual concentration of CyMe$_4$-BTBP was studied by HPLC-APCI-MS as a function of the absorbed dose. Also, complementary chromatogram where presence of degradation products in the samples by tandem LC-MS were confirmed (Figure 79). From obtained data can be seen that stability of CyMe$_4$-BTBP in contact with HNO_3 is higher (across all irradiated temperatures) than in the case of irradiation in absence of aqueous phase. This stabilization effect may be also ascribed to some capture of free radicals created during the radiolysis by HNO_3 [83]. In the next step, the influence of HNO_3 concentration (2, 4 and 8 M) present during the irradiation on the properties of the irradiated solvent was tested (Table 14). The concentrations of the initial extractant decrease independently on the HNO_3 concentration in the range of 2M to 8M HNO_3, however the presence of aqueous phase has significant effect on stability.

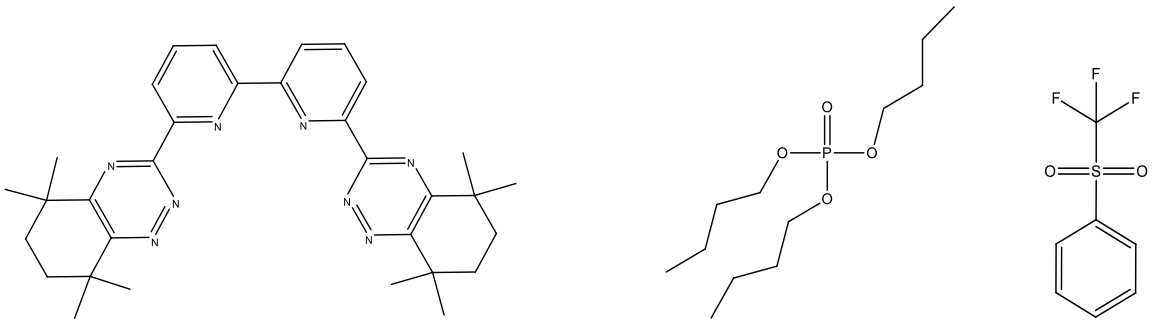

Figure 78: Chemical structure of CyMe$_4$-BTBP, FS-13 and TBP, respectively.

Table 12: Residual concentrations of CyMe$_4$-BTBP (70% FS-13 and 30% TBP) on absorbed dose, *D*, at different temperatures.

		***c* [mmol/l]**			
		15 °C	**25 °C**	**35 °C**	**45 °C**
***D*[kGy]**	**0**	10.0	10.0	10.0	10.0
	50	5.9	7.2	7.7	7.2
	100	6.3	6.3	6.2	6.7
	200	4.7	4.8	5.0	5.1
	350	3.7	3.7	3.6	3.6
	500	2.8	2.7	2.7	2.8

This project has received funding from the EURATOM research and training programme 2014–2018 under grant agreement No. 755171. The content of this deliverable reflects only the authors' view. The European Commission is not responsible for any use that may be made of the information it contains.

Table 13: Residual concentrations of $CyMe_4$-BTBP (70% FS-13 and 30% TBP, 4 M HNO_3) on absorbed dose, *D*, at different temperatures.

		c [mmol/l]			
		15 °C	**25 °C**	**35 °C**	**45 °C**
***D*[kGy]**	**0**	10.0	10.0	10.0	10.0
	50	7.9	7.9	8.0	7.0
	100	7.3	7.5	7.6	7.9
	200	6.7	6.7	6.8	7.3
	350	6.1	5.9	6.4	6.1
	500	5.6	5.4	N/A	5.3

N/A - The sample was not available.

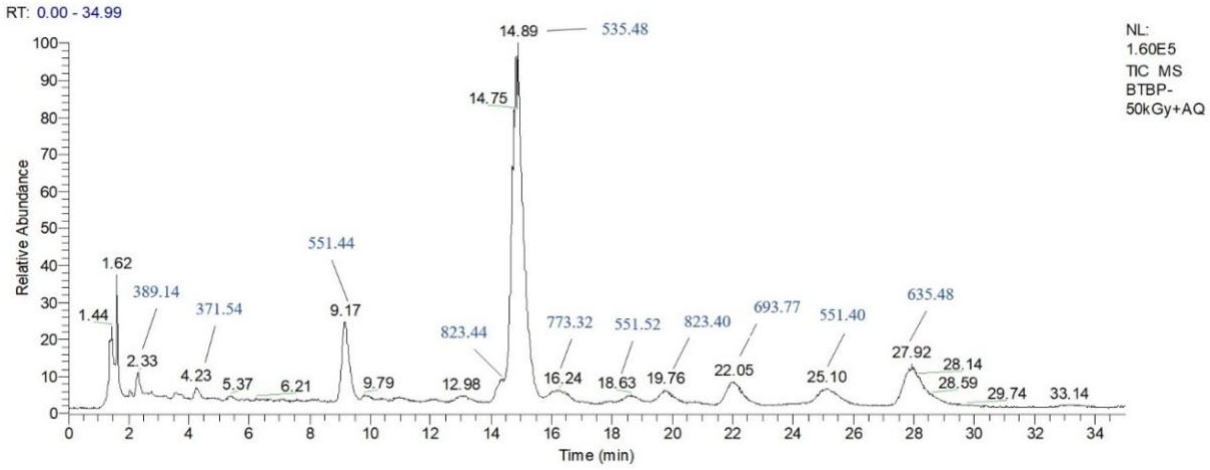

Figure 79: LC-MS chromatogram with isocratic elution of $CyMe_4$-BTBP (70% FS-13 and 30% TBP, 4 M HNO_3) irradiated dose: 50 kGy; flow rate 0.3 mL/min; column: Gemini-NX C18 110 Å (3 µm, 150 x 2.00 mm *I.D.*); mobile phase: 10 mM DEAO pH 8.2 with 78% ACN. The peaks are labelled with mass of the residual $CyMe_4$-BTBP and degradation products. Three peaks with *m/z* = 551 are observed indicating presence of isomeric hydroxyderivatives.

Table 14: Residual concentrations of $CyMe_4$-BTBP based on different absorbed dose, *D*, irradiated in the presence of aqueous phase.

		c [mmol/l]		
		2 M	**4 M**	**8 M**
***D*[kGy]**	**0**	10.0	10.0	10.0
	50	8.4	7.9	8.0
	100	7.7	7.5	7.5
	200	6.8	6.7	6.8
	350	6.0	5.9	6.0
	500	5.0	5.4	5.3

Secondly, attention was paid on deeper analyses of the supplied samples from CTU and Chalmers, irradiated during extension of the previous Project. By LC-MS determined composition of degradation products depend, if the sample were irradiated in neat solvent, in contact with HNO_3, or in GANEX solvent containing TBP.

This project has received funding from the EURATOM research and training programme 2014–2018 under grant agreement No. 755171. The content of this deliverable reflects only the authors' view. The European Commission is not responsible for any use that may be made of the information it contains.

Surprisingly enough, the series containing 70% FS-13 and 30% TBP gave the clearest image. Though there was a large solvent peak on HPLC, retention behaviour of most of degradation products could be adjusted to allow for their better integration. Combining the small scale isolations of the components by HPLC with mass spectrometry, two main peaks of degradation products could be isolated by HPLC, in essentially pure form, and have been identified by MS to correspond most probably to mono- and dihydroxy derivatives of $CyMe_4$-BTBP (Table 15). However, there could be several other isomeric species of dihydroxy derivative in the samples as suggest MS of other isolated HPLC fractions, which correspond to small, less resolved peaks (mixed) on the chromatograms. It can be seen, the mono derivative interconverts gradually to dihydroxy derivative as the dose increases and then to some other products. Apparently, these species were more deeply degraded, had lower molecular mass, and could not be resolved yet from solvent peak on chromatograms. According to MS and LC-MS analyses, the samples contained small amounts of other components, which correspond to *m/z* values 346, 371, 523, 532, 557, 573 and 603.

Table 15: Concentration of two main degradation products in supplied sample from CTU and Chalmers.

Sample	Dose [kGy]	BTBP *c* [mmol]*	BTBP-OH [%]	σ_r	BTBP-$(OH)_2$ [%]	σ_r
BTBP+FS13+TBP (Ganex solvent), 1M HNO_3						
G1M20	20	1.18	19.0	3.71	1.6	4.87
G1M50	50	0.56	31.0	3.93	5.3	2.11
G1M100	100	0.04	16.8	2.98	23.8	3.10
G1M200	200	0.02	4.3	4.44	34.2	3.00
G1M500	500	0.01	10.7	3.23	9.3	2.22
BTBP+FS13+TBP (Ganex solvent), 2M HNO_3						
G2M20	20	2.85	34.6	4.01	1.4	1.82
G2M50	50	0.61	61.8	5.47	7.7	6.15
G2M100	100	0	36.5	1.77	23.2	1.57
G2M200	200	0	22.1	1.01	24.4	0.99
G2M500	500	0	12.1	0.72	21.4	1.13
BTBP+FS13+TBP (Ganex solvent), 4M HNO_3						
G4M20	20	2.33	37.8	2.54	1.0	1.75
G4M50	50	0.42	68.2	0.91	4.9	1.36
G4M100	100	0.28	73.8	3.14	11.2	5.14
G4M200	200	0.02	25.1	0.64	37.3	0.57
G4M500	500	0.01	30.4	1.53	15.9	1.02

Subsequently, a series of 4 samples of volume 5.0 mL each had been irradiated after discussion at Chalmers facility by uniform dose 500 kGy either in presence or absence of aqueous phase (4 M HNO_3). As could be seen in Table 16, contact with acid plays again positive role on stability of the systems in cases, when FS-13 or octanol were used as diluents. Complete degradation was observed in octanol sample without contact with acid. Furthermore, the degradation products in this case are different than in other samples and correspond apparently to adducts with octanol. The degradation products in other samples mainly corresponded to peaks that are less retained than $CyMe_4$-BTBP. Presence of hydroxy derivative was observed by HPLC in orange sample in octanol and in lower concentration in green sample. The composition differs depending on the solvent,

This project has received funding from the EURATOM research and training programme 2014–2018 under grant agreement No. 755171. The content of this deliverable reflects only the authors' view. The European Commission is not responsible for any use that may be made of the information it contains.

conditions used during irradiation (i.e. in neat solvent or in contact with HNO_3). Nevertheless, the amounts of isolated products from samples were not sufficiently high for performing NMR characterizations. For this purpose would be needed either bigger-volume samples or higher initial concentration of the ligand. Also the irradiation doses should be set up in such manner that the concentrations of individual degradation products in the irradiated samples are higher.

Table 16: Concentrations of $CyMe_4$-BTBP found in the irradiated samples.

Sample	Diluent	Contact	Dose [kGy]	Residual conc. [%][a]	BTBP *c* [mmol][a]	σ_r
Red Big	70% FS-13, 30%	4M HNO_3	500	70.1	7.06	4.98
Green Big	70% FS-13, 30%	No	500	35.2	3.52	1.81
Orange Big	70% Oct, 30% TBP	4M HNO_3	200	62.9	6.29	1.81
Pink Big	70% Oct, 30% TBP	No	200	0.0	0.00	-

a) Calculated based on Standards small samples supplied.

DEGRADATION OF $CYME_4$-BTBP UNDER SPECIFIC CONDITION IN BIG-SCALE

ANALYSIS BY HPLC-APCI-MS

In this initial task, attention was paid to continuing on deeper analyses of the samples with main focus on formed degradation products, their identification and relative abundance in the sample. The various $CyMe_4$-BTBP samples of concentrations 50 mM in big-volume of solvent (up to 50 mL) Blue (70% FS-13, 30% TBP) and Red (70% octanol, 30% TBP) were prepared by Chalmers and CTU, and irradiated by doses 1200 and 300 kGy, respectively. These conditions were chosen to closely follow the results obtained during the previous research, when the irradiations were performed in smaller volumes and in lower concentrations of the samples (5 or 10 mM) in both solvents. The aim was to approach degradation in the samples around 80- 90% and thus generate high concentration of degradation products. Results from analytical determination of $CyMe_4$-BTBP residual content by HPLC with UV detection are summarized in Table 17. It can be seen, that the degradation of the original ligand only slightly exceeded 50% or remained even lower. A new tandem LC-MS method was developed for more detailed analysis of the samples that enabled monitoring of molecular peaks of individual degradation products on chromatograms. This method was used for analyses of both samples and fractions from *semi*-preparative LC and HPLC separations. Illustration of analysis of both samples is depicted in Figure 80 and Figure 81. The Figures show basic differences in composition of degradation products observed by HPLC with MS detection, depending on the solvent used (samples were irradiated either in 1-octanol or FS-13 with 30% TBP). In fact, the results verified very high stability of the ligand in 50 mM concentration in the Ganex solvents towards radiation, however concentrations of isolatable degradation products remained quite low.

This project has received funding from the EURATOM research and training programme 2014–2018 under grant agreement No. 755171. The content of this deliverable reflects only the authors' view. The European Commission is not responsible for any use that may be made of the information it contains.

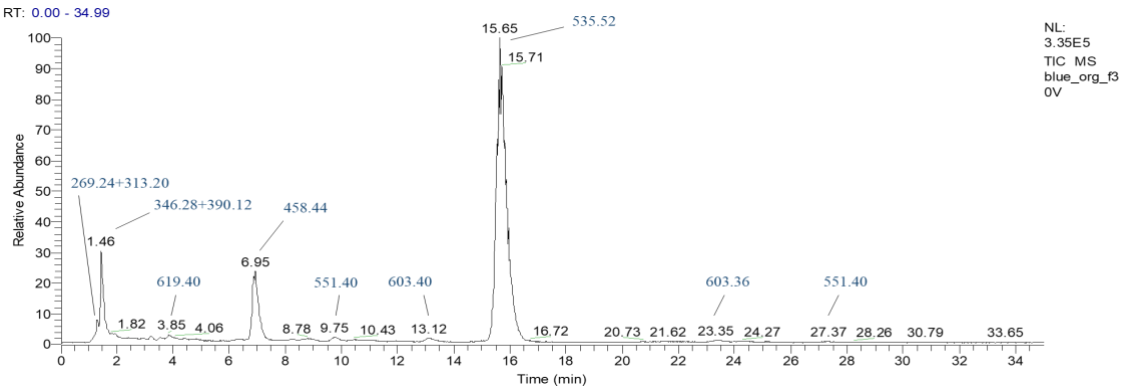

Figure 80: Chromatogram with isocratic elution of sample Blue in organic phase; measured with PDA and MS detection (blue digits); flow rate 0.3 ml/min; column: Gemini-NX C18 110 Å (3 µm, 150 x 2.00 mm *I.D.*); mobile phase: 10 mM DEAO pH 8.2 with 78% ACN. The peak at 458.44 corresponds to $CyMe_4$-BTP, which was present as an impurity in the sample.

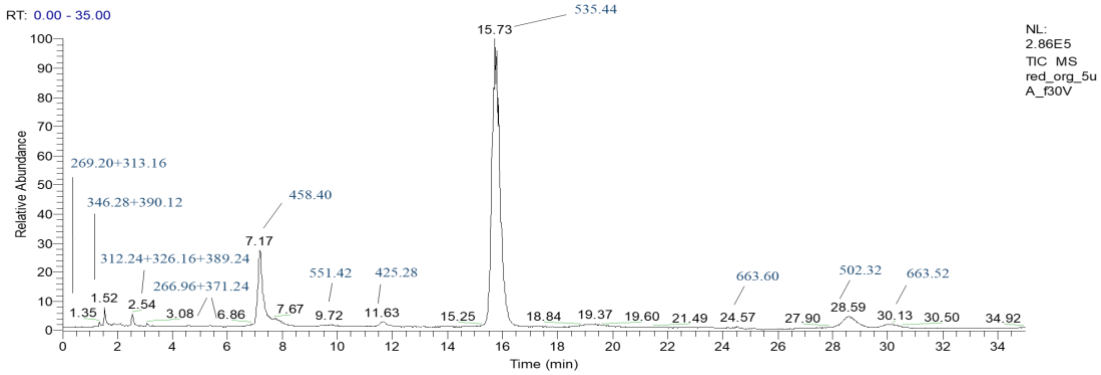

Figure 81: Chromatograms with isocratic elution of sample Red in organic phase; measured with PDA and MS detection (blue digits); flow rate 0.5 mL/min; column: Gemini-NX C18 110 Å (3 µm, 150 x 3.00 mm *I.D.*); mobile phase: 10 mM DEAO pH 8.2 with 78% ACN.

Table 17: Residual concentrations of $CyMe_4$-BTBP found in the irradiated samples. Irradiated at Chalmers or CTU*.

Sample	Diluent	Initial conc. [mM]	Dose [kGy]	Residual conc. [%][a]	BTBP *c* [mM][a]	σ_r
Blue Big	70% FS-13, 30% TBP	50	1200	63.6	31.83	4.60
Red Big	70% Oct, 30% TBP	50	300	44.3	22.1	1.41
Blue Big *	70% FS-13, 30% TBP	50	1200	42.6	21.3	1.72

a) Calculated based on content of Yellow Standard supplied with the series. The samples were irradiated in contact with 4 M HNO_3.

The larger samples from Chalmers Univ. were already consumed for semi-preparative separations before finishing complete isolation and characterization of degradation products by HPLC, MS and NMR. Thus, an additional sample (volume up to 20 mL) from Blue series of same initial concentration and with the identical dose was kindly supplied by our partner from CTU. This was used for continued isolations of degradation products and to for accumulating larger quantities of degradation products for more reliable ^{1}H NMR characterization. What is worth mentioning is that more pronounced degradation and slight differences in degradation products distribution were observed. This is exemplified by LC-MS analysis which is shown in Figure

This project has received funding from the EURATOM research and training programme 2014–2018 under grant agreement No. 755171. The content of this deliverable reflects only the authors' view. The European Commission is not responsible for any use that may be made of the information it contains.

82. The samples differed mainly in concentration of lower mass products corresponding to degradation of lateral rings. The samples from CTU were further used for continuations of *semi*-preparative separations of the degradation products by HPLC.

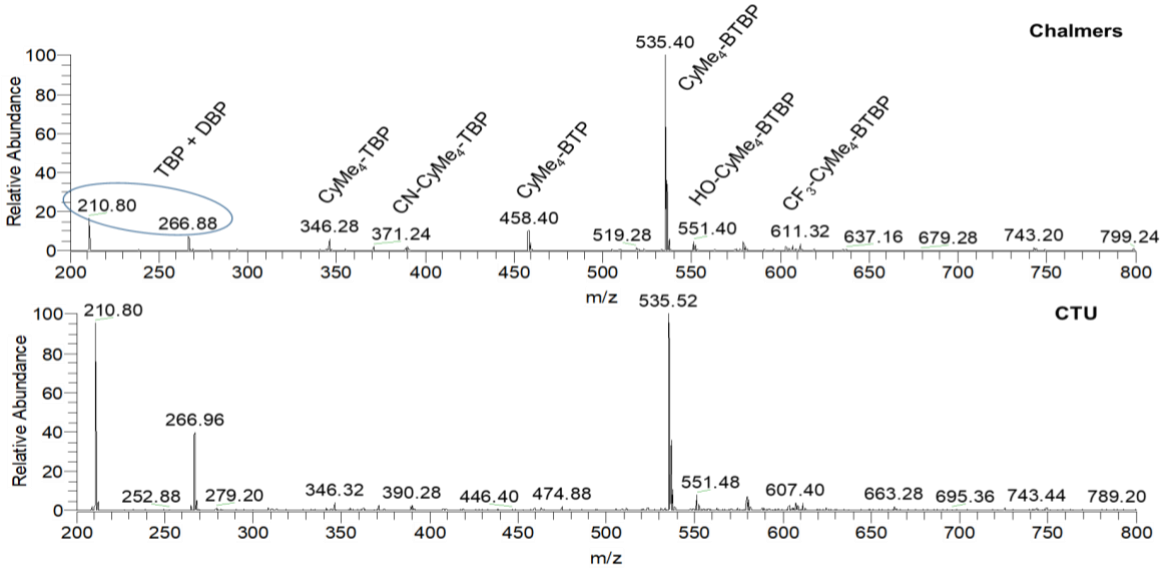

Figure 82: Comparison of MS spectra of Blue sample (50 mM, Ganex, 70% FS-13 and 30% TBP) irradiated by 1200 kGy, supplied from Chalmers and CTU.

SEMI-PREPARATIVE SEPARATIONS

Because of the small quantities of the degradation products and high solvent load in each sample it was not possible to separate the products during single separation run. Also, whereas higher mass degradation products could be separated from the solvent peaks by selected two-step procedure, lower mass or higher polarity degradation products remained close or in overlay with solvent peaks, what along lower stability complicated their further isolation and NMR characterization. Thus, isolation of low retained compounds was based on several repetitions of to be able to concentrate the individual species from each fraction. But even so, the low retained fractions were still loaded with some residual content of TBP or/and FS-13. Considering the NMR characterization, an advantage is that the diagnostics peaks for $CyMe_4$-BTBP and similar compounds are found in the range of aromatic (between ca. 9.5 - 7.5) and aliphatic (between ca.1.9 - 1.3 ppm) regions and thus, do not interfere with those for TBP and FS-13 shifted upfield and downfiled, resp. ^{1}H NMR signals of the collected fractions were, mostly, sufficiently strong and allowed for assignments of chemical shifts of some individual degradation products. As expected, some of the products were identical in both irradiated samples. The structure of one of the main assumed degradation product occurring in both sample series with retention time close to 7.00 min and corresponding *m/z* = 458 that showed clear symmetric NMR spectrum could be unambiguously assigned. NMR and MS spectra correspond to $CyMe_4$-BTP, *i.e.* compound that probably persisted in the sample as impurity from synthesis or handling (Figure 83). Another mass with *m/z* = 532 was initially suspected also to be degradation product, was then finally explained in terms of a TBP dimer, based on NMR and MS-MS fragmentation experiments (Figure 84). Based on performed fragmentation, was found that *m/z* = 210 not corresponding to degradation product, but to a dibutyl phosphate BDP which arose upon solvent irradiation from TBP.

This project has received funding from the EURATOM research and training programme 2014–2018 under grant agreement No. 755171. The content of this deliverable reflects only the authors' view. The European Commission is not responsible for any use that may be made of the information it contains.

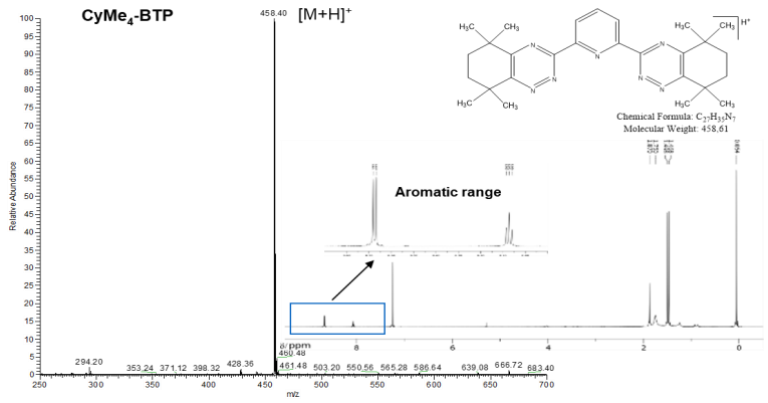

Figure 83: Obtained mass spectrum of $CyMe_4$-BTP and its ^1H NMR measurement.

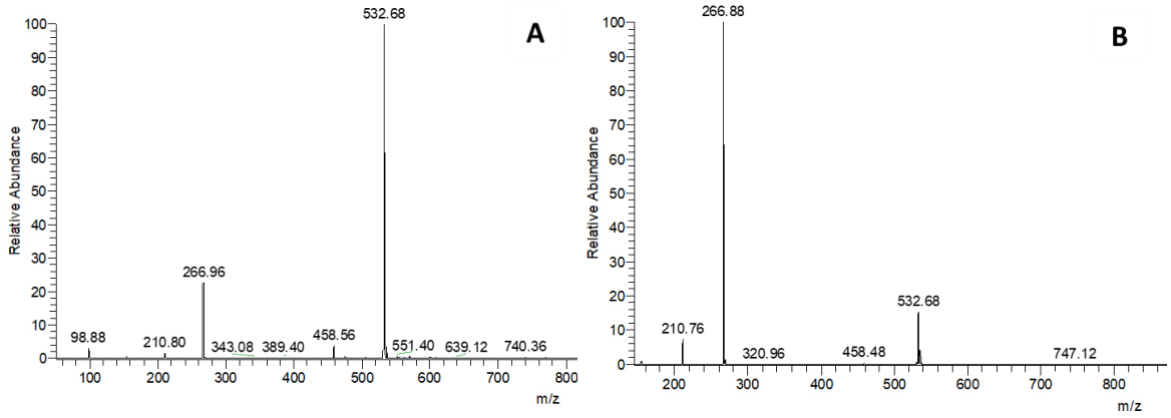

Figure 84: Plot of the mass spectra of the selected fraction containing TBP not fragmented (A) and with source fragmentation (B).

BLUE SERIES

Blue series Irradiated in FS-13 and TBP along with quite high amount of undestroyed $CyMe_4$-BTBP ligand with *m/z* = 535, that could be isolated back, HO-$CyMe_4$-BTBP with *m/z* = 551, was observed and successfully separated and measured by both LC-MS and ^1H NMR (Figure 85). According to NMR, the hydroxy group in the most abundant isomer is most probably sitting at one of the two pyridine rings in the central bipyridine unit in the apical *para*-position to the nitrogen atom. Another main degradation product with *m/z* = 603 (Figure 86) that was however identified mainly by MS and LC, corresponds probably to transfer of CF_3 moiety from FS-13 solvent to $CyMe_4$-BTBP molecule. No clear NMR spectra could be obtained for this compound, possibly due to presence of poorly resolved different isomeric forms in the corresponding isolated fraction. Therefore, the position of CF_3 fragment on the $CyMe_4$-BTBP scaffold remains unclear. From lower molecular mass compounds, several degradation products could be isolated. One of separated degradation product with *m/z* = 346 is depicted in Figure 86. According to NMR and MS evidence, its structure probably corresponds to degraded $CyMe_4$-BTBP molecule, from which one cyclohexane ring was completely lost together with all methyl groups on that side.

This project has received funding from the EURATOM research and training programme 2014–2018 under grant agreement No. 755171. The content of this deliverable reflects only the authors' view. The European Commission is not responsible for any use that may be made of the information it contains.

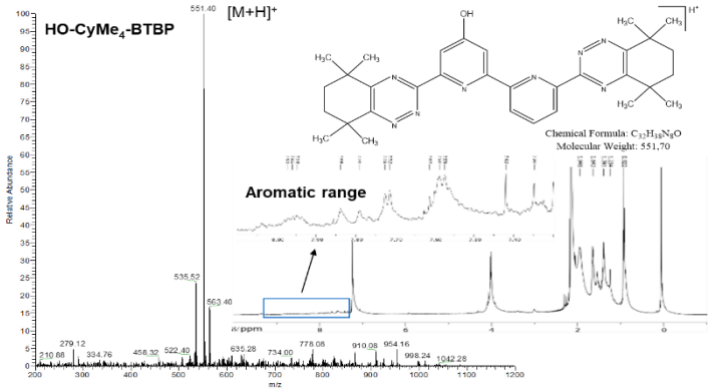

Figure 85: Mass spectra and ^{1}H NMR of HO-CyMe$_4$-BTBP.

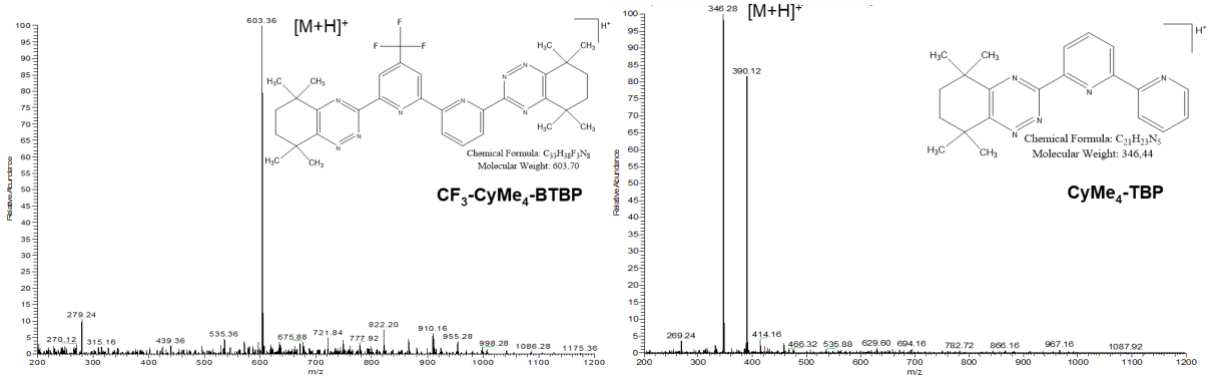

Figure 86: Plot of the mass spectra of the selected individual separated fractions Blue and possible structure of CyMe$_4$-BTBP degradation products, based on consideration from ^{1}H NMR, MS and LC-MS results.

Another isolated compound with *m/z* = 371 corresponds, according to ^{1}H NMR and MS, also to a molecule, which symmetry was lost. This compound has unaffected central bipyridyl unit together with CyMe$_4$ part on one side, but the lateral cyclohexane ring attached to triazinyl are most probably cleaved from the other side, with formation of nitrile group on one pyridine of the rings as a result. The ^{1}H NMR and MS spectra for fraction that correspond to this CyMe$_4$-BTBP degradation product are shown in Figure 87.

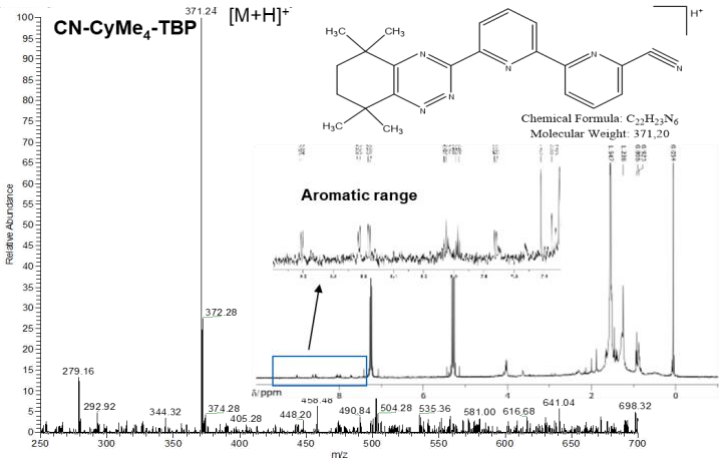

Figure 87: Obtained mass spectra and ^{1}H NMR of CN-CyMe$_4$-TBP.

This project has received funding from the EURATOM research and training programme 2014–2018 under grant agreement No. 755171. The content of this deliverable reflects only the authors' view. The European Commission is not responsible for any use that may be made of the information it contains.

RED SERIES

The compounds with m/z = 207, 346, 371, 458, 551 present also in Blue series and described above could be isolated. Along with them, a different degradation products of $CyMe_4$-BTBP could be isolated, which shows a molecular mass 663. The compound with *m/z* = 663 corresponds to addition product of octanol that was used as solvent (1-octanol, M.W. = 130) (Figure 88). The site of substitution seems to correspond to bypyridine central unit of $CyMe_4$-BTBP, probably to an apical position *para*- to the nitrogen atom, although some evidence may also suggest for presence of other isomer with *meta*-substituted ring. Another adduct containing two solvent molecules of 1-octanol attached $CyMe_4$-BTBP scaffold (*m/z* = 791) was observed as small abundant peak in the MS spectra of Red sample and some highly retained fractions. This however could not be isolated in a sufficient quantity. These results complement the previous analytical results described in already submitted manuscript that indicated formation of adduct with octanol. Apparently, these addition species form important class of degradation products in the systems containing octanol [84].

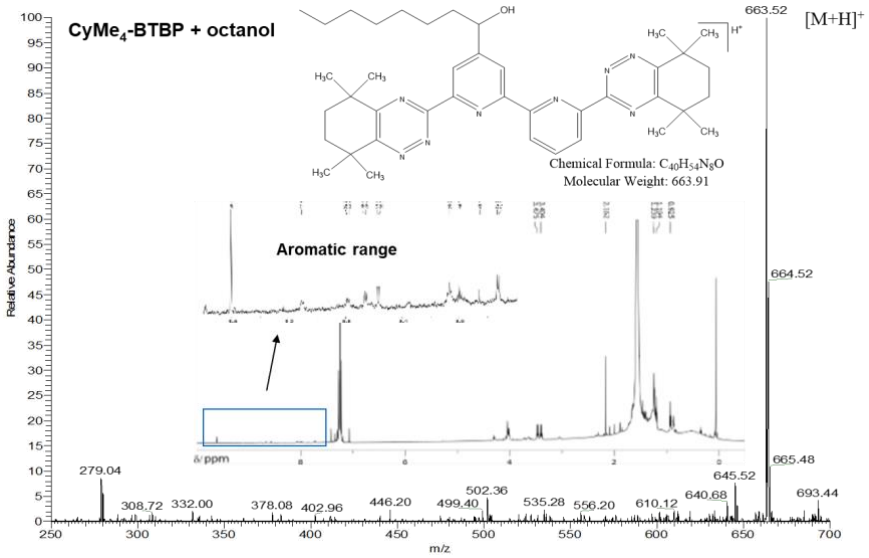

Figure 88: Mass spectrum of the selected individual separated fraction (Red).

ADDITIONAL CHALMEX SOLVENT RESISTANCE STUDIES

RADIOLYTIC STABILITY

Irradiation experiments were performed on two separate series in addition to a reference series:

- 25 mM $CyMe_4$-BTBP in 30% TBP and 70% FS-13 in contact with nitric acid
- 25 mM $CyMe_4$-BTBP in 30% TBP and 70% FS-13 without contact with nitric acid
- All samples that were irradiated without acid contact, were pre-contacted with acid regardless. This was done both to dissolve the ligand, but also to mimic the foreseen industrial process where the organic phase will have been in contact with nitric acid.

This project has received funding from the EURATOM research and training programme 2014–2018 under grant agreement No. 755171. The content of this deliverable reflects only the authors' view. The European Commission is not responsible for any use that may be made of the information it contains.

The reference series was 25 mM $CyMe_4$-BTBP in 30% TBP and 70% FS-13 (in contact with nitric acid) kept in a water bath or heating cabinet at 50°C for the same respective time as the irradiations were performed at. As soon as the irradiations were performed, the extraction tests were performed as quickly as allowed by the capacity of the shaking machine (typically ranging from 10 minutes to 2 hours). 5 µL of the following respective stock solutions were added to a fresh aqueous phase (4M HNO_3), so that the total volume of the aqueous phase was 300 µL:

- $^{241}Am(III)$ (2.2 MBq mL^{-1}) in 4M HNO_3
- $^{152}Eu(III)$ (30.6 kBq mL^{-1}) in 4M HNO_3
- $^{238}Pu(IV)$ (0.28 Bq mL^{-1}) in 4M HNO_3

Samples were shaken by a mechanical shaker (IKA, VIBRAX VXR 1.500 rpm) at 25°C. The shaker can fit 10 samples, but all triplicate specimens were contacted in the same batch in the mechanical shaker to limit varying effects of time on the degradation of ligand/extraction efficiency.

The distribution ratios as a function of received dose to the organic phase can be seen in Figure 89 for the Am and Eu, and in Figure 90 for Pu and Np for all respective irradiation series. From the Am distribution ratios it is evident that the distribution ratios remain very high (D> 75) even after significant doses. For the Eu extraction, a similar decrease in D-values is seen as for the Am extraction. This is surprising as NMR analysis on the solvent shows that the % $CyMe_4$-BTBP ligand remaining in the solvent is reduced to 2.7% after 100 kGy, as seen in Table 18 [85]. Clearly, the degradation products of $CyMe_4$-BTBP are also potent extracting agents. Please also refer to work done by IIC for more details on the analytics of specific degradations products (See D2.1 and Degradation of $CyMe_4$-BTBP sections in this deliverable).

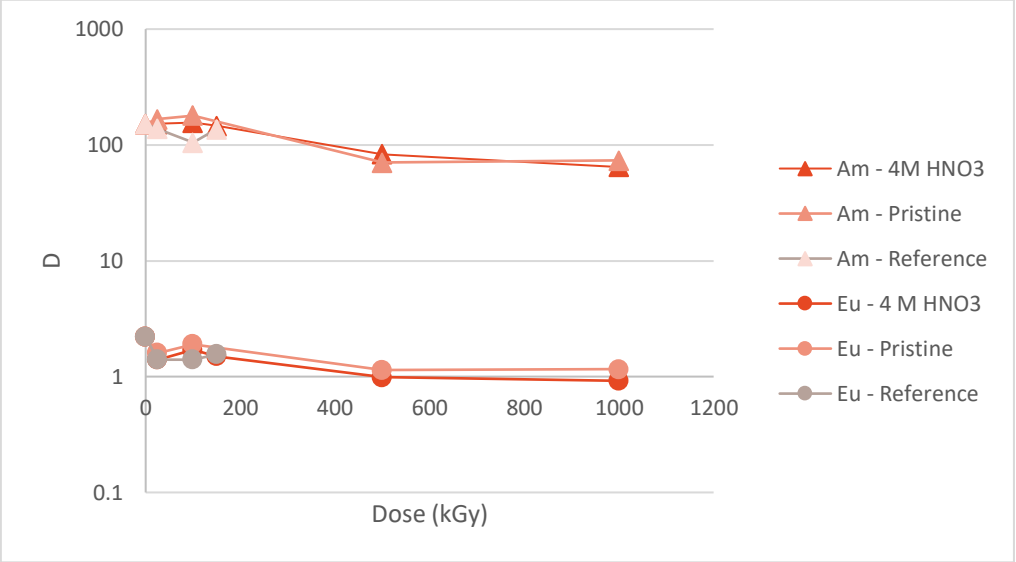

Figure 89. The distribution ratio of americium and europium as a function of dose for organic phases irradiated in the presence of 4M HNO_3, pristine and reference solution (kept at 50 C).

The distribution ratios of plutonium and neptunium as a function of received dose is found in Figure 90. It appears that the D-values for plutonium increases with increasing dose to the solvent. This is probably due to the formation of dibutyl phosphate (DBP) and monobutyl phosphate (MBP), which are known to increase the distribution ratio of plutonium [86].

This project has received funding from the EURATOM research and training programme 2014–2018 under grant agreement No. 755171. The content of this deliverable reflects only the authors' view. The European Commission is not responsible for any use that may be made of the information it contains.

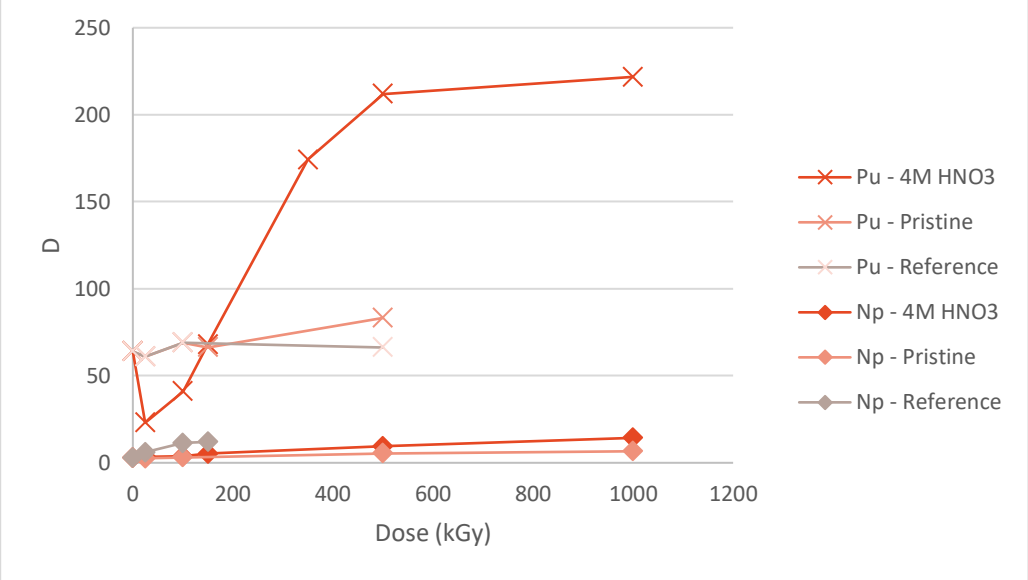

Figure 90. The distribution ratios (D) of Pu and Np extraction as a function of dose received to the organic phase.

Table 18. The concentration CyMe4-BTBP measured in the organic phase as a function of dose.[85]

Dose (kGy)	C (mM)	%	± (%)
0	10.0	100	3.3
50	3.7	37	1.8
100	0.27	2.7	3.8
200	0.00	0.0	0.0
500	0.07	0.7	2.2

HYDROLYTIC AND THERMAL STABILITY

The hydrolytic stability of the solvent was investigated by leaving the solvent in contact with nitric acid over various time periods and measuring the amount of remaining $CyMe_4$-BTBP compared to the initial amount. It is clear that under room temperature, the ligand does not degrade, as seen in Table 19.

Extraction experiments were also performed with different temperatures to establish any effect on the extraction, as temperature fluctuations in industrial processes are common. A slight decrease in D-values is seen for increasing temperatures (Figure 91) for both the Am and the Eu extraction. This indicates an exothermic extraction reaction. It is also seen that selectivity is maintained at higher temperatures.

This project has received funding from the EURATOM research and training programme 2014–2018 under grant agreement No. 755171. The content of this deliverable reflects only the authors' view. The European Commission is not responsible for any use that may be made of the information it contains.

Table 19. The concentration of CyMe4-BTBP in the solvent as a function of time left in contact with nitric acid.[85]

Age (Weeks)	C (mM)	%	± (%)
0	10.0	100	3.3
1	9.3	93	2.9
2	9.5	95	1.6
3	10.0	100	0.2
6	9.7	97	4.5
7	9.7	97	1.9

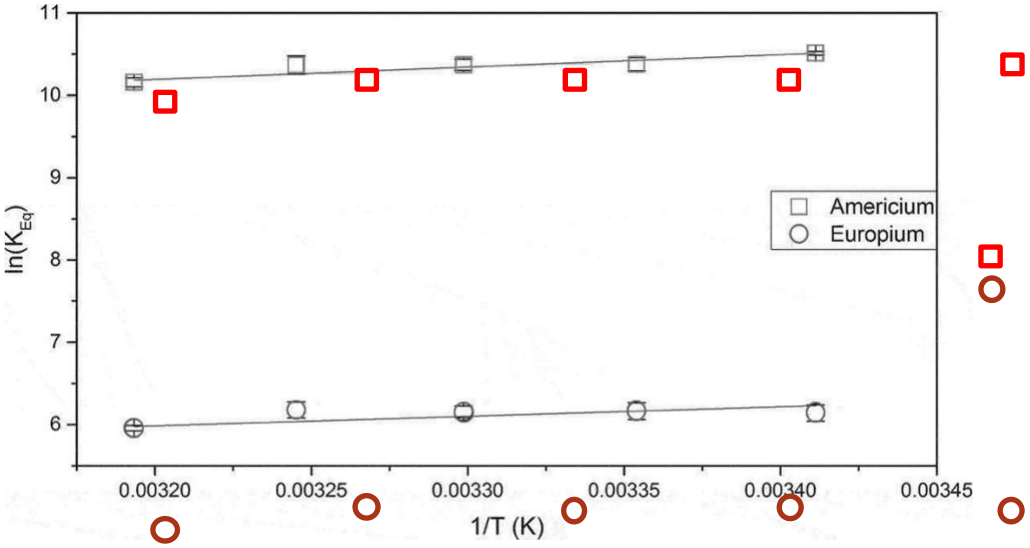

Figure 91. The logarithm if the extraction equilibrium constant as a function of 1/T (K). The organic phase was 10 mM $CyMe_4$-BTBP and 77% w/w FS-13 and 23% w/w TBP.

CORROSION STUDIES

310 SS and 316L SS were immersed in the CHALMEX solvent and placed in a gamma irradiation field to receive a significant amount of dose to determine the effect on the steel. SEM imaging and EDX analysis was performed before and after irradiation. While the 316L SS showed significant degrees of pitting corrosion, as seen in Figure 92, the 310 SS proved much more resistant to corrosion (both by SEM image and EDX analysis), as seen in Figure 93.

This project has received funding from the EURATOM research and training programme 2014–2018 under grant agreement No. 755171. The content of this deliverable reflects only the authors' view. The European Commission is not responsible for any use that may be made of the information it contains.

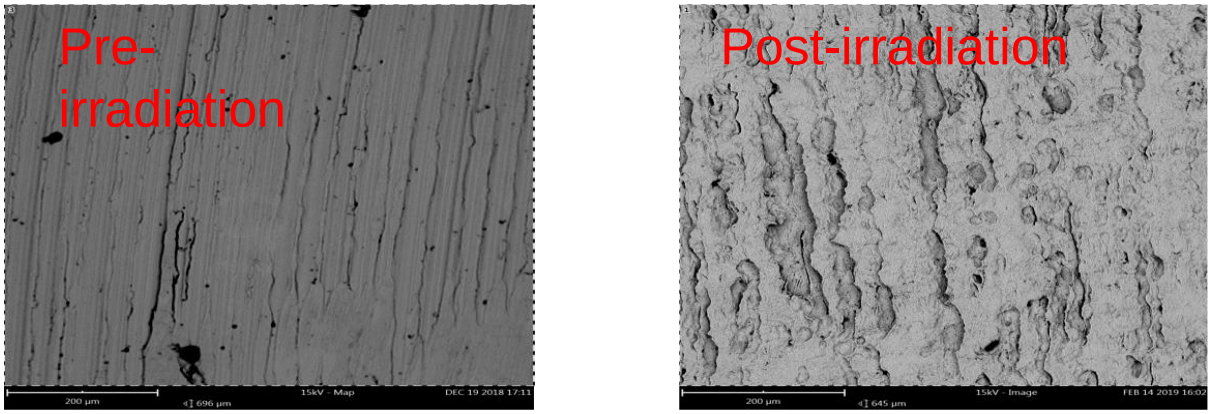

Figure 92. Before- and after- SEM image of 316L SS immersed in the CHALMEX solvent and exposed to a total dose of 2300 kGy.

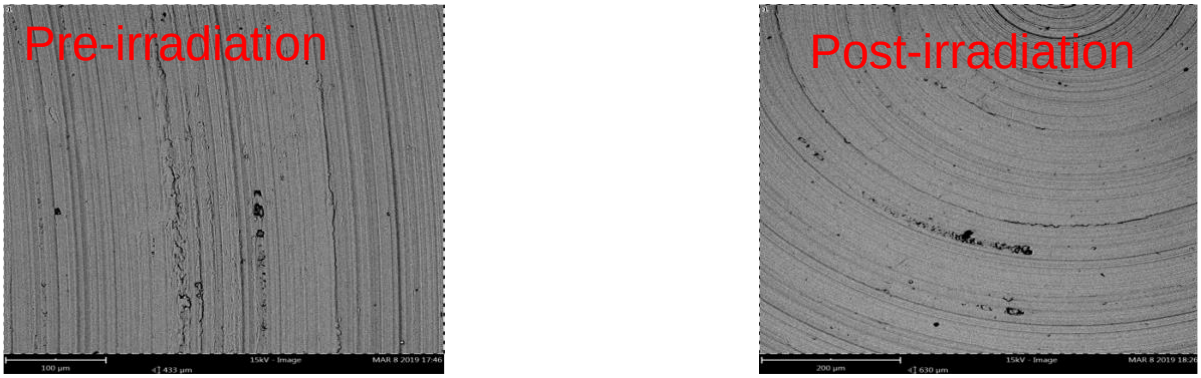

Figure 93. Before- and after- SEM image of 310 SS immersed in the CHALMEX solvent and exposed to a total dose of 2150 kGy.

This project has received funding from the EURATOM research and training programme 2014–2018 under grant agreement No. 755171. The content of this deliverable reflects only the authors' view. The European Commission is not responsible for any use that may be made of the information it contains.

REFERENCES

[1] D. Warin, "Future nuclear fuel cycles: prospect and challenges for actinide recycling," in *IOP Conference Series: Materials Science and Engineering*, 2010, vol. 9, no. 1: IOP Publishing, p. 012063.

[2] C. Poinssot, C. Rostaing, S. Greandjean, and B. Boullis, "Recycling the actinides, the cornerstone of any sustainable nuclear fuel cycles," *Procedia Chemistry,* vol. 7, pp. 349-357, 2012.

[3] J.-M. Adnet *et al.*, "Development of new hydrometallurgical processes for actinide recovery: GANEX concept," 2005.

[4] M. Miguirditchian, C. Sorel, B. Camès, I. Bisel, and P. Baron, "Extraction of uranium (VI by N,N-di(2-ethylhexyl)isobutyramide (DEHIBA): from the batch experimental data to the countercurrent process," in *Solvent extraction: fundamentals to industrial applications. Proceedings ISEC 2008 International Solvent Extraction conference*, B. A. Moyer Ed. Montreal, Canada: Can. Inst. Min. Metall. Pet., 2008, ch. 581, pp. 721-726.

[5] M. Miguirditchian, H. Roussel, L. Chareyre, and P. Baron, "HA demonstration in the Atalante facility of the GANEX 2nd cycle for the grouped TRU extraction," in *GLOBAL 2009*, Paris, France, 2009, La Grange Park, Illinois: American Nuclear Society, p. 9378.

[6] M. Carrott *et al.*, "Development of a new flowsheet for co-separating the transuranic actinides: the "EURO-GANEX" process," *Solvent Extraction and Ion Exchange,* vol. 32, pp. 447-467, 2014.

[7] M. Carrott *et al.*, "Distribution of plutonium, americium and interfering fission products between nitric acid and a mixed organic phase of TODGA and DMDOHEMA in kerosene, and implications for the design of the "EURO-GANEX" process," *Hydrometallurgy,* vol. 152, pp. 139-148, 2015/02/01/ 2015, doi: http://dx.doi.org/10.1016/j.hydromet.2014.12.019.

[8] R. Malmbeck *et al.*, "Homogenous recycling of transuranium elements from irradiated fast reactor fuel by the EURO-GANEX solvent extraction process," *Radiochimica Acta,* vol. 107, no. 9-11, pp. 917-929, 2019, doi: doi:10.1515/ract-2018-3089.

[9] E. Aneheim, C. Ekberg, and M. R. S. J. Foreman, "A TBP/BTBP-Based GANEX Separation Process – Part 3: Fission Product Handling," *Solvent Extraction and Ion Exchange,* vol. 31, no. 3, pp. 237-252, 2013/05/01 2013, doi: 10.1080/07366299.2012.757158.

[10] E. Aneheim *et al.*, "A TBP/BTBP-based GANEX Separation Process—Part 2: Ageing, Hydrolytic, and Radiolytic Stability," *Solvent Extraction and Ion Exchange,* vol. 29, no. 2, pp. 157-175, 2011/03/18 2011, doi: 10.1080/07366299.2011.539462.

[11] E. Aneheim, C. Ekberg, A. Fermvik, M. R. S. J. Foreman, T. Retegan, and G. Skarnemark, "A TBP/BTBP-based GANEX Separation Process. Part 1: Feasibility," *Solvent Extraction and Ion Exchange,* vol. 28, no. 4, pp. 437-458, 2010/06/11 2010, doi: 10.1080/07366299.2010.480930.

[12] J. Halleröd, C. Ekberg, and E. Aneheim, "Phenyl trifluoromethyl sulfone as diluent in a grouped actinide extraction process: extraction properties of the solvent components TBP and CyMe4-BTBP," *Journal of Radioanalytical and Nuclear Chemistry,* vol. 307, no. 3, pp. 1711-1715, 2016/03/01 2016, doi: 10.1007/s10967-015-4416-7.

This project has received funding from the EURATOM research and training programme 2014–2018 under grant agreement No. 755171. The content of this deliverable reflects only the authors' view. The European Commission is not responsible for any use that may be made of the information it contains.

[13] P. Baron *et al.*, "A review of separation processes proposed for advanced fuel cycles based on technology readiness level assessments," *Progress in Nuclear Energy,* vol. 117, p. 103091, 2019/11/01/ 2019, doi: https://doi.org/10.1016/j.pnucene.2019.103091.

[14] E. D. Collins *et al.*, "State-of-the-art report on the progress of nuclear fuel cycle chemistry," OECD-NEA, Paris, France, 2018.

[15] M.-C. CHARBONNEL, "Importance of stability studies in the development of a new solvent extraction process for the multi-recycling of uranium and plutonium from spent nuclear fuels," presented at the Radical Behaviour 2018, Würzburg, 2018.

[16] J. Drader *et al.*, "Radiation chemistry of the branched-chain monoamide di-2-ethylhexyl-isobutyramide," *Solvent Extraction and Ion Exchange,* vol. 35, no. 7, pp. 480-495, 2017.

[17] P. N. Pathak, R. Veeraraghavan, D. R. Prabhu, G. R. Mahajan, and V. K. Manchanda, "Separation Studies of Uranium and Thorium Using Di-2-Ethylhexyl Isobutyramide (D2EHIBA)," *Separation Science and Technology,* vol. 34, no. 13, pp. 2601-2614, 1999/01/01 1999, doi: 10.1081/SS-100100793.

[18] N. Condamines and C. Musikas, "The extraction by N,N-dialkylamides. II. Extraction of actinide cations," *Solvent Extraction and Ion Exchange,* vol. 10, pp. 69-100, 1992.

[19] G. Modolo, A. Geist, and M. Miguirditchian, "10 - Minor actinide separations in the reprocessing of spent nuclear fuels: recent advances in Europe," in *Reprocessing and Recycling of Spent Nuclear Fuel*, R. Taylor Ed. Oxford: Woodhead Publishing, 2015, pp. 245-287.

[20] M. Miguirditchian *et al.*, "HA demonstration in the Atalante facility of the Ganex 1st cycle for the selective extraction of Uranium from HLW," in *Proceedings of GLOBAL*, 2009, pp. 1032-1035.

[21] M. Carrott *et al.*, "Solvent extraction behavior of plutonium (IV) ions in the presence of simple hydroxamic acids," *Solvent Extraction and Ion Exchange,* vol. 25, no. 6, pp. 723-745, 2007.

[22] R. Taylor *et al.*, "The applications of formo-and aceto-hydroxamic acids in nuclear fuel reprocessing," *Journal of alloys and compounds,* vol. 271, pp. 534-537, 1998.

[23] H. Galán, A. Núñez, A. G. Espartero, R. Sedano, A. Durana, and J. de Mendoza, "Radiolytic stability of TODGA: characterization of degraded samples under different experimental conditions," *Procedia Chemistry,* vol. 7, pp. 195-201, 2012.

[24] G. Modolo, H. Asp, C. Schreinemachers, and H. Vijgen, "Development of a TODGA based process for partitioning of actinides from a PUREX raffinate Part I: Batch extraction optimization studies and stability tests," *Solvent Extraction and Ion Exchange,* vol. 25, no. 6, pp. 703-721, 2007.

[25] Y. Sugo, Y. Sasaki, and S. Tachimori, "Studies on hydrolysis and radiolysis of N, N, N', N'-tetraoctyl-3-oxapentane-1, 5-diamide," *Radiochimica Acta,* vol. 90, no. 3, pp. 161-165, 2002.

[26] C. A. Zarzana *et al.*, "A Comparison of the γ-Radiolysis of TODGA and T(EH)DGA Using UHPLC-ESI-MS Analysis," *Solvent Extraction and Ion Exchange,* vol. 33, no. 5, pp. 431-447, 2015, doi: 10.1080/07366299.2015.1012885.

This project has received funding from the EURATOM research and training programme 2014–2018 under grant agreement No. 755171. The content of this deliverable reflects only the authors' view. The European Commission is not responsible for any use that may be made of the information it contains.

[27] L. Berthon and M.-C. Charbonnel, "Radiolysis of solvents used in nuclear fuel reprocessing," in *Ion exchange and solvent extraction*: CRC Press, 2009, pp. 443-527.

[28] L. Berthon *et al.*, "Use of chromatographic techniques to study a degraded solvent for minor actinides partitioning: qualitative and quantitative analysis," CEA VALRHO, 2004.

[29] L. Berthon, J. Morel, N. Zorz, C. Nicol, H. Virelizier, and C. Madic, "DIAMEX process for minor actinide partitioning: hydrolytic and radiolytic degradations of malonamide extractants," *Separation Science and Technology,* vol. 36, no. 5-6, pp. 709-728, 2001.

[30] H. Galán, D. Munzel, A. Núñez, U. Müllich, J. Cobos, and A. Geist, "Stability and recyclability of SO3-Ph-BTP for i-SANEX process development," in *Proc. Internat. Solvent Extr. Conf.(ISEC 2014)*, 2014, pp. 137-143.

[31] G. P. Horne, S. P. Mezyk, N. Moulton, J. R. Peller, and A. Geist, "Time-resolved and steady-state irradiation of hydrophilic sulfonated bis-triazinyl-(bi) pyridines–modelling radiolytic degradation," *Dalton Transactions,* vol. 48, no. 14, pp. 4547-4554, 2019.

[32] D. Peterman *et al.*, "Performance of an i-SANEX System Based on a Water-Soluble BTP under Continuous Irradiation in a γ-Radiolysis Test Loop," *Industrial & Engineering Chemistry Research,* vol. 55, no. 39, pp. 10427-10435, 2016/10/05 2016, doi: 10.1021/acs.iecr.6b02862.

[33] A. Geist, "Impacts on process safety from radiolytic degradat. and gas generat.in TODGA&TWE-21 based solvents," SACSESS D11.4.

[34] A. Geist, "Identification of losses of extractants and diluents and their effects in the different processes," SACSESS D12.3.

[35] A. Geist, "Description of loading issues in the different processes and identificationof possible solutions," SACSESS D12.4.

[36] H. Galán *et al.*, "Influence of gamma radiation on extraction systems based on diglycolamides and water soluble SO3-Ph-BTP such the Euro-GANEX process," in *ISEC 2017*, Japan, November 5-9, 2017.

[37] A. Nunez, H. Galan, and J. Cobos, "TODGA degradation compounds: properties and effects on extraction systems-5400," in *GLOBAL 2015 Proceedings*, 2015.

[38] A. N. H. Galán, I. Sánchez-García, L. Serrano, J. Cobos, "Status on solvent clean- up & recycling," GENIORS D3.4

[39] I. Sánchez-García, L. Bonales, H. Galán, J. Perlado, and J. Cobos, "Radiolytic degradation of sulphonated BTP and acetohydroxamic acid under EURO-GANEX process conditions," *Radiation Physics and Chemistry,* vol. 183, p. 109402, 2021.

[40] G. P. Horne *et al.*, "Gamma Radiolysis of Hydrophilic Diglycolamide Ligands in Concentrated Aqueous Nitrate Solution," (in English), *Dalton Trans.,* vol. 48, pp. 17005–17013, 2019, doi: 10.1039/C9DT03918J.

This project has received funding from the EURATOM research and training programme 2014–2018 under grant agreement No. 755171. The content of this deliverable reflects only the authors' view. The European Commission is not responsible for any use that may be made of the information it contains.

[41] I. Sánchez-García, H. Galán, J. Perlado, and J. Cobos, "Development of experimental irradiation strategies to evaluate the robustness of TODGA and water-soluble BTP extraction systems for advanced nuclear fuel recycling," *Radiation Physics and Chemistry,* vol. 177, p. 109094, 2020.

[42] A. Casnati, "Stability studies of stripping agents.," Deliverable 2.2 of GENIORS project.

[43] B. Gruner, "Stability and safety studies of hold extraction systems (1 for each CyMe4BTBP, HyidroBTBP, TODGA & PTD)," D2.1 GENIORS Project.

[44] I. Sánchez-García, L. J. Bonales, H. Galán, J. M. Perlado, and J. Cobos, "Spectroscopic study of acetohydroxamic acid (AHA) hydrolysis in the presence of europium. Implications in the extraction system studies for lanthanide and actinide separation," *New Journal of Chemistry,* vol. 43, no. 39, pp. 15714-15722, 2019.

[45] I. Sánchez-García, L. J. Bonales, H. Galán, J. M. Perlado, and J. Cobos, "Advanced direct method to quantify the kinetics of acetohydroxamic acid (AHA) by Raman spectroscopy," *Spectrochimica Acta Part A: Molecular and Biomolecular Spectroscopy,* vol. 229, p. 117877, 2020.

[46] I. Sánchez-García, H. Galán, J. M. Perlado, and J. Cobos, "Stability studies of GANEX system under different irradiation conditions," *EPJ Nuclear Sciences & Technologies,* vol. 5, p. 19, 2019.

[47] F. P. L. Andrieux, C. Boxall, and R. Taylor, "The hydrolysis of hydroxamic acid complexants in the presence of non-oxidizing metal ions 1: Ferric ions," *Journal of solution chemistry,* vol. 36, no. 10, pp. 1201-1217, 2007.

[48] A. Geist *et al.*, "Actinide (III)/lanthanide (III) separation via selective aqueous complexation of actinides (III) using a hydrophilic 2, 6-bis (1, 2, 4-triazin-3-yl)-pyridine in nitric acid," *Solvent Extraction and Ion Exchange,* vol. 30, no. 5, pp. 433-444, 2012.

[49] H. Galán, A. Núñez, I. Sánchez, S. Durán, L. Serrano, and J. Cobos, "1st half yearly partner activity report of GENIORS project (HYPAR-1_CIEMAT). ," Reporting period: 1/06/2017-30/11/2017.

[50] H. Galán, A. Núñez, I. Sánchez, S. Durán, L. Serrano, and J. Cobos, "2nd half yearly partner activity report of GENIORS project (HYPAR-2_CIEMAT). ," Reporting period: 1/12/2017-30/05/2018.

[51] H. Galán, A. Núñez, I. Sánchez, S. Durán, L. Serrano, and J. Cobos, "3rd half yearly partner activity report of GENIORS project (HYPAR-3_CIEMAT). ," Reporting period: 1/06/2018-30/11/2018.

[52] H. Galán, A. Núñez, I. Sánchez, S. Durán, L. Serrano, and J. Cobos, "4th half yearly partner activity report of GENIORS project (HYPAR-4_CIEMAT). ," Reporting period: 1/12/2018-30/05/2019.

[53] H. Galán, A. Núñez, I. Sánchez, S. Durán, L. Serrano, and J. Cobos, "5th half yearly partner activity report of GENIORS project (HYPAR-5_CIEMAT). ," Reporting period: 1/06/2019-30/11/2019.

This project has received funding from the EURATOM research and training programme 2014–2018 under grant agreement No. 755171. The content of this deliverable reflects only the authors' view. The European Commission is not responsible for any use that may be made of the information it contains.

[54] M. Sypula *et al.*, "Use of polyaminocarboxylic acids as hydrophilic masking agents for fission products in actinide partitioning processes," *Solvent Extraction and Ion Exchange,* vol. 30, no. 7, pp. 748-764, 2012.

[55] R. Malmbeck, D. Magnusson, and A. Geist, "Modified diglycolamides for grouped actinide separation," *Journal of Radioanalytical and Nuclear Chemistry,* journal article vol. 314, no. 3, pp. 2531–2538, December 01 2017, doi: 10.1007/s10967-017-5614-2.

[56] E. Macerata *et al.*, "Hydrophilic clicked 2, 6-bis-triazolyl-pyridines endowed with high actinide selectivity and radiochemical stability: toward a closed nuclear fuel cycle," *Journal of the American Chemical Society,* vol. 138, no. 23, pp. 7232-7235, 2016.

[57] E. Mossini *et al.*, "Radiolytic degradation of hydrophilic PyTri ligands for minor actinide recycling," *Journal of Radioanalytical and Nuclear Chemistry,* vol. 322, no. 3, pp. 1663-1673, 2019.

[58] C. Wagner *et al.*, "Time-resolved laser fluorescence spectroscopy study of the coordination chemistry of a hydrophilic CHON [1, 2, 3-triazol-4-yl] pyridine ligand with Cm (III) and Eu (III)," *Inorganic chemistry,* vol. 56, no. 4, pp. 2135-2144, 2017.

[59] H. Galán *et al.*, "Gamma-Radiolytic Stability of New Methylated TODGA Derivatives for Minor Actinide Recycling," (in English), *Dalton Trans.,* vol. 44, no. 41, pp. 18049-18056, 2015, doi: 10.1039/c5dt02484f

[60] A. Wilden *et al.*, "Unprecedented Inversion of Selectivity and Extraordinary Difference in the Complexation of Trivalent *f*-Elements by Diastereomers of a Methylated Diglycolamide," (in English), *Chem. Eur. J.,* vol. 25, no. 21, pp. 5507-5513, 2019, doi: 10.1002/chem.201806161.

[61] Y. Sugo *et al.*, "Influence of diluent on radiolysis of amides in organic solution," *Radiation Physics and Chemistry,* vol. 76, no. 5, pp. 794-800, 2007, doi: 10.1016/j.radphyschem.2006.05.008.

[62] A. Wilden *et al.*, "Radiolytic and Hydrolytic Degradation of the Hydrophilic Diglycolamides," (in English), *Solvent Extr. Ion Exch.,* vol. 36, no. 4, pp. 347-359, 2018, doi: 10.1080/07366299.2018.1495384

[63] V. Hubscher-Bruder *et al.*, "Behaviour of the Extractant Me-TODGA Upon Gamma Irradiation: Quantification of the Degradation Compounds and Individual Influences on Complexation and Extraction," (in English), *New J. Chem.,* vol. 41, pp. 13700-13711, 2017, doi: 10.1039/C7NJ02136D.

[64] M. J. Carrott, C. R. Gregson, and R. J. Taylor, "Neptunium extraction and stability in the GANEX solvent (0.2 M TODGA / 0.5 M DMDOHEMA / kerosene)," (in English), *Solvent Extr. Ion Exch.,* vol. 31, no. 5, pp. 463-482, 2013, doi: 10.1080/07366299.2012.735559.

[65] B. J. Mincher, M. Precek, S. P. Mezyk, G. Elias, L. R. Martin, and A. Paulenova, "The redox chemistry of neptunium in γ-irradiated aqueous nitric acid," (in English), *Radiochim. Acta,* vol. 101, no. 4, pp. 259-266, 2013/04/01 2013, doi: 10.1524/ract.2013.2013.

This project has received funding from the EURATOM research and training programme 2014–2018 under grant agreement No. 755171. The content of this deliverable reflects only the authors' view. The European Commission is not responsible for any use that may be made of the information it contains.

[66] G. P. Horne, T. S. Grimes, B. J. Mincher, and S. P. Mezyk, "Reevaluation of Neptunium-Nitric Acid Radiation Chemistry by Multiscale Modeling," (in English), *J. Phys. Chem. B,* Article vol. 120, no. 49, pp. 12643-12649, Dec 2016, doi: 10.1021/acs.jpcb.6b09683.

[67] M. Sypula *et al.*, "Use of polyaminocarboxylic acids as hydrophilic masking agents for fission products in actinide partitioning processes," (in English), *Solvent Extr. Ion Exch.,* vol. 30, no. 7, pp. 748-764, 2012, doi: 10.1080/07366299.2012.700591.

[68] P. Weßling, U. Müllich, E. Guerinoni, A. Geist, and P. J. Panak, "Solvent extraction of An(III) and Ln(III) using TODGA in aromatic diluents to suppress third phase formation," *Hydrometallurgy,* vol. 192, p. 105248, 2020/03/01/ 2020, doi: https://doi.org/10.1016/j.hydromet.2020.105248.

[69] T. H. Siddall, "Effects of Structure of N,N-Disubstituted Amides on Their Extraction of Actinide and Zirconium Nitrates and of Nitric Acid," (in English), *J Phys Chem-Us,* vol. 64, no. 12, pp. 1863-1866, Dec 1960, doi: 10.1021/j100841a014.

[70] B. Verlinden *et al.*, "First-principles study of the radiolytic degradation of diglycolamides: the role of solvation thermodynamics," (in English), *Physical Chemistry Chemical Physics,* vol. submitted, 2021.

[71] H. Galán, A. Núñez, I. Sánchez, L. J. Bonales, S. Durán, and L. Serrano, "7th half yearly partner activity report of GENIORS project (HYPAR-7_CIEMAT). ," Reporting period: 1/06/2019-30/11/2019.

[72] A. Wilden *et al.*, "JUELICH contribution in the Deliverable 6.2 of GENIORS project: Optimized flowsheets for homogeneous recycling of advanced MOX fuel in GEN IV reactors.."

[73] G. Modolo *et al.*, "6th half yearly partner activity report of GENIORS project (HYPAR-5_JUELICH). ," Reporting period: 1/06/2019-30/11/2019.

[74] G. Modolo, A. Wilden, D. Schneider, Z. Paparigas, B. Verlinden, and F. Kreft, "5th half yearly partner activity report of GENIORS project (HYPAR-6_JUELICH).", Reporting period: 1/12/2019-31/05/2020.

[75] A. Casnati *et al.*, "Assessment of applications of PTD in i-SANEX and EUROGANEX processes, GENIORS - D6.1 ".

[76] P. Ekeblad and K. Erne, "Non-aqueous acid-base titrations in pharmaceutical analysis," *Journal of Pharmacy and Pharmacology,* vol. 6, no. 1, pp. 433-439, 1954.

[77] H. Fricke, "Chemical dosimetry," *Radiation dosimetry,* vol. 2, pp. 167-239, 1966.

[78] X. Heres, M. Montuir, and J. L. Girotto, "PUREX-Amide process: estimation of the dose received by the solvent.," ed: CEA, 2021.

[79] L. Berthon and C. M.C., "Ion Exchange and Solvent Extraction: A Series of Advances, Volume 19 (Vol. 19). ," B. A. Moyer Ed.: CRC Press., 2009.

[80] I. Sanchez-García and H. Galán, "CIEMAT HPLC-MS mTDDGA measurements," ed, 2021.

[81] M. Charbonnel and L. Berthon, "CEA technical note.," 2021.

This project has received funding from the EURATOM research and training programme 2014–2018 under grant agreement No. 755171. The content of this deliverable reflects only the authors' view. The European Commission is not responsible for any use that may be made of the information it contains.

[82] P. Distler *et al.*, "Stability of Different BTBP and BTPhen Extracting or Masking Compounds Against Gamma Radiation," *to be submitted.,* 2021.

[83] H. Schmidt, A. Wilden, G. Modolo, J. Švehla, B. Grüner, and C. Ekberg, "Gamma radiolytic stability of CyMe4BTBP and the effect of nitric acid," *Nukleonika,* vol. 60, no. 4, pp. 879-884, 2015.

[84] H. Schmidt *et al.*, "Gamma and pulsed electron radiolysis studies of CyMe4BTBP and CyMe4BTPhen: identification of radiolysis products and effects on the hydrometallurgical separation of trivalent actinides and lanthanides," 2021, submitted. .

[85] J. Halleröd *et al.*, "On the Basic Extraction Properties of a Phenyl Trifluoromethyl Sulfone-Based GANEX System Containing CyMe4-BTBP and TBP," *Solvent Extraction and Ion Exchange,* vol. 36, no. 4, pp. 360-372, 2018/06/07 2018, doi: 10.1080/07366299.2018.1497043.

[86] V. B. Shevchenko and V. S. Smelov, "The effect of mono- and dibutyl phosphates on the extraction of plutonium with tributyl phosphate," *The Soviet Journal of Atomic Energy,* vol. 5, no. 5, pp. 1455-1459, 1958/11/01 1958, doi: 10.1007/BF01498488.

This project has received funding from the EURATOM research and training programme 2014–2018 under grant agreement No. 755171. The content of this deliverable reflects only the authors' view. The European Commission is not responsible for any use that may be made of the information it contains.